Aus dem Institut für Zell- und Neurobiologie
der Medizinischen Fakultät Charité – Universitätsmedizin Berlin

DISSERTATION

The integrity of basal forebrain neurons depends on permanent expression of Nkx2-1: potential for understanding haploinsufficiency in humans.

zur Erlangung des akademischen Grades
Doctor of Philosophy in Medical Neurosciences
(PhD in Medical Neurosciences)

vorgelegt der Medizinischen Fakultät
Charité – Universitätsmedizin Berlin

von

Lorenza Magno

aus Bergamo

Gutachter/in: 1. Priv.-Doz. Dr. Med. T. Naumann

2. Prof. Dr. H.-D. Hofmann

3. Prof. Dr. H. Schwegler

Datum der Promotion: 01.11.2010

CONTENTS

LIST OF FIGURES

ABBREVIATIONS

AChE	acetylcholine esterase
CB	calbindin
cf.	compare
ChAT	choline acetyltransferase
CNS	central nervous system
CPu	caudate-putamen
CR	calretinin
GAD67	glutamate decarboxylase 67
GPe	globus pallidus external segment
GPi	globus pallidus internal segment
hDB-SI	horizontal limb of the diagonal band-substantia innominata
IHC	immunohistochemistry
ISH	*in situ* hybridization
LGP	lateral globus pallidus
LS	lateral septum
MGE	medial ganglionic eminence
MS	medial septum
MSDB	medial septum-diagonal band complex
MSvDB	medial septum-ventral limb of the diagonal band
PB	phosphate buffer
POA	preoptic area
PV	parvalbumin
SOM	somatostatin
SVZ	subventricular zone
VZ	ventricular zone

1. INTRODUCTION

1.1. BRAIN-THYROID-LUNG SYNDROME: A MYSTERIOUS DISEASE EMERGING IN POSTNATAL LIFE

The brain-thyroid-lung syndrome was first identified in patients screened for congenital hypothyroidism which also displayed neurological impairments. The occurrence of neurological symptoms and developmental delay in patients affected by congenital hypothyroidism has been attributed to the lack of thyroid hormones in the developing CNS (Gruters et al., 2004). However, the neonatal screening program allows immediate initiation of thyroid hormone therapy, thus preventing the onset of these deficits. Notably, despite early hormone substitution, in some cases the neurological outcome is poor. Thus, the symptoms of such patients are more likely related to other defects, such as underlying genetic defects, rather than to the consequence of hypothyroidism (Moya et al., 2006). Initially two studies found deletions of the chromosome 14q13, encompassing the *NKX2-1* locus, in patients displaying neurological symptoms in combination with thyroid abnormalities and / or respiratory distress (Devriendt et al., 1998; Iwatani et al., 2000). These descriptions encouraged the investigation of the *NKX2-1* gene in patients showing this peculiar combination of symptoms. So far, several heterozygous mutations affecting the *Nkx2-1* locus have been described to cause specific dysfunctions of the CNS, sometimes accompanied by disturbances of thyroid gland and the lungs (Breedveld et al., 2002a; b; Krude et al., 2002; Asmus et al., 2005; do Carmo Costa et al., 2005; Moya et al., 2006; Devos et al., 2006; Provenzano et al., 2008; for review see: Kleiner-Fisman and Lang, 2007).

The “brain-thyroid-lung” syndrome emerges early in childhood and is characterized by a variable combination of hypothyroidism (including high thyroid-stimulating-hormone levels), respiratory distress, and dysfunctions of the motor system (for review see: Kleiner-Fisman and Lang, 2007). The latter include delayed development of speech and motor abilities, persistent ataxia, dysarthria, muscular hypotonia, hyperextendable knee joints, muscular atrophy of the lower limbs, and choreoathetosis, which is described as rapid involuntary and slow writhing movements of the limbs, face and trunk. The term “benign hereditary chorea” was used referring to mutations of NKX2-1 only causing neurological symptoms described above. However, the spectrum of the disorder is more

complex and the term “brain-thyroid-lung” syndrome more adequately emphasizes the involvement of multiple organ systems (Kleiner-Fisman and Lang, 2007). The severity of the symptoms varies between the patients and depends on the type of mutation affecting the *NKX2-1* gene. In most cases the symptoms become less severe or even disappear once adulthood is reached. So far, according to the clinical studies, no psychiatric or cognitive abnormalities have been found in most of the patients, and only some individuals fail to finish school and show mild mental abnormality (Breedveld et al., 2002b; Willemsen et al., 2005; Moya et al., 2006). Morphological abnormalities in the brains were described in only a few cases. In one study, magnetic resonance imaging revealed mild malformations of the basal ganglia, including reduced size of the globus pallidus and no defined separation into a lateral and a medial part. Moreover, a cystic mass was found in a position cranio-dorsal to the pituitary (Krude et al., 2002). Overall, these few cases cannot explain the complex motor disturbances described for all *NKX2-1*-haploinsufficient patients.

In humans only heterozygous mutations of *NKX2-1* have been identified. Besides large chromosomal deletions (Iwatani et al., 2000; Breedveld et al., 2002b), missense, nonsense and point mutations have also been described to cause this brain-thyroid-lung triad (Krude et al., 2002; Pohlenz et al., 2002; Willemsen et al., 2005).

Heterozygous mutations of the NKX2-1 locus result in haploinsufficiency, a rare genetic phenomenon related to semi-dominant genes. Since these genes only fulfill their normal function in the presence of both wild-type alleles, loss of one allele already results in corresponding defects (for review see: Nutt and Busslinger, 1999). In some cases the mutation results in a frameshift leading to the synthesis of a truncated protein (Krude et al., 2002). Most of the mutations reported so far are described to affect the DNA-binding properties of the transcription factor (Krude et al., 2002; Breedveld et al., 2002b).

1.2. NKX2-1 PROTEIN AND GENE

Nkx2-1 was initially discovered in the thyroid gland of rodents. The transcription factor was first isolated in 1989 as a thyroid specific DNA-binding activity that interacts with the rat thyreoglobulin gene and was therefore called “Thyroid Transcription Factor 1” (TTF-1; Civitareale et al., 1989). Subsequently, another study identified Nkx2-1 by its ability to bind to an enhancer in the human thyroid peroxidase gene, leading to its

designation as Thyroid-specific Enhancer-binding-protein (T/Ebp; Mizuno et al., 1991). In cloning experiments the so called TTF-1 was recognized as a novel homeodomain containing protein closely related to members of the Drosophila NK-2 family (Guazzi et al., 1990; Kim et al., 2006). Thus, the protein was then named Nkx2-1.

NKX2-1 belongs to the Homeobox gene family. These genes encode transcription factors containing a 60 amino acids-homeodomain that mediates binding to DNA (Gehring et al., 1994). The homeodomain was cloned and analyzed in a large number of organisms ranging from yeast to humans, and it was found to be evolutionary conserved among the species (Kim and Nirenberg, 1989; Vollmer and Clerc, 1998; Mark et al., 1997). Homeodomain proteins act as nuclear transcriptional regulators, functioning at different protein concentration thresholds. (Vollmer and Clerc, 1998). Several studies on purified homeodomain polypeptides demonstrated that they consist of a tri-α-helical domain. The second and third helices form a helix-turn-helix motif that recognizes and binds to the major groove of the DNA (Kissinger et al., 1990).

In addition to the conserved homeodomain, proteins from the Nk/Nkx class contain a short 17-amino acid-long highly conserved sequence called the “conserved peptide”, whose function remains unknown (Price et al., 1992). The sequences of human, rat and mouse protein are 98% identical with absolute conservation of the homeodomain (Bingle, 1997).

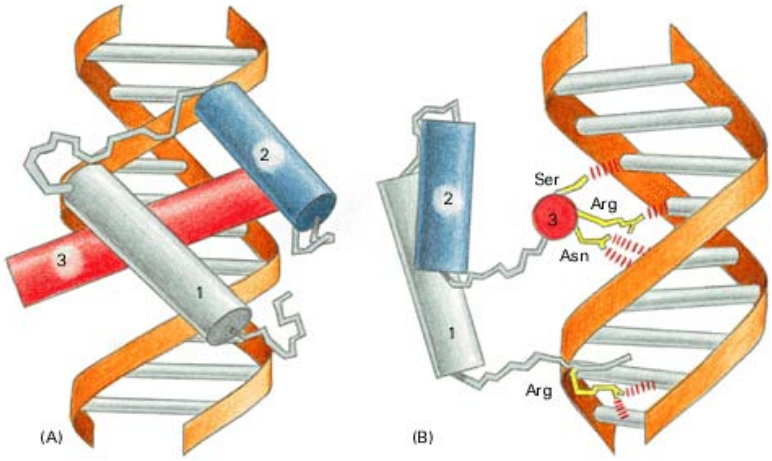

Figure 1. Interaction between the homeodomain and DNA (Albert, 2002).

NKX2-1 gene is localized on chromosome 14 in humans and on chromosome 12 in rodents. The genomic clones have been isolated from rat (Endo et al., 1994), human

(Ikeda et al., 1995) and mouse (Oguchi et al., 1995). These studies have shown that *Nkx2-1* consists of two exons separated by an intron of approximately 900 nucleotides. More recently it was reported that the human *NKX2-1* gene consists of three exons and two introns. The newly found ATG falls upstream of the previously called exon I (Hamdan et al., 1998). Two splicing isoforms encoding for 401 amino acid-long and 371 amino acid-long proteins were also identified in the pulmonary epithelium (Li et al., 2000). However, the existence and exact location of exon 1 upstream of the so called exon 2 containing the main ATG is not well defined in the mouse genome.

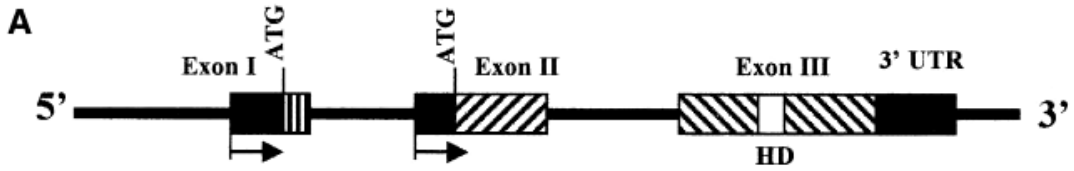

Figure 2. Schematic diagram of the NKX2-1 gene encoding for two isoforms with different N-terminus (Li et al., 2000).

1.3. EXPRESSION OF NKX2-1

1.3.1. Prenatal expression

During development of vertebrates Nkx2-1 is specifically expressed in the developing brain, as well as in the Anlagen of the lungs and the thyroid gland (Lazzaro et al., 1991; Price et al., 1992; Fig. 3). In rodents, *Nkx2-1* mRNA was observed in two discontinuous regions of the developing brain, the floor of the telencephalic vesicles, and the Anlagen of the hypothalamus. *Nkx2-1* transcripts were detected at day 10.5 post coitum in rats (Lazzaro et al., 1991), and embryonic stage 8.75 in mice (Price et al., 1992; Shimamura et al., 1995). *Nkx2-1* expression is strongly upregulated from E10 onwards in the hypothalamic primordium and in ventral parts of the immature telencephalon of the mouse brain, including the MGE, the preoptic area (POA) and the anterior entopeduncular region (AEP; Shimamura et al., 1995; Sussel et al., 1999; Puelles et al., 2000; Flames et al., 2007; Garcia-Lopez et al., 2008; Abellan and Medina, 2009).

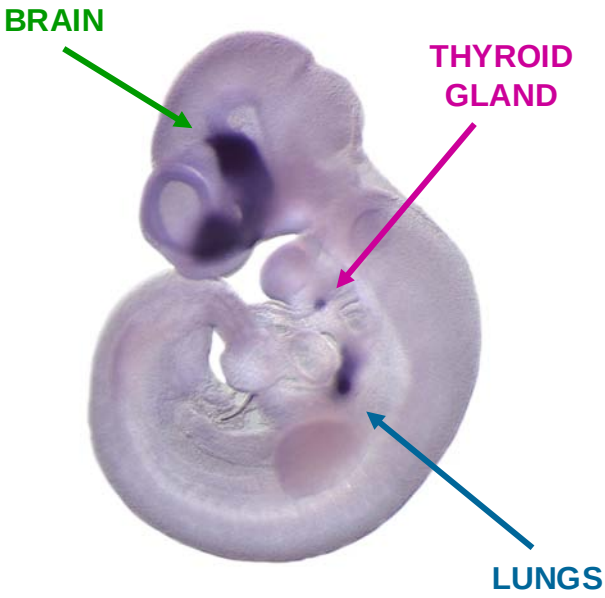

Figure 3. Whole mount in situ hybridization for Nkx2-1 on E10 mouse embryo (Schrumpf P., Charitè, Berlin).

Analysis of the *Nkx2-1* knockout mice gave the first direct evidence of Nkx2-1 function in the morphogenesis of the lungs, the brain and the thyroid gland. Homozygous *Nkx2-1*$^{-/-}$ mutants were generated by inserting a cassette in the middle of the homeobox sequence of the *Nkx2-1* gene resulting in the synthesis of a truncate non-functional protein (Kimura et al., 1996). The mutants die at birth due to agenesis of the lungs, and the Anlage of the thyroid gland is eliminated very early during embryogenesis through apoptotic mechanism.

Extensive defects were found in the brain in all structures originating from the Nkx2-1-positive neuroepithelium. The ventral part of the septal area appear to be fused in the midline, and the typical structure of the nucleus of the diagonal band is missing (Kimura et al., 1996; Fig. 4). In the basal ganglia the globus pallidus, is absent and, conversely, the striatum is enlarged (Sussel et al., 1999).

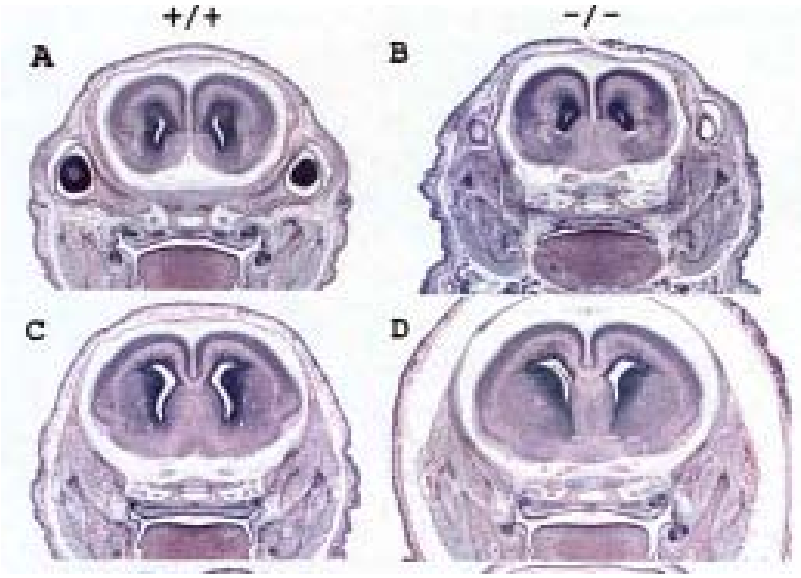

Figure 4. Coronal sections at the level of the septal complex of E18.5 control (+/+) and Nkx2-1 knockout (-/-) mice (Kimura et al., 1996).

As described above, Nkx2-1 expression was found not only in the developing telencephalon, but also in the Anlage of the hypothalamus. In line with this, the preoptic and hypothalamic areas of *Nkx2-1*$^{-/-}$ mice are severely affected. The ventromedial and dorsomedial nuclei are underdeveloped and appear to be fused in the midline. Several hypothalamic structures, such as the arcuate and premammillary nuclei, are almost absent, whereas the pituitary gland and the mammillary bodies are completely missing. (Kimura et al., 1996).

1.3.2. Postnatal expression

Several studies have shown that the expression of Nkx2-1 extends at least into the early postnatal life of rodents. In the telencephalon, Nkx2-1 immunoreactivity was observed in the globus pallidus and striatum until the third postnatal week (Marin et al., 2000).

Nkx2-1 expression in the hypothalamus and other diencephalic structures was described to be involved in the control of various vegetative functions. Preoptic neurons expressing the luteinizing hormone-releasing hormone, and preproenkephalin-positive neurons of the ventromedial hypothalamic nucleus, transiently regulate the expression of *Nkx2-1* prior to puberty and participate in the control of sexual maturation and

reproductive behavior (Lee et al., 2001). Other Nkx2-1-positive neuronal subsets, mainly located in hypothalamic nuclei surrounding the third ventricle and in the lateral hypothalamic area, are involved in regulating feeding behavior and body weight (Kim et al., 2006). In the subfornical organ, an elevated level of the *Nkx2-1* mRNA was observed after water deprivation, which points to a role in regulation of body fluid homeostasis and blood pressure (Son et al., 2003). Furthermore, it has been shown that GFAP-positive cells of the posterior lobe of the pituitary gland, probably pituicytes, express Nkx2-1 throughout life (Nakamura et al., 2001).

Notably, mice heterozygous for the disrupted *Nkx2-1* allele are born and develop normally, they appear to be healthy and fertile (Pohlenz et al., 2002). These mice showed normal thyroid gland size and normal T4 hormone levels, but elevated levels of thyroid-stimulating-hormones. *Nkx2-1*$^{+/-}$ mice were tested with the rota-rod test, a typical behavioral paradigm to assess motor coordination. The performances of mutants were described as slightly worse than controls, however, corresponding malformations were not detected in the telencephalon of the heterozygous mutants as the various structures of the brain were described as morphologically normal at the “gross level”. (Pohlenz et al., 2002).

Two recent reports demonstrated that Nkx2-1 protein is required in adult mice for the maintenance of the normal architecture and function of the differentiated thyroid gland (Kusakabe et al., 2006), and for the hypothalamic control of puberty and reproductive function (Mastronardi et al., 2006). In the first case, a partial loss of Nkx2-1 in follicular cells of the thyroid gland led to atrophy / degeneration of the follicles, which caused a severe increase in the level of thyroid-stimulating-hormone (Kusakabe et al., 2006). In the second case, synapsin I-driven deletion of the *Nkx2-1* gene in terminally differentiated neurons of the forebrain led to hypothalamic dysfunctions such as delayed puberty and reduced reproductive capacity. In contrast, functions depending on the ventral telencephalic structures (e.g. the basal ganglia and the cholinergic centers) were not affected after conditional deletion of Nkx2-1 in mature neurons. As a matter of fact, conditional mutants didn’t show impaired performances when tested for general locomotor activity and motor coordination. Furthermore, no deficits of cognitive functions were found that could be related to the loss of Nkx2-1 in basal forebrain cholinergic neurons (Mastronardi et al., 2006).

1.4. CELLULAR EXPRESSION OF NKX2-1 IN THE TELENCEPHALON

In the developing telencephalon, cells produced in the ventricular zone (VZ) of each proliferative domain (or their smaller subdivisions) move to the subventricular zone (SVZ) and start migrating either radially to the mantle zone or tangentially to adjacent and more distant regions (Fig. 5). It has been shown that projection neurons and interneurons migrate following a radial or a tangential route, respectively (Marin et al., 2000; Wichterle et al., 2001). The development of the compartments formed mainly by projection neurons is thus a result of radial migration (Rakic, 1974; Nadarajah et al., 2001). Other precursors mainly deriving from the subpallial progenitor zones tangentially migrate and integrate in the cortex and other telencephalic compartments (Anderson et al., 1997; Wichterle et al., 1999, Lavdas et al., 1999; Marin and Rubenstein, 2001; Letinic et al., 2002). Upon the exit from the cell cycle, these cells start differentiating into the various types of interneurons (Letinic et al., 2002), which, in general, represent a minor subpopulation of the target region. The appearance of the mature neuronal phenotype, marked by the expression of calcium binding proteins, neuropeptides or neurotransmitters, occurs, in most cases, at later stages or even after birth (PV, Schlosser et al., 1999; ChAT, Bender et al., 1996).

The phenotype of the knockout mice showed that Nkx2-1 is involved in the production of various cell types. Subsets of telencephalic neurons were either eliminated or reduced in Nkx2-1 mutants. Immunohistochemical analysis of prenatal mutants at E18.5 revealed a 40% reduction in the number of glutamate decarboxylase 67 (GAD67)-positive interneurons of the cerebral cortex, even if the structure appeared histologically normal. In line with this, neuronal cell numbers for hippocampal GABAergic interneurons co-expressing neuropeptide-Y (NPY), calbindin (CB), or somatostatin (SOM) were also significantly lower at E18.5 (Pleasure et al., 2000). Moreover, in the mutant striatum a partial loss of interneurons was observed. Choline acetyltransferase (ChAT)-, parvalbumin (PV)-, SOM-, NPY-, nitric oxide synthase-, and calretinin (CR)-positive neurons were either severely reduced or totally absent (Marin et al., 2000). In addition, cholinergic basal forebrain neurons expressing the high affinity nerve growth factor receptor trkA were not detectable (Sussel et al., 1999). Time-specific ablation of Nkx2-1 in the progenitor cells of the VZ demonstrated a critical role of Nkx2-1 in the temporally regulated production of the MGE-derived neurons (Miyoshi et al., 2007; Butt et al., 2008). Nkx2-1 could determine cell fate by directly regulating the expression of

other transcription factors, such as the members of the LIM homeobox family Lhx6 and Lhx7 (Grigoriou et al., 1998; Marin et al., 2000).

Furthermore, Nkx2-1 function in postmitotic neurons was described to be essential for their migration to the correct targets. While postmitotic interneurons destined for the cortical mantle downregulate Nkx2-1 synthesis, ventrally oriented neurons forming the basal ganglia maintain expression of Nkx2-1 (Nobrega-Pereira et al., 2008).

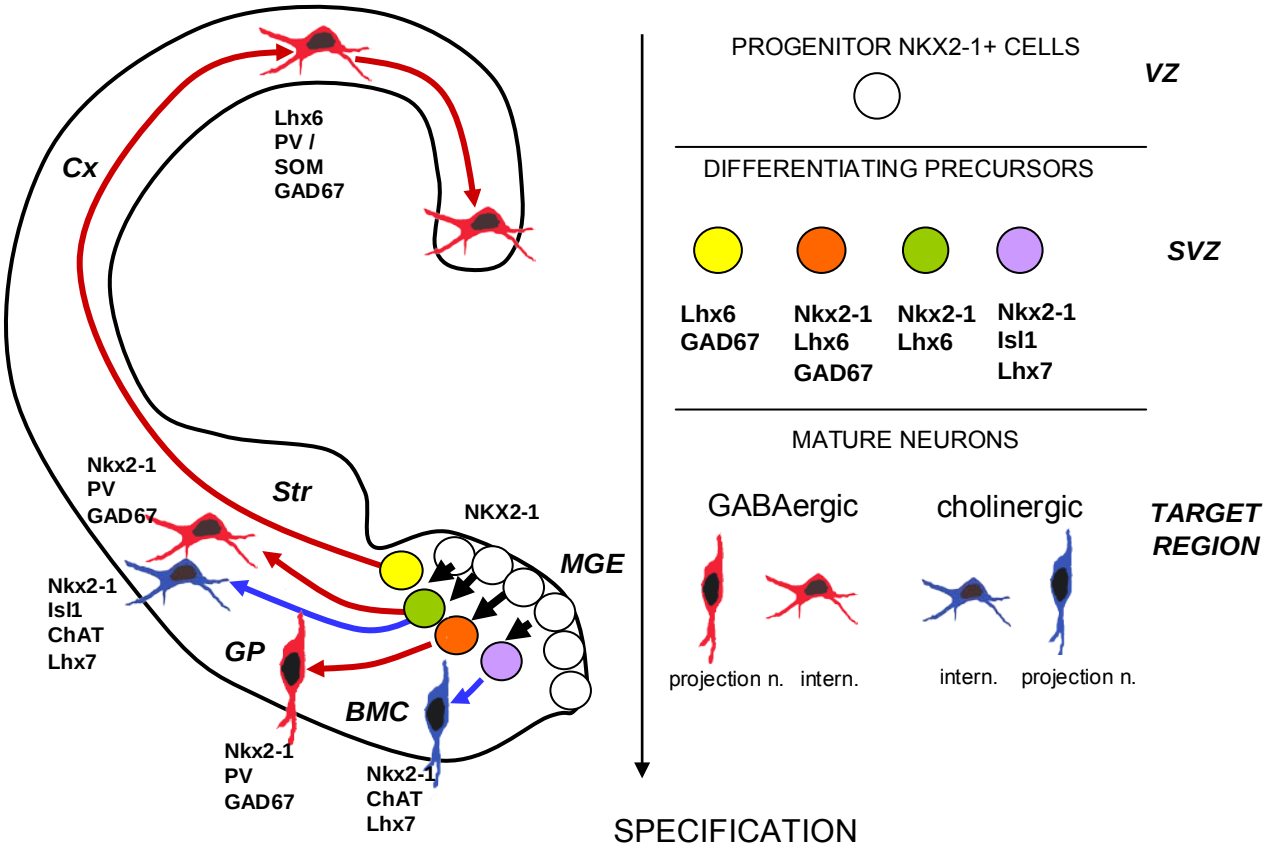

Figure 5. Left. Schematic diagram showing the origin and migration routes of NKX2-1-positive-MGE derived neurons. Right. Scheme showing the progressive specification of the neuronal populations from the Nkx2-1 undifferentiated progenitor pool. Cx, cortex; BMC, nucleus magnocellularis basalis; GP, globus pallidus; Str, striatum.

1.5. AIM OF THE STUDY

NKX2-1 haploinsufficiency in humans causes a peculiar syndrome characterized by a variable combination of symptoms related to the function of the CNS, the thyroid gland and the lungs. Interestingly, neurological symptoms do not appear in *NKX2-1*-haploinsufficient patients before the first year of age. The delay in speech development, together with persisting defects in movement coordination, suggests that the long-lasting expression of NKX2-1 in the basal ganglia is needed for the sufficient maturation of these abilities. Thus, the symptoms described for *NKX2-1*-haploinsufficiency could be a result of both prenatal and postnatal lack of NKX2-1 protein function. Notably, morphological abnormalities were hardly found in the brains of the patients which could be linked to the disorder.

Data obtained from rodents have been unable to convincingly explain the symptoms of human NKX2-1-haploinsufficiency so far. Firstly, prenatal inactivation of Nkx2-1 resulted in severe morphological alterations of the basal ganglia and various nuclei of the diencephalon, whereas such anatomical defects were rarely found in the patients. Secondly, postnatal conditional mutation of the transcription factor led to hypothalamic dysfunctions, but no impairments regarding motor coordination or cognitive functions were detected for these mutants. In contrast, the onset and the features of the disease indicate that the postnatal expression of NKX2-1 is necessary for the correct maturation of motor abilities. Moreover, only some preliminary data show the presence of hypothalamic dysfunctions in these patients (S. Schrittert, Doctoral dissertation, Charitè Univ., Berlin).

The conflicting results intrigued us to find an explanation for the human symptoms at a cellular level. This study was therefore aimed to determine which cell types might be affected by Nkx2-1 mutation. We first investigated to what extent neurons in the postnatal and adult mouse forebrain maintain Nkx2-1 expression. Since our results showed that mainly cholinergic and PV-expressing GABAergic neurons express Nkx2-1 postnatally, we then generated two conditional mouse lines with time- and cell type-specific ablation of *Nkx2-1*. Cre-recombinase expression under the control of the GA67 and ChAT promoter ensured *Nkx2-1* ablation during embryonic and postnatal development, respectively. Investigation of mutant mice with anatomical and behavioral analysis allowed us to assess the impact of the transcription factor during the prenatal and postnatal period on the development and maintenance of cholinergic and

parvalbumin-expressing GABAergic neurons. Finally, in order to ensure that the observation obtained for mice could be applied to the human pathology, we examined NKX2-1 expression in the human brain.

2. MATERIALS AND METHODS

2.1. MOUSE LINES AND STRAINS, GENERATION OF CONDITIONAL MICE AND GENOTYPING

2.1.1. Animals

All animals were housed on a 12/12 hour light/dark cycle with access to food and water *ad libitum* and in accordance with institutional guidelines for animal welfare.
Behavioral tests were performed according to the state authority of Berlin, Landesamt für Gesundheit und Soziales (LAGeSo; permit #G0004/09).

2.1.2. Transgenic lines

GAD67-cre line
The *GAD67-cre* line was generated by A. Vogt (Doctoral dissertation, Heidelberg Univ., Heidelberg). The mice were accurately characterized and a detail description is provided in the doctoral dissertation of A. Vogt (Heidelberg). Briefly, the targeting vector used for generating *GAD67-cre* transgenic mice contained a 21 kb fragment of the murine *GAD67* gene spanning parts of exon 1 up to intron 6. The Cre-recombinase cDNA was placed 30 bp upstream of the translational start codon of *GAD67* (Fig. 6). The targeting vector was electroporated into E14 embryonic stem cells and correctly targeted ES cells were injected into C57Bl/6 blastocysts. Knockin mice were bred with C57Bl/6 mice to obtain a uniform genetic background. The heterozygous mice are viable and fertile, and no abnormal phenotype was detected in these mice.

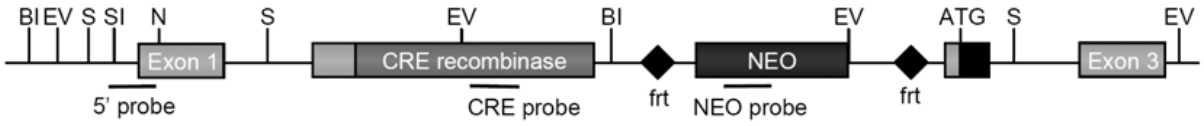

Fig 6. Diagram of the GAD67-cre allele.

ChAT-cre line

The *ChAT-cre* line was purchased from The Jackson Laboratories (Charles River, Sulzfeld, Germany; *stock number #6410*). The targeting vector was designed to contain an internal ribosome entry site-linked Cre-recombinase gene (IRES-Cre) downstream of the stop codon of the *ChAT* gene. Thus, Cre-recombinase expression is controlled by the endogenous gene promoter. ChAT expression was described to be unaffected and Cre-recombinase activity was reported in all cholinergic neurons (The Jackson Laboratories). The construct was electroporated into 129S6/SvEvTac-derived W4 embryonic stem (ES) cells. Correctly targeted ES cells were injected into C57Bl/6 blastocysts and the chimeric mice were bred to C57Bl/6 mice. The resulting mutant offspring were bred to wild type siblings. The heterozygous mice are viable and fertile and no abnormal phenotype was detected in these mice.

Nkx2-1 floxed line

The *Nkx2-1 floxed* line ($Nkx2\text{-}1^{fl/fl}$) was kindly provided by Dr. Shioko Kimura, and has been described in detail elsewhere (Kusakabe et al., 2006). Briefly, assuming that the exon containing a start codon ATG is the first exon, two loxP site were inserted respectively between exon 1 and exon 2 (Fig. 7). Chimeric male mice were subsequently bred with C57Bl/6 females.

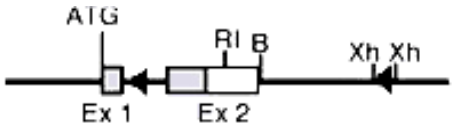

Figure 7. Diagram of the Nkx2-1 floxed allele. Exons are numbered, and the position of the loxP sites is indicated by arrowheads (Kusakabe et al., 2006).

ROSA26-floxed line

The *ROSA26-floxed* line (Soriano, 1999) was purchased by The Jackson Laboratories (*stock number # 2073).*

This transgenic line was generated to contain the gene encoding for β-galactosidase (lacZ) and an upstream floxed Neo cassette which prevents its translation. In cells expressing Cre-recombinase the NEO cassette is excised and the lacZ gene is

transcribed into a product that can be visualized either by X-Gal staining or by immunohistochemistry using an antibody against β-galactosidase. Homozygous mice are viable and fertile, and no abnormal phenotype was detected in these mice.

Generation of conditional mutants

For generation of conditional mice, the two Cre-lines were crossed with *Nkx2-1*$^{fl/fl}$ mice. Subsequently, Cre-positive mice of the F1 generation were bred with the homozygous floxed mice in order to delete *Nkx2-1* in GAD67- or ChAT-positive cells. For our experiments we used the following genotypes: *GAD*$^{+/+}$*;Nkx2-1*$^{fl/fl}$ and *ChaT*$^{+/+}$*;Nkx2-1*$^{fl/fl}$ (controls, referred as *GAD//fl/fl* & *ChAT//fl/fl*); *GAD*$^{cre/+}$*;Nkx2-1*$^{fl/+}$ *and ChaT*$^{cre/+}$*;Nkx2-1*$^{fl/+}$ ("heterozygous" controls, referred as *GAD-cre+/-//fl/+* & *ChATcre+/-//fl/+*); *GAD*$^{cre/+}$*;Nkx2-1*$^{fl/fl}$ and *ChaT*$^{cre/+}$*;Nkx2-1*$^{fl/fl}$ (mutants, referred as *GADcre+/-//fl/fl* & *ChATcre+/-//fl/fl*). We investigated the effects of *Nkx2-1* deletion in ChAT-expressing cells (postnatal mutation: ChATcre+/-//fl/fl; corresponding control: ChAT//fl/fl) and compared the results with those obtained following GAD67-driven inactivation of the transcription factor (prenatal mutation: GADcre+/-//fl/fl; controls: GAD//fl/fl). We have also performed a detailed analysis of GADcre+/-//fl/+ and ChATcre+/-//fl/+ mice. Since no significant differences were observed regarding cell numbers, axonal pattern, and performances in the behavioral tests compared with the corresponding fl/fl controls, these results are not included in the present study.

2.1.3. Genotyping

Mouse tail biopsies were digested and processed by using Invisorb Spin Tissue Mini kit (Invitek GmbH, Berlin, Germany). The following primers and annealing temperatures (Ta) have been used to detect the Cre, the floxed constructs or the wild type alleles in the genome:

GAD67-cre primer pair (designed by A.Vogt, Heidelberg)
CCGGCGCCCCTTAGCTGTGAG
GGTTCTTGCGAACCTCATCACTCG
Ta= 63°C

Chat-cre first primer pair (to detect the wild type allele; The Jackson Laboratories)

GTTTGCAGAAGCGGTGGG
AGATAGATAATGAGAGGCTC
Ta= 55°C

Chat-cre second primer pair (to detect the Cre transgenic allele; Jackson Lab)
AGATAGATAATGAGAGGCTC
CCTTCTATCGCCTTCTTGACG
Ta= 55°C

Nkx2-1 foxed primer pair (Neo primers; Kusakabe et al., 2006)
TGCCGTGTAAACACGAGGAC
GACTCTCAAGCAAGTCCATCC
Ta= 55°C
In addition, an internal primer mapping the sequence between the first two primers was designed to confirm the genotyping of these mice
(GAAGTGGCGAAAGCTACAGG; K. Paulick, Berlin-Buch).

ROSA26 floxed *primer pair* (designed by K. Paulick, Berlin-Buch)
LacZa *TCCCAACAGTTGCGCAGCCTGAAT*
LacZ b *ATATCCTGATCTTCCAGATAACTGCCG*
Ta=63°C

The following reagents were used for the PCR reaction: GoTaq polymerase (Promega, Madison, WI) and Deoxynucleotide Mix10 mM (Sigma-Aldrich, Inc., St. Louis, MO). The PCR conditions consisted of an initial activation step of 5 min at 95°C and 35 cycles as follows: 30 s of denaturation at 94°C, 30 s of annealing (see above for the specific Ta), 40 or 30 s extension at 72°C, and a final extension of 5 min at 72°C.

2.2. HUMAN TISSUE

We investigated tissue samples of the basal ganglia of two human brains. The samples were obtained from normal human brains during routine autopsies (males: 21 & 42

years old) in accordance with local ethical committee guidelines. The subjects died of non-neurological causes.
The samples were sliced fresh into thick slabs (1 cm), frozen in liquid nitrogen, and then stored at -80°C. The slabs containing parts of the basal ganglia were cut with the cryostat into 100-µm-thick coronal sections that were serially collected in cold 0.1 M phosphate buffer (PB).

2.3. HISTOCHEMISTRY AND IMMUNOFLUORESCENCE

2.3.1. Animal groups and tissue preparation

Wild type CD1 and C57Bl/6 (BL6) and conditional mutant mice (see chapter above) of either sex were used. For the analysis of Nkx2-1 expression in wild type mice, the following age-groups were selected for immunohistochemistry (IHC) and *in situ* hybridization (ISH): P0 (CD1: n = 6; BL6: n = 6), P2 (CD1: n = 4; BL6: n = 3), P5 (CD1: n = 8; BL6: n = 5), P8 (CD1: n = 3; BL6: n = 2), P10 (CD1: n = 5; BL6: n = 5), P11 (CD1: n = 2; BL6: n = 2), P15 (CD1: n = 6; BL6: n = 6), P20 (CD1: n = 2; BL6: n = 2), 4 – 6 weeks (“young adult mice”; CD1: n = 12; BL6: n = 12), 2 – 4 months (“adult mice”; CD1: n = 9; BL6: n = 9), and 6 months (“aged mice”; CD1: n = 5; BL6: n = 5). For real-time PCR we used brains of CD1 mice as follows: P0, P8, P15 and adult (4 weeks, n = 4 each). For stereology sections from the brains of transgenic P15 (n = 6), and 3 month old (n = 12) mice were used. The behavioral tests were performed on a total of 45 mice (see below for specific group numbers).
Early postnatal animals (P0, P2) were anesthetized with a mixture of ketamine, xylazine, and acepromazine (0.3 ml / 20 g body weight; i.m.), quickly decapitated, and the brains subsequently stored in a fixative containing 4% paraformaldehyde (PFA) in 0.1 M phosphate buffer (PB; pH 7.35) overnight. From the age P5 onwards, the mice were anesthetized as described above and perfused transcardially first with saline (0.9% NaCl) followed by 4% PFA in 0.1 M PB. 0.1% glutaraldehyde was added to the fixative if the brains were later to be used for electron microscopy (see Hollerbach et al., 1998). All brains were removed from the skull and postfixed in PFA overnight. The brains were subsequently cut coronally (P0, P2: 100 µm; all others: 50 or 100 µm) on a vibratome and the sections stored in PB until further processing.

All mice used for RNA extraction were sacrificed by cervical dislocation. The brains were rapidly dissected on ice, frozen in liquid nitrogen, and stored at -80°C until use.

2.3.2. Immunohistochemistry for Nkx2-1

Some of the brains were exclusively immunolabeled for Nkx2-1 to obtain a detailed expression pattern for the transcription factor along the rostro-caudal axis of the basal forebrain at different postnatal ages. After treatment of the vibratome sections with 0.6% H_2O_2 in 0.1 M PB for 20 min to inactivate endogenous peroxidase activity, the "free floating" sections were pre-incubated in a solution containing 5% normal goat serum (NGS; Vector Laboratories, Burlingame, CA), 1% bovine serum albumin (BSA), and 0.3% Triton X-100 (TX) in 0.1 M PB for 1 h at room temperature (RT) to block unspecific binding sites and facilitate penetration of the antibodies. If the sections were later to be used for fine-structural analysis, TX was omitted.

Nkx2-1 immunohistochemistry was performed using a polyclonal rabbit antibody mapping the first 190 amino acids of the Nkx2-1-sequence (Santa Cruz Biotechnology, Santa Cruz, CA). The antibody was diluted 1:2000 in 0.1 PB containing 2% NGS and 0.2% TX for 48 hours at 4 °C, followed by incubation with biotinylated goat anti-rabbit IgG (Vector Laboratories, Burlingame, CA), diluted 1:250 in PB for 2 hours at RT and, subsequently, Vectastain ABC reagent (1:250; Elite Vectastain ABC kit, Vector Laboratories, Burlingame, CA) for 1 hour. The sections were carefully rinsed with several changes of PB between all incubation steps. The tissue-bound peroxidase was detected by incubating the sections with 3,3'-diaminobenzidine (DAB; 0.07%) and H_2O_2 (0.001%) in 0.1 M PB. To enhance the staining intensity 1% cobalt chloride and 1% nickel ammonium sulphate were added to the DAB solution (Adams, 1981). This modification always resulted in dark violet to nearly black labeling of cell nuclei. In control experiments the primary antibody was omitted and no immunostaining was detected under this condition.

The labeling was found to be highly specific, and it was confirmed by the use of two other antibodies against Nkx2-1. Indeed, IHC with a polyclonal rabbit antibody (Biopat Immunotechnologies, Italy, 1:2000) or a monoclonal goat antibody (Santa Cruz Biotechnology, Santa Cruz, CA; 1:1000) resulted in the same labeling pattern as obtained by using the antibody specified above. After several washes in 0.1 M PB, the sections used for light microscopy were mounted onto gelatin-coated slides, dried,

dehydrated, and coverslipped using Shandon Xylene Substitute Mountant (Thermo Fisher Scientific, Pittsburgh, PA).

2.3.3. Immunohistochemistry for neuronal markers and β-Galactosidase

Sections were pre-incubated in solutions containing 10% normal serum of the species in which the secondary antibody was raised (see secondary antibodies below), 5% BSA, and 0.2% TX in 0.1 M PB for 1 hour at RT. The blocking steps for ChAT- and $p75^{NTR}$-IHC were slightly modified as follows: 5% BSA containing 1% TX (for ChAT), and 2% TX alone (for $p75^{NTR}$).

The primary antisera (see Table 1 for a detailed description of the antibodies, dilutions and companies) were incubated overnight at RT or 48 hours at 4°C in a solution containing 0.2% TX and 10% of the corresponding normal sera. The sections were subsequently transferred to solutions containing biotinylated goat anti-rabbit IgG (for PV, CR, $p75^{NTR}$, β-Gal), biotinylated horse anti-mouse IgG (for CB, NeuN), biotinylated rabbit anti-rat IgG (for SOM), or biotinylated rat anti-goat IgG (for ChAT; all secondary antibodies: Vector Laboratories, Burlingame, CA), diluted 1:250 in PB for 2 hours at RT. Subsequent visualization of the labeling by ABC and DAB reactions was performed as described above. After intense rinsing in PB, the double-labeled sections were further processed for light microscopy as described before. Immunofluorescence labeling (IF) for β-Gal and ChAT or PV was performed as described for IHC. After overnight incubation with the primary antisera and careful rinsing the sections were incubated with Alexa-labeled secondary antibodies (Invitrogen, Karlsruhe, Germany).

2.3.4. Double-immunohistochemistry for Nkx2-1 and neuron-specific proteins

To further characterize the Nkx2-1-immunoreactive cells in mouse and human brains several antibodies known to be specific for neuronal marker proteins were tested in double-labeling experiments (see Table 1). After careful rinsing, Nkx2-1-labeled sections (see above) were pre-incubated in solutions containing 10% normal serum of the species in which the secondary antibody was raised (see secondary antibodies above), 5% BSA, and 0.2% TX in 0.1 M PB for 1 hour at RT. As for Nkx2-1 IHC (see above), TX was omitted in all incubation steps if sections were later to be processed for fine-structural analysis. ABC reaction and development of the color reaction was

performed as described for Nkx2-1 IHC, except that enhancement of staining intensity was omitted. Our double-stainings thus resulted in violet to black labeling of the cell nuclei for Nkx2-1, whereas staining for the neuronal marker proteins resulted in brown labeling of the cytoplasms and their processes. After intense rinsing in PB, the double-labeled sections were further processed for light microscopy as described before.

IF on human tissue was performed on cryosections. The primary antibodies and dilutions used for the double-IF experiments are shown in Table 1. After overnight incubation and careful rinsing the sections were incubated with Alexa-labeled secondary antibodies (Invitrogen, Karlsruhe, Germany).

Table 1. List of primary antibodies used for IHC and IF

Name	Company	Dilution
polyclonal rabbit anti-TTF1	Biopat Immunotechnologies, Italy	1:2000
polyclonal rabbit anti-TTF1 (C-terminus)	Santa Cruz Biotechnology, Santa Cruz, CA	1:1000
polyclonal rabbit anti-TTF1	Santa Cruz Biotechnology, Santa Cruz, CA	1:2000 IHC, 1:500 IF
polyclonal rabbit anti-parvalbumin (PV)	Swant, Bellinzona, Switzerland	1:5000 IHC
monoclonal mouse anti-PV	Swant, Bellinzona, Switzerland	1:500 IF
monoclonal mouse anti-calbindin (CB)	Swant, Bellinzona, Switzerland	1:5000 IHC
polyclonal rabbit anti-calretinin (CR)	Swant, Bellinzona, Switzerland	1:5000 IHC
polyclonal goat anti-ChAT	Chemicon Int. Inc., Temecula, CA	1:100 IHC; 1:500 IF
polyclonal rat anti-SOM	Chemicon Int. Inc., Temecula, CA	1:2500
polyclonal rabbit anti-human $p75^{NTR}$	Promega, Madison, WI	1:1000
polyclonal rabbit anti-β-Galactosidase (β-Gal)	Cappel	1:3000
monoclonal mouse anti GAD67	Chemicon Int. Inc., Temecula, CA	1:1000 IF
monoclonal mouse anti-NeuN	Chemicon Int. Inc., Temecula, CA	1:1000 IHC and IF

2.3.5. Stereological cell counts

Sections from mutant and control mouse brains (n = 6 each group) intended for stereological cell counts were stained for PV, ChAT and NeuN.

Stereological cell counts (Stereo Investigator software: MicroBright- Field, Inc., Colchester, VT; version 4.31) were performed for ChAT- and PV-immunoreactive (ir) neurons in the caudate-putamen, the medial septum-vertical limb of the diagonal band complex, the horizontal limb of the diagonal band-substantia innominata, and the lateral globus pallidus (for detailed description see Fig. 8). For the latter, total neuronal cell numbers and the total volume were additionally estimated by using IHC for NeuN and subsequent stereology.

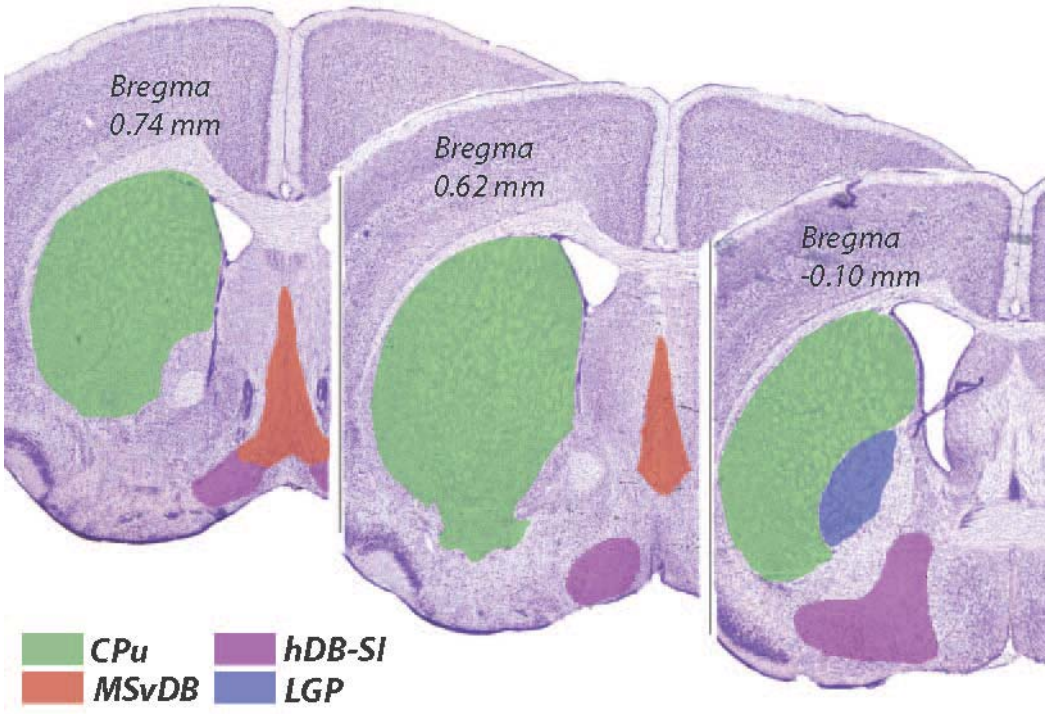

Figure 8. Representative sections showing the regions investigated with stereological cell counts at three different levels along the rostrocaudal axis of the mouse brain. (original figures are taken from Paxinos G, 2001). Whereas the borders of the MSvDB, the CPu, and the LGP are well described in the literature, no common definition of the so-called "substantia innominata" exists yet. For practical reasons we used the abbreviation "hDB-SI" because the horizontal part of the diagonal band mainly contributes to this region (left & middle sections). At a more caudal level (right section), neurons of the substantia innominata and the magnocellular preoptic nucleus were also included in the estimations of the total cell numbers for the hDB-SI.

The optical dissector / fractionator method was applied for the various regions as previously described (Naumann et al., 2002). The sections were visualized on a computer screen attached to an Olympus BX60 microscope F5 (Olympus Optical Co. Ltd., Düsseldorf, Germany). A computer-controlled stepper motor stage and focus assembly allowed movement in the x-, y-, and z-axes. Cell counts were performed using the Stereo Investigator software (MicroBright- Field, Inc., Colchester, Vt; version 3.0). The region of interest was first marked for each section using low power magnification (objective 4X/0.10). The following parameters were used: counting frame 50 X 30 µm, guard zone 2 µm, counting depth 10 µm. Thereafter, using high power magnification (oil objective 100X / 1.35) immunoreactive neurons which fulfilled the criteria of the unbiased counting rules were marked and added to the probe run list (as recommended by the “Stereo Investigator” manual).
A smaller frame size (30 x 18 µm) was used for estimation of the numbers of NeuN-positive cells in the LGP. The volume calculation for the LGP was based on the following parameters: “region investigated” (LGP), number of sections and section thicknesses. Cell numbers of the various nuclei represent data obtained from one side of the brain.

2.3.6. AChE-staining

After cutting at the vibratome, free floating brain sections assigned to AChE and Nissl staining were directly mounted onto gelatin-coated slides. Sections were processed for acetylcholine esterase (AChE) histochemistry (cf. Mesulam et al., 1983; Kermer et al., 1995). The slides were subsequently dehydrated and coverslipped using Shandon Xylene Substitute Mountant (Thermo Fisher Scientific, Pittsburgh, PA).

2.3.7. X-Gal staining

5-Bromo-4-chloro-3-indolyl-β-D-galactosidase (X-Gal) staining was performed as described earlier (Bonnerot and Nicolas, 1993). The free floating sections were washed three times with 1x PB, transferred to the staining solution (5 mM $K_4Fe(CN)_6$, 5mM $K_3Fe(CN)_6$, 2mM $MgCl_2$, 2 mg/mL X-Gal in dimethylformamide / 1x PBS) and subsequently incubated at 37 °C in the dark overnight. After three washes for 5 minutes

with 1x PB, most of the sections were mounted on slides and coverslipped as described above for the immunohistochemistry procedure. Some sections were further processed for Nkx2-1 IHC in order to detect cells expressing the cre-recombinase.

2.3.8. Semithin preparations and electron microscopy

After IHC sections selected for fine-structural analysis were osmicated (1% osmium tetroxide in 0.1 M PB) individually for 25-45 minutes in order to avoid extensive darkening of the tissue, subsequently rinsed in PB, dehydrated in ethanol (block-stained with 1% uranylacetate and 1% phosphor tungstic acid in 70% ethanol), and flat-embedded in Epon. After hardening, the sections were studied light-microscopically and selected cells were photographed at higher magnification. Small tissue samples containing these cells were re-embedded in plastic capsules and closely trimmed. Afterward, the embedded tissue blocks underwent semithin sectioning (1-2 µm thickness) followed by ultrathin sectioning. All cuts were performed on a Reichert Ultracut S. Semithin sections were fixed on slides, counter-stained with 1% toluidine blue or methylene blue, and coverslipped. The ultrathin sections were mounted on single-slot grids coated with Formvar film and examined using a Zeiss EM 900 electron microscope.

2.4. *IN SITU* HYBRIDIZATION

2.4.1. Riboprobe synthesis

The digoxigenin-labeled RNA probes were generated by *in vitro* transcription from various vectors. Plasmids (pBluescript; SK polylinker; Stratagene, La Jolla, CA) containing a 478bp mouse *Nkx2-1* cDNA fragment (corresponding to the 3' UTR of *Nkx2-1* gene sequence; between position 2250 and 2701) were linearized either with *Spe*I or with *Xho*I (New England BioLabs Inc., Ipswich, MA) to generate antisense or sense *Nkx2-1* probes, respectively. The *GAD67* RNA probe was transcribed from pBluescript transcription vectors (SK polylinker; Stratagene, La Jolla, CA) containing the sequence of the *GAD67* cDNA of rat (Erlander et al., 1991). The plasmids were linearized with *Not*I (New England BioLabs Inc., Ipswich, MA). Plasmids containing the

sequences of Lhx6 and Lhx7 were linearized either with *Not*I (Lhx6) or with *Spe*I (Lhx7; New England BioLabs Inc., Ipswich, MA) to generate antisense probes. The pGEM-T-easy vector containing a 700 bp fragment of *Lhx7* cDNA was kindly provided by G. Fishell (New York University School of Medicine, New York), and the Lhx6 plasmid was kindly provided by V. Pachnis (National Institute for Medical Research, London). In all cases, *in vitro* transcription was performed as recommended by the manufacturer with 1 g plasmid template DNA using the DIG-RNA labeling kit and appropriate enzymes (T3 polymerase for *GAD67* and *Lhx6* antisense probes, *Nkx2-1* and *Lhx7* sense probes; T7 polymerase for *Nkx2-1* and *Lhx7* antisense probe) for 2 h at 37 °C (Roche Biochemicals, Mannheim, Germany). After transcription reaction, the DNA template was digested using DNAse I (Sigma-Aldrich, Inc., St. Louis, MO).

The DIG-labeled RNA probes were purified with RNA Clean-up (Machery-Nagel GmbH & Co. KG, Düren, Germany) and controlled on 1% agarose gel. The probes were resuspended in DEPC-treated water. Subsequently, formamide was added to achieve a final concentration of 50% of the total volume and the solution was then stored at -80°C until use. A semi-quantitative analysis of probe concentration was performed by dot test.

2.4.2. *In situ* hybridization

For all steps of the ISH, RNAse-free DEPC-treated (Sigma-Aldrich, Inc., St. Louis, MO) or autoclaved solutions were used. ISH experiments were performed on 50 µm “free floating” sections collected in 2X SSC (0.3 M NaCl and 0.3 M sodium citrate in DEPC-treated water). The sections were then equilibrated for 15 minutes in a solution of 2X SSC and hybridization buffer (HB) at 1:1. Two different HBs were used for Nkx2-1 and GAD67 ISH. Sections assigned to Nkx2-1 ISH were pre-incubated for 1 hour at 60 °C in the following HB: 2X SSC, 50% formamide, 0.5X Denhardt’s solution, 5X dextran sulphate (all: Sigma-Aldrich, Inc., St. Louis, MO), 1.5% Herring sperm DNA, 0.1% E. coli tRNA (Roche Biochemicals, Mannheim, Germany), and DEPC-treated water to 40 ml. Sections selected for *GAD67*, *Lhx6* and *Lhx7* ISH were pre-incubated for 1 hour at 70 °C in the following HB: 50% formamide, 5X SSC, 5X Denhardt’s solution, 50 µg/ml tRNA, 10 µg/ml Sperm DNA, and DEPC-treated water to 50 ml.

Digoxigenin-labeled probes were used at concentrations of 400 ng per ml HB. Hybridization temperatures were 60 °C for *Nkx2-1*, 70 °C for *GAD67* and *65* °C for *Lhx6* and *Lhx7* probes. After hybridization overnight, the sections were washed in a series of

citrate buffers of increasing stringency as follows: 2X SSC twice for 20 minutes at RT, 2X SSC-50% formamide for 15 minutes at 60 °C for *Nkx2-1*, 70 °C for *GAD67* and 65 °C for *Lhx6* and *Lhx7* probes, followed by 0.1X SSC-50% formamide for 20 minutes, and finally 0.1X SSC twice for 20 minutes. Sections were then rinsed in 0.1 M Tris-Buffer (TBS) twice for 10 minutes at RT prior to a blocking step with 1% Blocking Reagent (Boehringer Ingelheim, Heidelberg, Germany) in 0.1 M TBS. For detection of DIG-labeled hybrids, sections were incubated with an anti-DIG antibody coupled to alkaline phosphatase (1:2000; Roche Applied Science, Mannheim, Germany) in 0.1 M TBS overnight at 4 °C. Sections were then washed twice for 10 minutes in 0.1 M TBS, and incubated in B1 buffer (100 mM Tris, 100 mM NaCl, 50 mM $MgCl_2$; pH 9.5) for 15 minutes at RT.

Colorimetric detection was performed at RT by using Nitro Blue Tetrazolium (0.34 µg/µL; Roche Biochemicals, Mannheim, Germany) and 5-bromo-4-chloro-3-indolylphosphate (0.35 µg/µL; Roche Biochemicals, Mannheim, Germany) in B1 buffer. When color reaction was complete (approximately 5 hours for *Nkx2-1*; 3 hours for *Lhx6*, *Lhx7* and *GAD67*), sections were washed in double-distilled water.

2.4.3. *In situ* hybridization combined with immunohistochemistry

We combined ISH for *GAD67, Lhx6* or *Lhx7* with subsequent IHC for Nkx2-1 or SOM. ISH was first performed as described above. Since ISH staining results in violet to blue labeling of the mRNA precipitates, we modified the subsequent staining protocol for IHC accordingly. Enhancement of the DAB reaction by adding cobalt chloride and nickel ammonium sulphate was omitted, thus resulting in light-brown labeling of cells.

2.5. IMAGE PROCESSING

Images were captured using an Olympus digital camera (Olympus BX-51, Hamburg, Germany). Fluorescent images were obtained with a Leica confocal laser-scanning microscope (SL). They were then processed with Adobe Photoshop CS3 (Adobe Systems Inc., San Jose, CA) for general contrast and brightness enhancements and

color-level adjustments, and finally handled with Adobe Illustrator CS3 (Adobe Systems Inc., San Jose, CA) for final compositing of the figures.

2.6. REAL TIME PCR

2.6.1. RNA extraction

Total RNA was isolated from the mouse brains. The frozen brains were homogenized in 1 ml of TRIzol reagent (Invitrogen, Carlsbad, CA) per 100 mg of tissue. The aqueous and organic phases were separated by the addition of 0.2 ml of chloroform per 1 ml TRIzol reagent used, followed by centrifugation at 12.000 g for 15 min at 4 °C. RNA was precipitated from the aqueous phase with isopropanol (50% of the total volume), followed by centrifugation at 12.000 g for 10 min at 4 °C. The pellets were washed twice with 75% ethanol, dried at RT and resuspended in DEPC-treated water. RNA concentrations were determined using a BioMate™ 3 UV-Visible spectrophotometer (Thermo Fisher Scientific Inc, Pittsburgh, PA). Afterwards, 5 µg of total RNA was reverse transcribed in a total volume of 50 µL using High-Capacity cDNA Reverse Transcription Kits (Applied Biosystems Inc., Foster City, CA), according to the manufacturer's instructions. Reverse-transcribed cDNA samples were subsequently diluted 1:3.

2.6.2. Analysis of gene expression

Relative quantification of gene expression was performed by real-time PCR using 1 µL cDNA of P0, P8, P15 and 4-week-old CD1 mouse brains as a template (n = 4, each group). *Nkx2-1* and two endogenous control genes were measured at each stage with TaqMan Gene Expression Assays products on an ABI PRISM 7500 Fast Real-time PCR Detection System (Applied Biosystems Inc., Foster City, CA). *Nkx2-1*, *HPRT* and *GAPDH* TaqMan probes and primers were pre-tested. The probes contained a 6-carboxyfluorescein phosphoramidite (FAM dye) label at the 5' end and a minor groove binder and non-fluorescent quencher at the 3' end. The *Nkx2-1* assay is supplied with primers and probe concentrations of 18 µM and 5 µM, respectively. To validate the amplification efficiency of *GAPDH, HPRT* and *Nkx2-1*, standard curves were generated

using several cDNA dilutions from the RNA sample. For calibration and generation of standard curves, we employed cDNA derived from the lungs of adult CD1 mice, which are known to express high levels of this gene (Guazzi et al., 1990). Amplification efficiency for the target (*Nkx2-1*) and the references (*HPRT, GAPDH*) was approximately equal. As determined by the slope of the standard curves, they showed a PCR amplification efficiency of > 90%.

HPRT and *GAPDH* were chosen on the basis of an analysis of their relatively constant expression in postnatal mouse brain (Meldgaard et al., 2006). Since the normalization to the endogenous control genes *HPRT* and *GAPDH* led to similar results and conclusions, we present only the data normalized to *GAPDH* expression.

The result for the relative gene expression was calculated using the $2^{-\Delta CT}$ method. All PCR assays were performed in duplicate. Universal TaqMan master mix and optimized primer and probe sets were purchased from Applied Biosystems (Applied Biosystems Inc., Foster City, CA) and used according to the manufacturer's recommendations at a final volume of 20 µL. The thermal profile used for amplification was: 95 °C for 20 min for the enzyme activation, followed by 40 cycles of 95 °C for 3 s for denaturation, and 60 °C for 30 s for the annealing / extension.

2.7. BEHAVIORAL ANALYSIS

2.7.1. Morris Water Maze (MWM)

The water maze task was conducted according to earlier protocols (Bert et al., 2005) with the following groups: GADcre+/-//fl/fl (n = 7); GAD//fl/fl (n = 7); GADcre+/-//fl/+ (n = 7); ChATcre+/-//fl/fl (n = 9); ChAT//fl/fl (n = 8); ChATcre+/-//fl/+ (n = 8). A blue circular pool (120 cm in diameter, 36 cm height) was filled up with water till 24 cm (water temperature 21±1 °C). The pool was surrounded by several visual cues and indirectly illuminated. The water surface was made opaque by adding milk powder.

The test was performed during 11 days and consisted of different phases. On the first day of trial each mouse was allowed to swim in the pool for 90 s (adaptation trial). From experimental day 2 to day 9 the "place version" trial was performed: a submerged escape platform (1cm below the water level, 10 x 10 cm) was placed in the middle of

one of four virtual quadrants. The platform was located in the quadrant which was not preferred or avoided by the mice during the adaptation trial. Each day the animals were placed into the pool from three different starting points (left, opposite, and right respect to the platform quadrant). Animals which did not find the escape platform within 90 s were placed there by the experimenter. All mice remained on the platform for 30 s. Between the trials the animals were allowed to rest for 60 s in a heated cage. For each trial, the escape latency (s) and the swimming distance (cm) were measured by a computerized tracking system (VideoMot, TSE, Germany). The average swimming speed was calculated by the quotient of swimming distance and escape latency (cm/s). For each mouse the data of the three trials per day were averaged.
On experimental day 10 the platform was removed and the time spent in each quadrant during a single trial over 90 s was registered (spatial probe). In the last test (cued version, day 11), the platform was placed 1cm above the water surface and signaled by adding a white cylinder (diameter: 3cm; height: 4cm). The platform was located in the quadrant opposite to the intermediate position during the place version. The procedure was performed as described for the place version and the escape latency, and the swimming distance were measured for each trial.

2.7.2. Rota-rod

2 weeks after the MWM test, the animals (same groups as described above) were tested on an accelerating rota-rod (Ugo Basile, Italy) according to an earlier protocol (Bert et al., 2002). On the first day a trial was performed consisting of three sessions of 3 min each, at a constant speed of 4 rpm, with an intertrial interval of 1 h. The following day the mice were placed on the rotating drum with an accelerating speed up to 34 rpm over 300 s. The latencies of mice to fall from the accelerating rod were measured automatically.

2.8 STATISTICAL ANALYSIS

Differences between the experimental groups (cell counts, real time PCR) were determined by two tailed unpaired student t-test with confidence intervals of 95% and

were considered significant when $p < 0.05$. All calculations were performed with GraphPad Prism version 4.00 for Windows (GraphPad Software, San Diego, CA, USA). Since the behavioral data were not normally distributed (tested using the Shapiro-Wilk-method) non-parametric tests were generally chosen. Data of the MWM were analyzed using Friedman one-way ANOVAs by ranks, followed by post-hoc Dunnett´s method (place version, each group was analyzed separately), by Mann-Whitney-rank sum-tests (to detect differences between genotypes in the place version and cued version), and by Wilcoxon-matched pairs-tests (for the spatial probe). Data of the rota-rod test, elevated plus-maze test, and free exploratory paradigm were analyzed by Mann-Whitney-rank sum-tests. All analyses were performed with SigmaPlot version 11.0 (Systat Software Inc., Chicago, IL, USA). A difference was considered statistically significant at a p-value (two-tailed) < 0.05.

3. RESULTS

3.1. ANALYSIS OF NKX2-1 POSTNATAL EXPRESSION IN THE MOUSE BRAIN

As outlined in the introduction, several studies have suggested that the expression of Nkx2-1 continues into the postnatal life of rodents. However, at least for the telencephalon, these studies have only been performed up to 3 weeks after birth. Therefore, we first investigated whether Nkx2-1 is expressed in the adult and aged mouse brains. Moreover, since a detailed characterization of subcortical Nkx2-1 expressing neurons has not yet been performed, we used immunohistochemistry and *in situ* hybridization in order to identify Nkx2-1-positive cells in the forebrain.

3.1.1. Nkx2-1 protein is localized in cell nuclei of neurons

The employment of the three different antibodies against Nkx2-1 (see Materials and Methods) resulted in corresponding labeling of cells in many regions of the postnatal (Fig. 9) and adult / aged mouse forebrain (Figs. 9-16). Closer inspection of labeled profiles revealed that, due to their size, only compartments of cells were stained (e.g. Figs. 10a; b). After embedding of selected sections in resin, semithin sections were cut and counterstained with methylene blue or toluidine blue (Fig. 10e). The intense dark brown labeling of nuclei by the DAB reaction product corresponded with the known subcellular localization of transcription factors (e.g. Nkx2-1; Fig. 10e), and no staining of cytoplasm, processes, or long fiber tracts was observed. Since the contrast between unlabeled and labeled nuclei is less pronounced after processing of the tissue for electron microscopy (e.g. Figs. 10f; g), images mainly from semithin sections were selected for presentation of labeled neurons (e.g. Figs. 10e; 13c).

Nkx2-1 labeling was always detected in the nuclei of neurons. Expression of Nkx2-1 by non-neuronal cells was established to only a very limited extent in this study. For instance, high-level expression by glial cells was observed throughout life in the subfornical organ and the ependyma of the third ventricle (Figs. 11a; b) but not at all in the white matter tracts. However, we cannot exclude the possibility that in the

telencephalon, Nkx2-1 is expressed in non-neuronal cell types, as we did not investigate this question in detail.

3.1.2. Distribution of Nkx2-1-immunoreactive cells in the early postnatal and adult mouse brain

Around birth, Nkx2-1 immunoreactivity was mainly observed in subcortical structures of the forebrain. At P2, but also in adult stages, Nkx2-1-immunoreactive profiles were rarely seen in any part of the dorsal cortical mantle (e.g. primary motor and sensory cortex), and their number seemed to be only slightly higher in its lateral parts (Fig. 9). Similarly, in the various fields of the medial limbic cortices (Figs. 9a; b) and also in the bulbus olfactorius (not shown), Nkx2-1-labeled cell nuclei were only occasionally observed at birth or later. Conversely, dense labeling of cell nuclei was found in many compartments of the basal forebrain between the most rostral part of the caudate-putamen ("striatum"), at the level of the tenia tecti, and the caudal end of the hypothalamic region (Figs. 9a-c). After the first postnatal week (not shown) the number of labeled cell nuclei in these areas was obviously lower compared to P2, but was then indistinguishable from that of adult mice (cf. Figs. 9e-k; m-s).

At a more caudal level of the early postnatal forebrain, several regions contain Nkx2-1 positive nuclei (Figs. 9). Interestingly, a very dense accumulation of labeled cells was still visible near the ventral tips of the lateral ventricles (Fig. 9f). This stripe of cells extended along the stria terminalis towards the area of the bed nucleus of the stria terminalis (Figs. 9b; f), finally reaching the hypothalamus (Fig. 9b). Within the diencephalon, intense labeling for Nkx2-1 was observed in several nuclei of the hypothalamic region (Figs. 9c; j; r; k; s) as well as in the ependyma lining the third ventricle (Figs. 9c; j; k). Despite a clear reduction, a remarkable number of immunoreactive cells remained detectable at adult stages within these neuronal assemblies and in the caudal parts of the striatum (cf. Figs. 9g; o). In contrast to most of the meso- and neocortical fields, the allocortical hippocampal formation and parts of the subcortical amygdaloid complex always contained higher numbers of labeled cell profiles (cf. Figs. 9c; i; q)

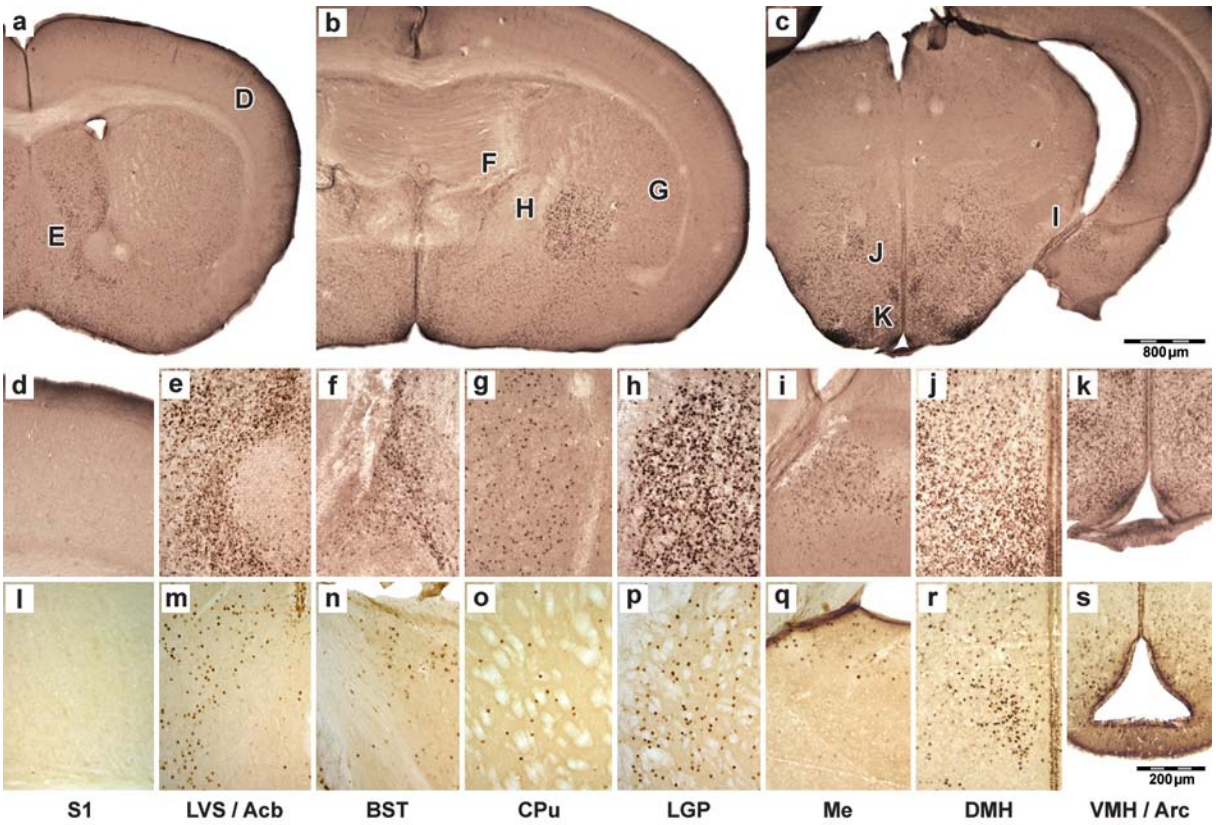

Figure 9. Distribution of Nkx2-1-immunreactive cells in the early postnatal and young adult mouse brain.

Coronal sections at the level of the medial septum (a), globus pallidus (b), hypothalamus (c). Nkx2-1 IHC for an early postnatal (P2; a-k) and adult (1 month; l-s) mouse brain is shown. No labeling was found in the sensory cortex (S1).

Most intense staining for Nkx2-1 was detected in the ventral tips of the subventricular zone lining the lateral ventricles / nucleus accumbens, (LVS / Acb; e), the nuclei of the septal complex (a), all parts of the striatum (CPu, b; g; LGP,h; p), the bed nucleus of the stria terminalis (BST, f; n).

At more caudal level, Nkx2-1 immunolabeling was found in the substantia innominata, the preoptic area, the medial amygdala (Me; I; q), and various hypothalamic nuclei (DMH, dorsomedial and VMH ventromedial hypothalamic nuclei; arcuate nucleus Arc).

The pattern of Nkx2-1-immunoreactive cells described here for the early postnatal mouse forebrain was partially maintained into adulthood and was then indistinguishable from that of aged mice (Fig. 16). Thus, our investigation of the adult mouse brain focused on Nkx2-1 expression in specific regions such as the basal ganglia and the

septal complex (see also Table in appendix for a complete list of the regions where Nkx2-1 immunoreactivity has been found).

3.1.3. Nkx2-1-immunoreactive neurons in the hypothalamic area of adult mice

Several reports have provided evidence for a robust postnatal expression of Nkx2-1 in certain regions of the rodent hypothalamus (see introduction). Never described before, the most intense darkening of the tissue following IHC for Nkx2-1 was regularly observed at the level of the mammillary complex and the neighboring hypothalamic nuclei (Figs. 10a; 11). To allow comparisons of Nkx2-1 labeled cells with those of other structures of the brain this observation was included in the present study.

In all animals analyzed between P0 and 6 months of age, a very strong labeling of cell nuclei was found in the mammillary bodies (Figs. 10a; b). By means of double-IHC, part of the Nkx2-1-positive cell profiles in the medial and lateral mammillary nuclei could be identified as PV- (Fig. 10c) or CB-containing (Fig. 10d) neurons. Analysis of Nkx2-1 immunolabeling in semithin sections (Fig. 10e) or in ultrathin sections (Figs. 10f; g) revealed that most of the neurons in this area express the transcription factor. All cell profiles show fine-structural characteristics of mature neurons and bear somatic input synapses (Figs. 10g; h; see also: Allen and Hopkins, 1988). No morphological differences could be detected between unlabeled (Fig. 10f) and Nkx2-1-positive neurons (Fig. 10g).

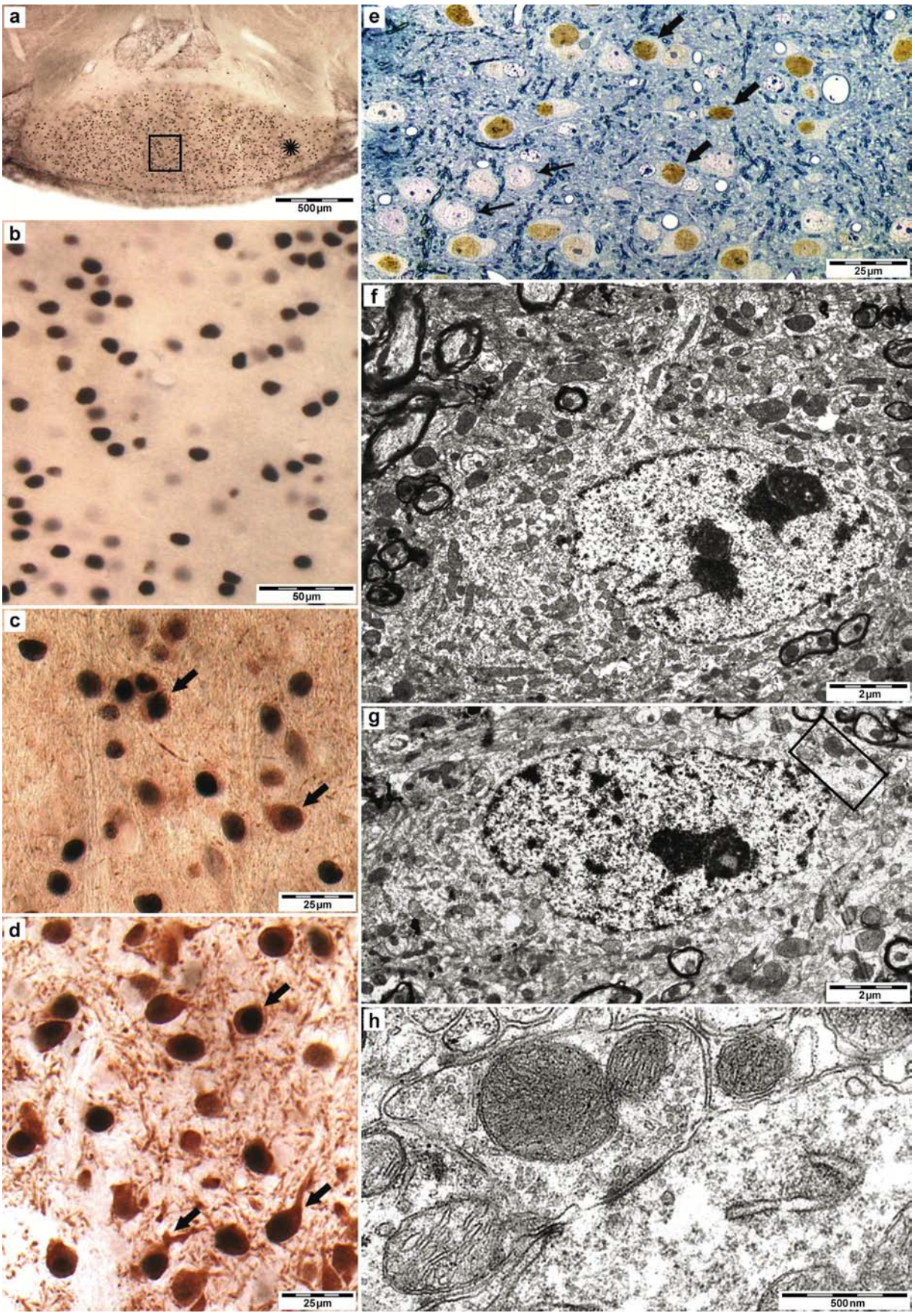

Figure 10. Nkx2-1 expression in the mammillary bodies of adult mice.

Coronal section showing staining for Nkx2-1 in the mammillary region (a); boxed area in "a" is shown at higher magnification in "b". Nkx2-1-positive cells were double-labeled for PV (c, arrows), and CB (d, arrows). Light brown labeling of the cytoplasm (neuronal markers) surrounds the dark brown staining of the nucleus (Nkx2-1).
Fine structural analysis was performed on the region marked by the asterisk in "a" (e-h); semithin section showing Nkx2-1 labeled (thick arrows) and unlabeled (thin arrows) neurons (e); electron microscopy for unlabeled (f) and Nkx2-1 labeled (g) neurons; synaptic contact (h).

Many other hypothalamic nuclei surrounding the third ventricle also express Nkx2-1 at a very high level. To further characterize these neurons we combined ISH for *GAD67* mRNA with subsequent IHC for Nkx2-1. As shown for the premammillary nuclei and the arcuate nucleus (Fig. 11; see also Yee et al., 2009) labeling for *GAD67* only partially overlaps with that of Nkx2-1. In addition, the ependyma of the third ventricle was always found to be immunoreactive for Nkx2-1 (Figs. 9c; j; r; 11a; b).

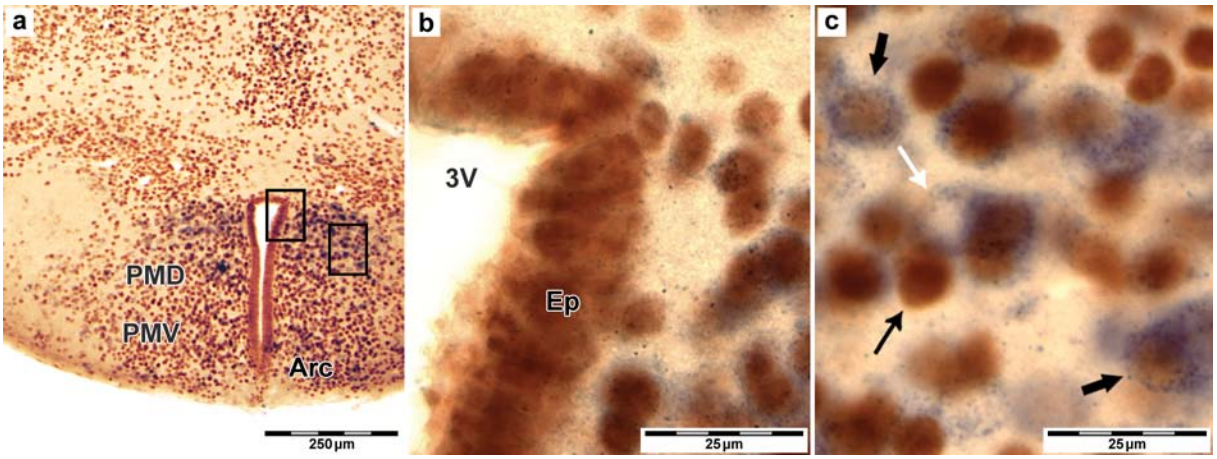

Figure 11. Nkx2-1 expression in the various nuclei of the hypothalamic region.
ISH for GAD67 combined with IHC for Nkx2-1 (a-c); left boxed area in "a" is shown at higher magnification (b; 3V, third ventricle; Ep, ependyma;); right boxed area in "a" is shown at higher magnification (c), double-labeled (thick black arrows), Nkx2-1 single-labeled (thin black arrow) and GAD67 single-labeled (white arrow) neurons.
Note that only a few Nkx2-1 positive nuclei were co-labeled with GAD67 in the ventral (PMV) and dorsal (PMD) parts of the premammillary nuclei (c) and in the arcuate nucleus.

3.1.4. Nkx2-1-positive cells in the ventral tips of the lateral ventricles

As outlined before, cells of the ventral tips of the lateral ventricles were always intensely labeled for Nkx2-1 and the extent of immunostaining was developmentally regulated. At P0 almost all the cells populating this region seem to be immunoreactive for the transcription factor. However, already at P10 the number of Nkx2-1-positive cells was strongly reduced (Fig. 12). Fine structural analysis of this region revealed that these cells show characteristics of progenitors. Obviously, distinct parts of the forebrain such as the SVZ of the lateral ventricles may continuously give rise to Nkx2-1-immunoreactive cells (Fig. 12b). In fact, the SVZ lining the lateral ventricles is described as one of the few constitutive neurogenic areas in the adult brain.

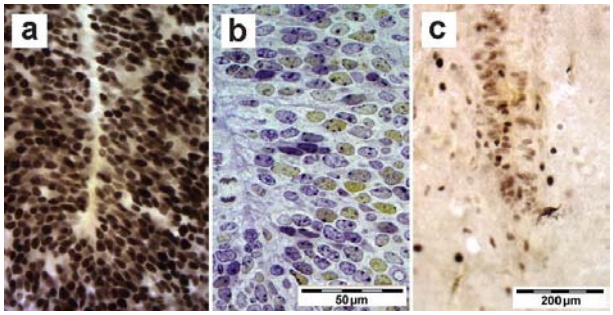

Figure 12. Nkx2-1 expression in the ventral tips of the lateral ventricles.
Coronal section of the lateral ventricles at P0 (a) and P10 (c); semithin section showing fine-structural characteristics of Nkx2-1 labeled cells (b; yellow nuclei). At P0 a large number of cells in the epithelium lining the lateral ventricles is strongly immunoreactive for Nkx2-1, but the amount of positive profiles is strongly reduced at P10.

3.1.5. Nkx2-1-immunoreactive neurons in the caudate-putamen and globus pallidus of adult mice

Nkx2-1 expression and function have not yet been studied in the ventral telencephalon of adult and aged rodent brain. With respect to motor disturbances, a detailed analysis of Nkx2-1 expression in the basal ganglia, controlling voluntary movement and posture, is therefore required.
The striatum, formed by the caudate nucleus and the putamen (CPu), is one of the largest components of the telencephalon. As already shown after birth (Fig. 9), but also

for adult (Figs. 9; 13) and aged animals (Fig. 10), many Nkx2-1-immunoreactive cells are detectable throughout the parenchyma. The cell nuclei are homogeneously distributed throughout the CPu and have a diameter of about 10 µm (Figs. 13b; d-f). In adult mice, many Nkx2-1-labeled cells could be identified as PV-immunoreactive neurons (insert in Fig. 13c) whereas co-labeling with antibodies against CB (Fig. 13d), CR (Fig. 13e), or SOM (not shown) was rarely observed. Interestingly, by using antibodies against ChAT a large number of Nkx2-1-positive profiles in the striatum could be identified as cholinergic neurons (Fig. 13f). SOM-expressing neurons have been reported to derive from the MGE (Marin et al., 2000). However, in this study only a very small number of striatal cells could be double-labeled for Nkx2-1 and SOM, and these cells were mainly observed in ventral parts of the striatum.

We analyzed part of the double-labeled neurons by means of fine-structural techniques. This method makes it possible to clearly distinguish between neurons expressing both Nkx2-1 and PV (or ChAT), those expressing only one or the other, and unlabeled neurons in semithin sections (Fig. 13c).

The second large component of the basal ganglia is formed by the lateral globus pallidus located medial to the CPu next to the internal capsule. At all ages analyzed, this structure was easily detectable due to the very high density of Nkx2-1-labeled profiles (Figs. 9; 16). Additional IHC for PV revealed that most, if not all, of the Nkx2-1-immunoreactive cells co-express this protein. Similar to the striatum, double-labeling experiments for Nkx2-1 and CR or CB were less successful, and only very few CB-stained neurons were found to be immunoreactive for Nkx2-1 too (not shown).

Taken together, Nkx2-1-labeled cells are widely distributed in the CPu and in the LGP of postnatal mice. In the adult (Fig. 13) and aged (Figs. 16b; c) mouse brain the majority of them could be identified as either GABAergic, mostly PV-positive, or cholinergic neurons (Fig. 13). The remaining neurons obviously belong to a very small group of GABAergic neurons that co-express CB, CR, SOM or other peptides / proteins. No labeling for Nkx2-1 was detected in non-neuronal cells during examination of basal ganglia sections at ultrastuctural level.

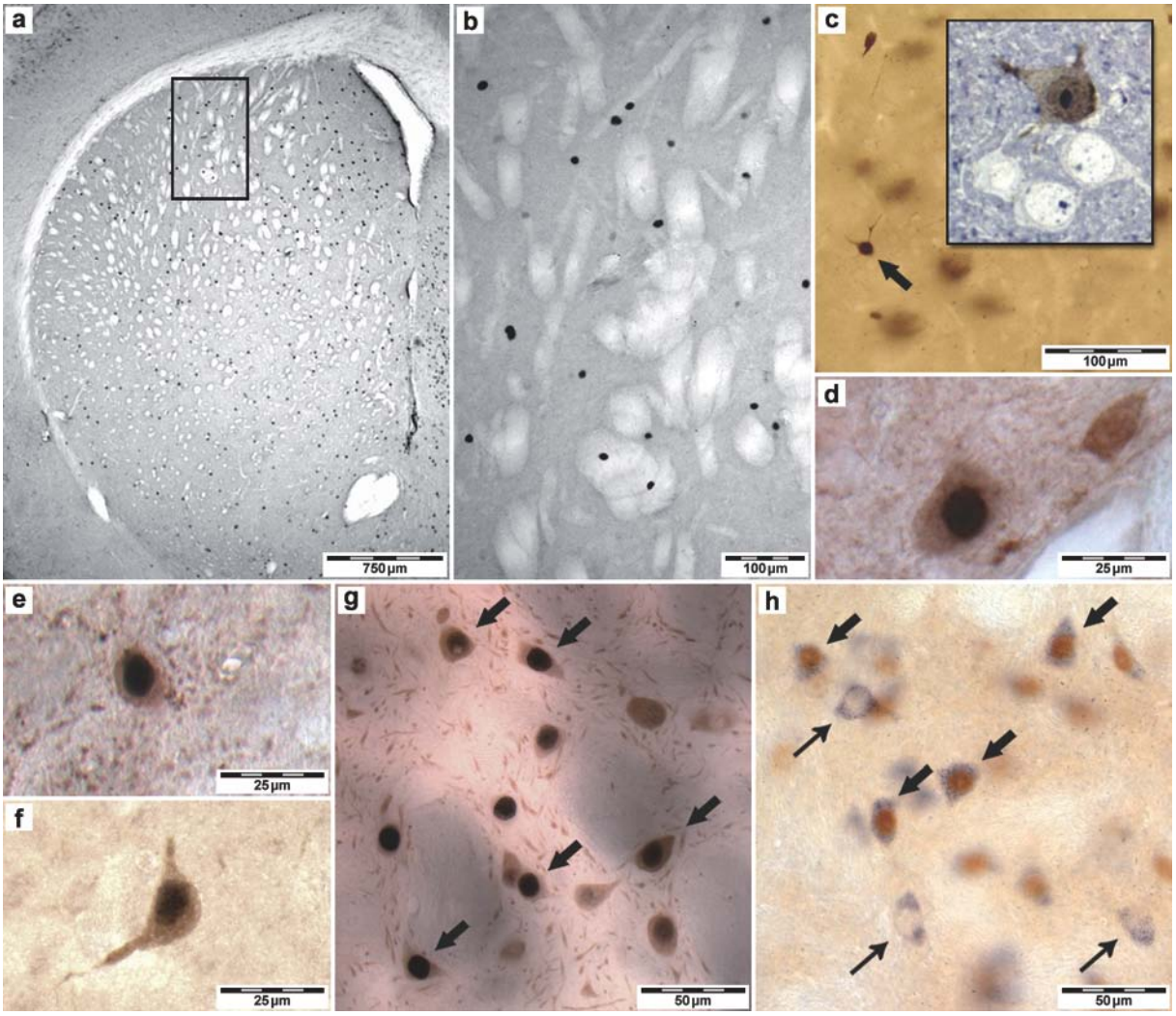

Figure 13. Neuronal expression of Nkx2-1 in the adult basal ganglia.
IHC for Nkx2-1 in the caudate-putamen (a-f); boxed area in "a" is shown at higher magnification in "b"; neuron double-labeled for Nkx2-1 and PV (c, thick arrow) analyzed at fine-structural level (c, inset); neurons double-labeled for Nkx2-1 and CB (d), CR (e) or ChAT (f).
IHC for Nkx2-1 in the lateral globus pallidus (g; h); neurons stained for Nkx2-1 and PV (g, thick arrows); neurons stained for Nkx2-1 and GAD67 mRNA (h, thick arrows); neurons single-labeled for GAD67 mRNA (thin arrows). Note that most, but not all GABAergic neurons express Nkx2-1.

3.1.6. Nkx2-1-immunoreactive neurons in the septal complex of adult mice

The septum is interposed among the cortical regions including the hippocampal formation dorsally, the lateral ventricle and nucleus accumbens laterally, and the preoptic region ventro-caudally. The septal complex belongs to those neuronal

assemblies that also contain high numbers of Nkx2-1-immunoreactive cells, not only during early postnatal development (Figs. 9), but also after maturation of the brain (Fig. 14; cf. Fig. 9). Even in adult and aged animals, intense labeling for Nkx2-1 was detectable in the intermediate part of the lateral septum (Figs. 9; 14; 16), in the medial septum and in the vertical and horizontal limbs of the diagonal band (Fig. 14). The number of labeled cell nuclei seemed to be lower in the most dorsal parts of the lateral septum and in neighboring areas including the nucleus accumbens (Fig. 14a) and more caudally, in the various subdivisions of the bed nucleus of the stria terminalis and the substantia innominata (Fig. 9n).

GABAergic neurons represent the dominant cell type in the septal complex (Figs. 14g; h), but cholinergic neurons also contribute substantially to the total number of neurons. According to their embryonic origin in the commissural preoptic area, which is one of the Nkx2-1-proliferative domains, a large number of Nkx2-1 immunolabeled profiles in the MSvDB of young adult and aged mice could be identified as cholinergic neurons after subsequent immunolabeling for $p75^{NTR}$ (Fig. 14b) or ChAT (Fig. 14e). Characterization of GABAergic neurons in the MSDB led to similar results as obtained for the basal ganglia. Most of the Nkx2-1-positive nuclei could be localized in neurons co-expressing PV (Fig. 14c). In addition, Nkx2-1-immunoreactive neurons co-expressing CB were rarely observed (Fig. 14d). Analysis of double-labeled cells in semithin or ultrathin preparations revealed that both cholinergic (Fig. 14e) and PV-containing GABAergic septal neurons (data not shown) showed all the characteristics of mature neurons (cf. Naumann et al., 1992a). Nkx2-1 immunoreactivity was never observed in non-neuronal cells of the adult septal complex.

Detection of GABAergic neurons in the lateral septum with antibodies against GABA or GAD67/65 is accompanied by some well-known difficulties (cf. Mugnaini, 1985; Kohler and Chan-Palay, 1983). Additionally, the expression level of calcium-binding proteins (e.g. PV) in this nucleus is much lower compared to that of the MSDB-complex or the cortical mantle. For this reason, we first analyzed solely Nkx2-1 labeled profiles using fine-structural methods. In all parts of the lateral septal nucleus DAB-precipitates could be localized within mature neurons (Fig. 14). Similar results were obtained for the neighboring nucleus accumbens (data not shown).

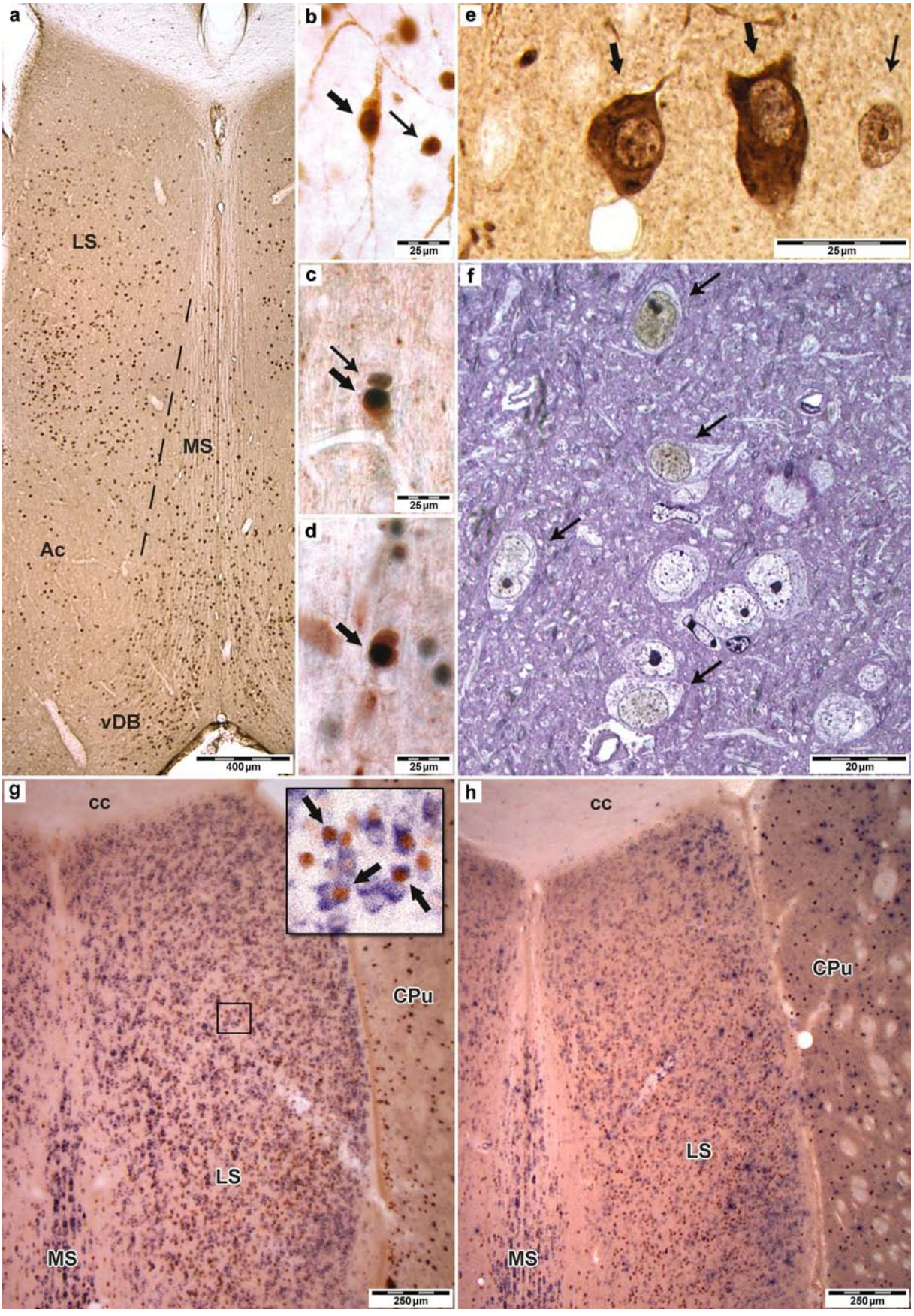

Figure 14. Nkx2-1 expressing neurons in the septal complex of adult mice.

ICH for Nkx2-1 in the septal complex including LS, lateral septum; MS, medial septum; Ac, nucleus accumbens; vDB, ventral limb of the diagonal band (a-e).
Neurons double-labeled (thick arrows) or single-labeled (thin arrows) for Nkx2-1 and p75NTR (b; e), PV (c), or CB (d a)are shown. Double-labeled cells display all characteristics of mature neurons.
Lateral septum (f-h); semithin sections showing Nkx2-1-immunoreactive neurons (f, arrows); ISH for GAD67 combined with IHC for Nkx2-1 at P11 (g, inset at higher magnification showing double-labeled neurons, arrows) and P35 (h); cc, corpus callosum.

To further characterize these Nkx2-1-immunoreactive neurons, we combined ISH for *GAD67* (a more appropriate method for labeling of GABAergic neurons in the LS) with IHC for Nkx2-1. In line with previous studies, the developing septal nuclei consist of densely packed GABAergic neurons (Fig. 14g) and the staining intensity for *GAD67* mRNA was found to be regulated during development (cf. Bender et al., 1996). Early postnatal GABAergic septal neurons show a very strong expression of *GAD67*, which is followed by a partial downregulation during maturation (cf. Figs. 14g; h). Accordingly, the ratio of lateral septal neurons expressing both *GAD67* and Nkx2-1 was found to be much higher in early postnatal mice (see inset in Fig. 14g) than in older animals. Subsequent staining for Nkx2-1 and various neuronal markers (e.g. CB and CR) only occasionally resulted in double-labeling of neurons.

3.1.7. Nkx2-1-immunoreactive neurons in cortical fields of adult mice

Nkx2-1-immunoreactive profiles were rarely observed in the various neocortical fields of early postnatal mice (Figs. 9). Accordingly, in frontal or parietal (Fig. 15) parts of the neocortex, as well as in mesolimbic fields such as the insular cortex and the retrosubicular region (not shown) of adult mice, we only occasionally found Nkx2-1-positive cells. However, their number appeared slightly higher in more ventral parts of the cortex including the perirhinal and piriform cortices and the olfactory tubercle (Fig. 15b). On the other hand, intense staining for Nkx2-1 was found within distinct subnuclei of the amygdala, a complex closely related to the cortex. Nkx2-1-immunolabeled cells formed a dense cluster at the level of the medial amygdala (Figs. 9; 15; cf. Xu et al., 2008). In our experiments, Nkx2-1-labeled cells in the medial amygdala could not be identified as cholinergic or GABAergic neurons.

In the allocortical dentate gyrus and hippocampus proper, many Nkx2-1-positive cells were detectable throughout life (Fig. 15d). Combined ISH for *GAD67* with IHC for Nkx2-1 revealed that most if not all of these cells belong to the GABAergic population (Fig. 15e). However, no strong overlap with calcium-binding protein staining was found.

In summary, Nkx2-1 is poorly expressed in the cortical mantle of the postnatal mouse. Only the hippocampal formation and certain nuclei of the amygdaloid complex contained higher numbers of Nkx2-1-immunoreactive cells, which are mostly GABAergic neurons.

The olfactory bulb, also belonging to the cortical structures, is one of the few brain regions that continuously receives newly generated cells throughout life. The progenitor cells reside in the subventricular zone lining the lateral ventricles and migrate via the rostral migratory stream to the bulb (Doetsch and Alvarez-Buylla, 1996). The Nkx2-1-positive cell-lineage of the ventral tips of the lateral ventricles (see above) have been described to contribute only in minor part to the cells of the olfactory bulb (Young et al., 2007), however, we detected Nkx2-1 positive-cells in the rostral migratory stream at all rostrocaudal levels and stages analyzed (not shown). Notably, only occasionally were these cells immunoreactive for Nkx2-1 at their final position (see above).

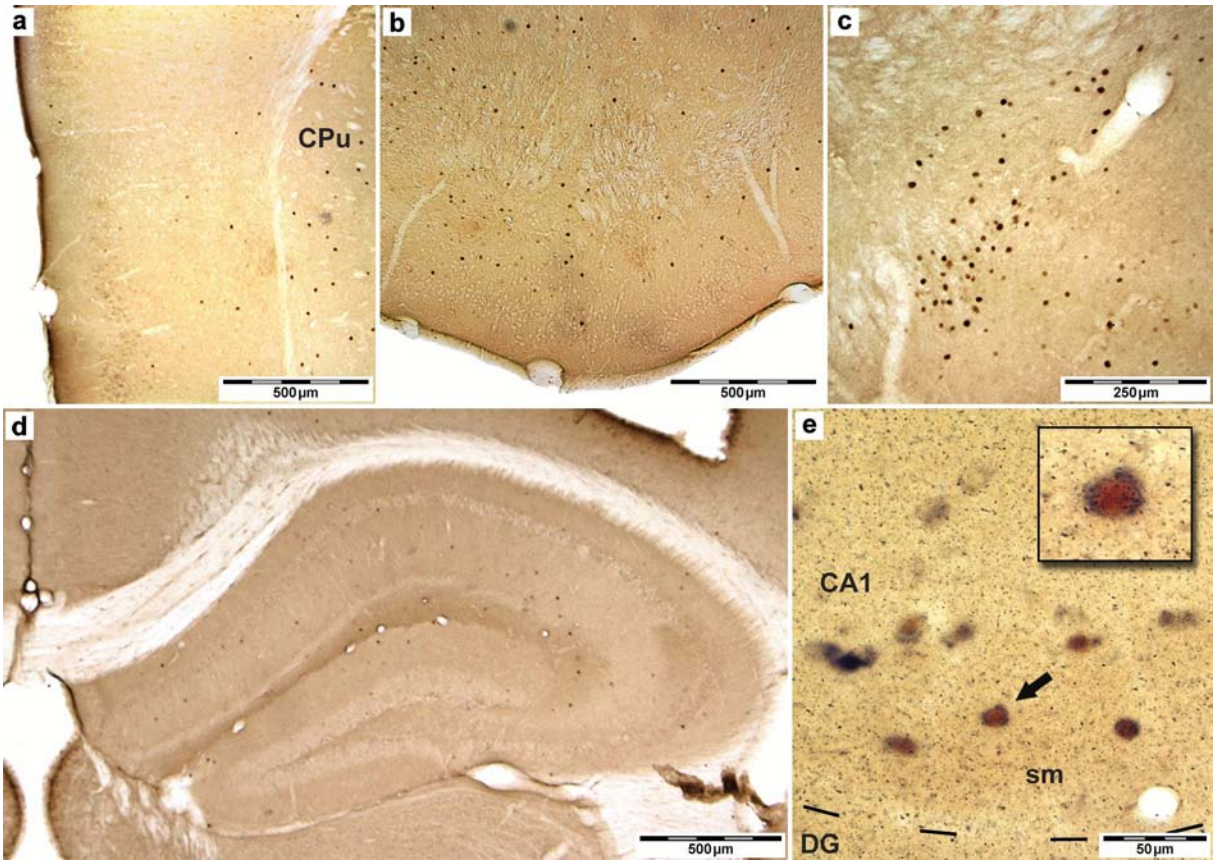

Figure 15. Neuronal expression of Nkx2-1 in the cortical / subcortical regions of the adult mouse brain.
IHC for Nkx2-1 in the parietal (a) and ventral cortices (b); the medial amygdala (c) and the hippocampal formation (d). Nkx2-1 positive nuclei were occasionally found in the neocortex, whereas a higher concentration was detected in allocortical structures.
ISH for GAD67 combined with IHC for Nkx2.1 at the level of the CA1 (e, double-labeled neuron marked by a thick arrow); Nkx2-1 and GAD67 co-labeled cells were *mainly located in the stratum moleculare (sm) and stratum oriens, sometimes in close proximity to the dentate gyrus (DG).*

3.1.8. Expression of Nkx2-1 in several regions of the aged mouse brain

In adult mice, Nkx2-1 immunolabeled neurons could be detected throughout the basal forebrain. Despite an obvious reduction of Nkx2-1-expressing neurons within the first two weeks after birth, a remarkable number of mature neurons is still strongly immunoreactive for Nkx2-1 at 6 months (Fig. 16), and until at least 1 year of age (not shown). As already shown for younger animals, these cells were mainly located in the basal ganglia (Figs. 16b; c), in the septal complex (Fig. 16a), and in the hypothalamus (Fig. 11). By means of double-labeling experiments for Nkx2-1 and PV or ChAT these cells could again be identified as cholinergic and PV-expressing GABAergic neurons.

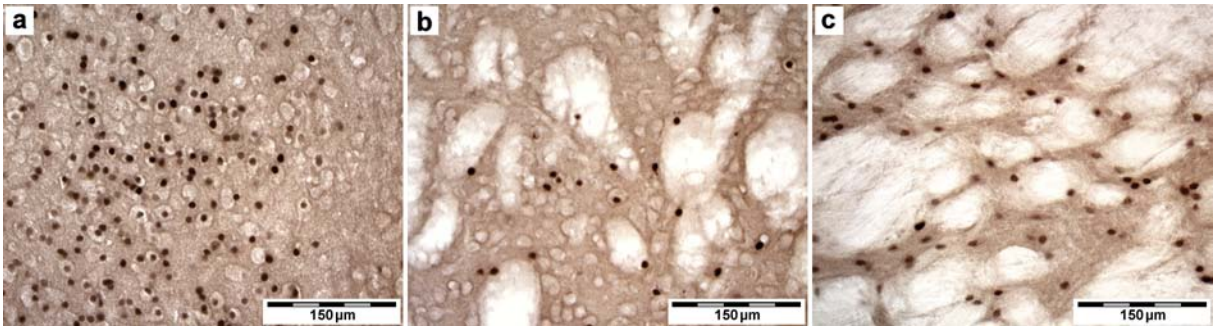

Figure 16. Nkx2-1 immunoreactive cells in several region of the aged mouse brain.
Sections of a 6 month old brain at the level of the lateral septum (a), the caudate-putamen (b), and the lateral globus pallidus (c). Note that labeled nuclei are still strongly immunoreactive for Nkx2-1 at 6 months of age.

3.1.9. Distribution and regulation of Nkx2-1 mRNA in the adult mouse brain

The staining pattern observed after IHC could simply reflect storage of the protein or, alternatively, mature neurons could constantly synthesize *Nkx2-1*. To assess which of these possibilities occurs, non-radioactive *in situ* hybridization for *Nkx2-1* was performed on coronal sections of an adult mouse brain. Staining for *Nkx2-1* mRNA resulted in distinct violet labeling of citoplasms. No staining of dendrites and axons was observed and no labeling was detected when the sense probe was used.

Not analyzed in detail but shown here for comparison, several compartments of the hypothalamic region displayed a very dense accumulation of *Nkx2-1* mRNA-expressing cells at all ages after birth. For instance, in the arcuate nucleus, in parts of the preoptic area and in many nuclei of the mammillary complex (Fig. 10e), the staining intensity for *Nkx2-1* mRNA was found to be much higher when compared with that of the various telencephalic structures (Figs. 10a-d).

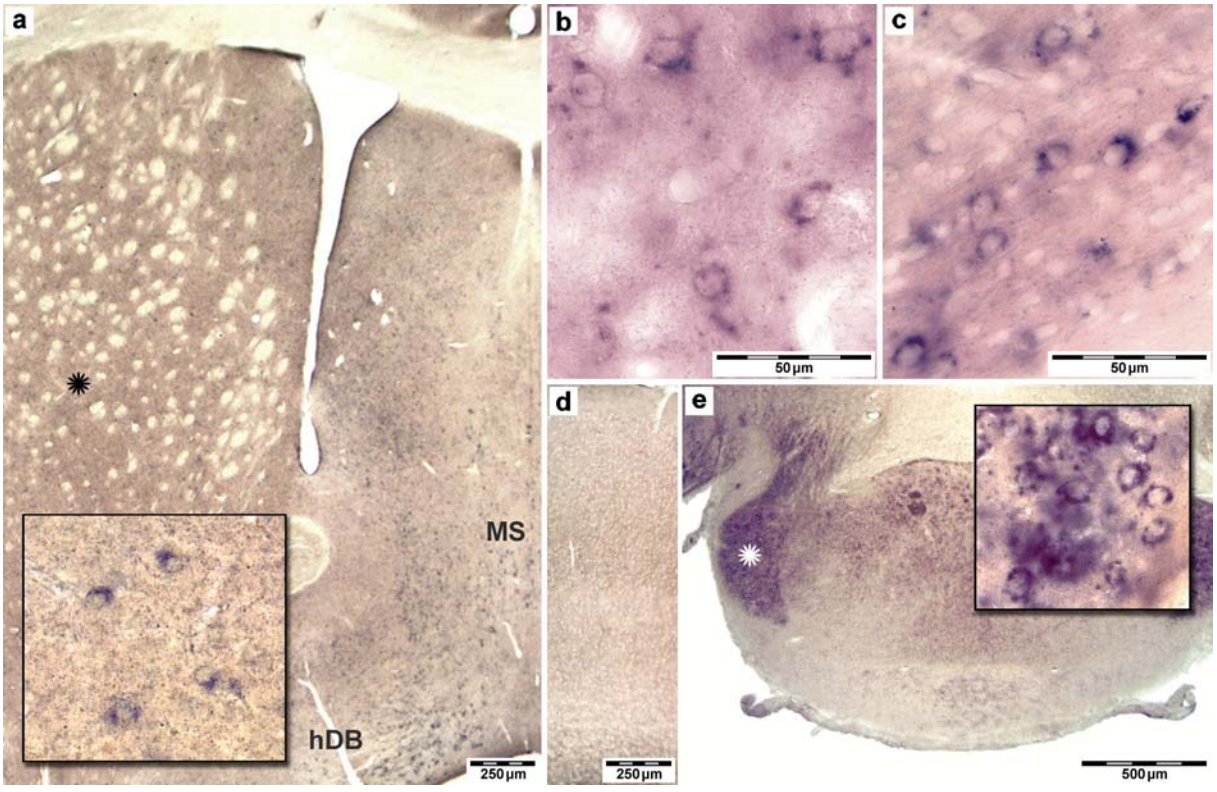

Figure 17. Nkx2-1 mRNA expression by ventral forebrain neurons of adult mice.

ISH for Nkx2-1 in the caudate putamen (a; inset: higher magnification from the area marked witha black asterisk), the MS (a), the LGP (b), the hDB (a; c), the cortex (d), and the mammillary bodies (e; inset: higher magnification from the area marked with a white asterisk).
Note that the most intense staining was found in the mammillary bodies (e) and in the hDB (c), reflecting the result obtained for Nkx2-1 IHC.

Indeed, in the striatum and the lateral globus pallidus ISH resulted in much weaker staining of individual cells compared to the mammillary complex (Fig. 17), and the complete staining pattern was only obtained after rather long incubation times. The number of labeled cells in these regions and their distribution seem to be comparable to those obtained after IHC for Nkx2-1 (cf. Figs. 11b; 17a). As for basal ganglia neurons, the distribution of the *Nkx2-1*-expressing septal cells corresponds to that of the Nkx2-1-immunoreactive neurons in this region. Nkx2-1 immunolabeled cells were rarely observed in the cortical mantle of postnatal mice. Accordingly, virtually no *Nkx2-1*-positive profiles could be detected in the various paleo- and neocortical fields (Fig. 17d). However, in the allocortical hippocampal formation, *Nkx2-1*-labeled cells were found at all developmental ages. The distribution of these cells resembled that of the *GAD67*-positive neurons and no labeling of granule cells and pyramids was observed.

Finally, we investigated whether changes in the extent of Nkx2-1 labeling over time, as revealed by IHC, are accompanied by regulation of the transcription factor at the mRNA level. We analyzed *Nkx2-1* mRNA expression at four different postnatal ages by means of real-time PCR. A large variability of *Nkx2-1* transcripts was observed at P0. In line with the observations obtained for the immunolabeling, a significant downregulation of *Nkx2-1* was detected between P0 and P8. Subsequently, no significant differences were found for mRNA levels at the other postnatal ages (Fig. 18).

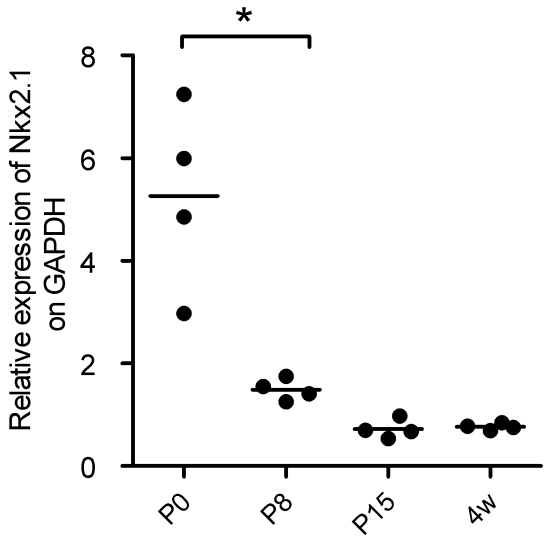

Figure 18. Quantitative real time PCR for Nkx2-1 in postnatal mouse brains.
*Value of each individual brain is shown as a dot, and the mean value as a bar; n = 4 each group; *p < 0.001.*

3.2. ABLATION OF *NKX2-1* IN THE MOUSE FOREBRAIN

3.2.1. General remarks

The neurological symptoms observed for NKX2-1-haploinsufficient patients could be caused by both the prenatal and the postnatal lack of the transcription factor. For the present study, we have therefore generated two conditional knockout lines in order to inactivate Nkx2-1 during embryogenesis or postnatally. Nkx2-1 becomes detectable during early embryonic development (around E9) in the neuroepithelium of ventro-medial parts of the telencephalic vesicle, which subsequently differentiate into the medial ganglionic eminence and the preoptic area (Sussel et al., 1999; Puelles et al., 2000). Notably, transcripts for *GAD67* have also been found as early as E10 as well as shortly thereafter, in differentiation zones of these regions (Katarova et al., 2000). Therefore, GAD67cre-driven ablation of Nkx2-1 occurs already at early embryonic stages in differentiating neurons. In contrast, ChAT-synthesis reaches mature levels around P15 in rodents (cf. Bender et al., 1996; Korsching, 1993). Thus, Cre-

recombinase expression under the control of the GAD67 and ChAT (ChAT) promoter ensured *Nkx2-1* ablation during embryonic and postnatal development, respectively.

To investigate the expression pattern of Cre-recombinase the cre-lines were bred with *ROSA26-floxed* reporter mice and the offspring were analyzed for β-galactosidase expression. Immunolabeling for β-galactosidase in the forebrain of *GAD67cre/ROSA* mice at embryonic stages was already described in the doctoral dissertation of A. Vogt (Heidelberg). Briefly, X-Gal staining experiments showed reporter expression in the olfactory bulb, the neocortex, the hippocampus, in developing caudate-putamen and the immature ventral forebrain regions, resembling the staining pattern expected for GAD67 (cf. Katarova et al., 2000).

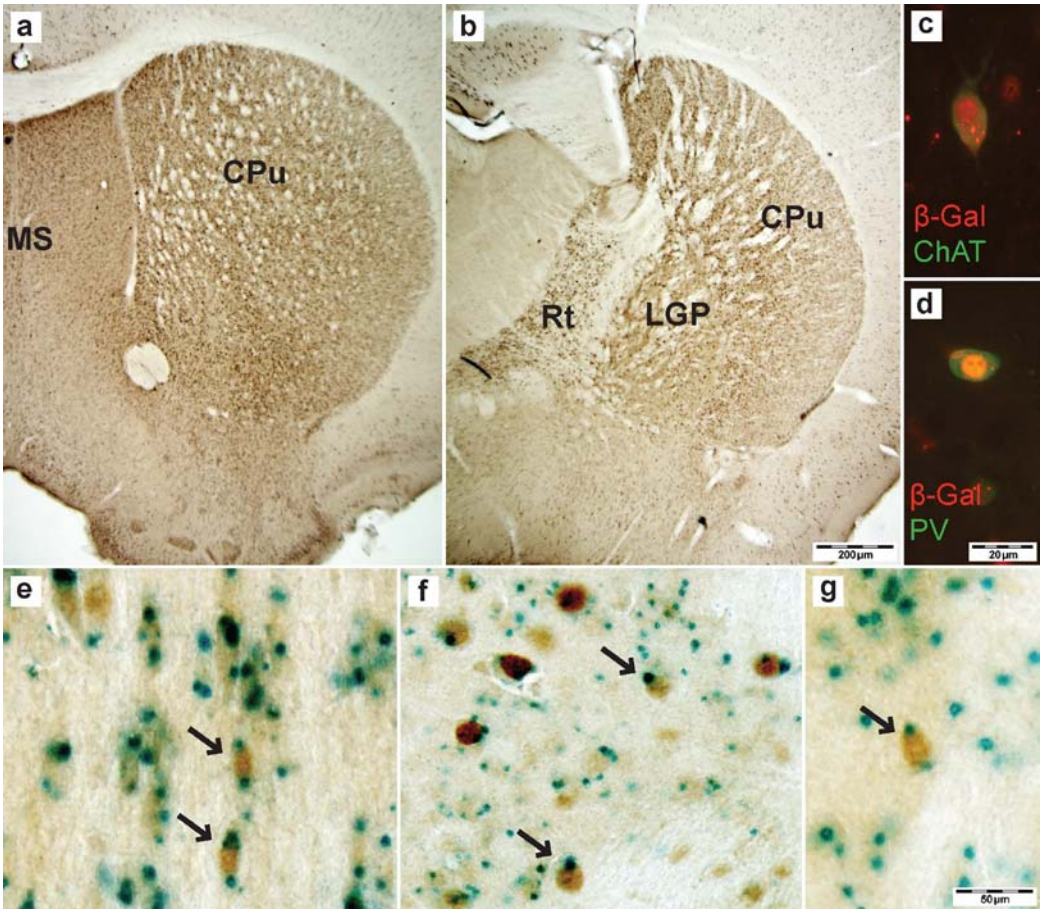

Figure 19. Expression of β-galactosidase in the adult GAD67cre/ROSA mice.
IHC for β-galactosidase at the level of the septal complex (a) and the basal ganglia (b). Note intense staining for β-Gal in the CPu, septal compex, LGP and reticular thalamic nucleus (Rt). Double immunofluorescence for β-galactosidase and ChAT (c, overlay) or PV (d, overlay).

X-Gal staining combined with IHC for Nkx2-1 in the MS (e), the CPu (f) and the LGP (g). X-Gal blue precipitate was detected in proximity of Nkx2-1-positive nuclei and is marked by arrows.

In the adult, brain β-galactosidase was found in the regions mentioned above including the septal complex and the lateral globus pallidus (Figs. 19a; b). Double immunofluorescence for β-galactosidase and ChAT (Fig. 19c) or PV (Fig. 19d) revealed that Cre-expression occurs efficiently in these neuronal populations. In addition, X-Gal staining was combined with IHC for Nkx2-1 to confirm that Cre-recombination takes place in Nkx2-1-expressing neurons. The punctuate staining due to β-galactosidase activity could be found in proximity of the Nkx2-1-positive nuclei in the various regions analyzed (Figs. 19e-g).

The expression pattern of β-galactosidase in the forebrain of *ChATcre/ROSA* mice was characterized by The Jackson Laboratories (Bar Harbor, ME, USA). β-galactosidase expression was reported in all cholinergic neurons of the ventral forebrain. By using a different indicator strains, Cre expression was detected in the striatum and in the cholinergic centers of the ventral forebrain (Madisen et al., 2009).

To characterize the general features of mutant mice we first analyzed the percentages of each genotype and the body weight. From a sample of 300 animals genotyped at weaning 27% were GADcre+/-//fl/+, 33% were GAD//fl/+, 23% were GAD//fl/fl, and 17% were GADcre+/-//fl/fl, indicating a loss of mutants during development. The sex ratio of the mutants was slightly altered, with males representing 45% of the total number. GADcre+/-//fl/fl mice that survived beyond the 3 months of age generally showed normal morphology of the organs. However, at P15 a significant reduction in the weight was already detected in comparison to the corresponding controls for both males and females (Fig. 20).

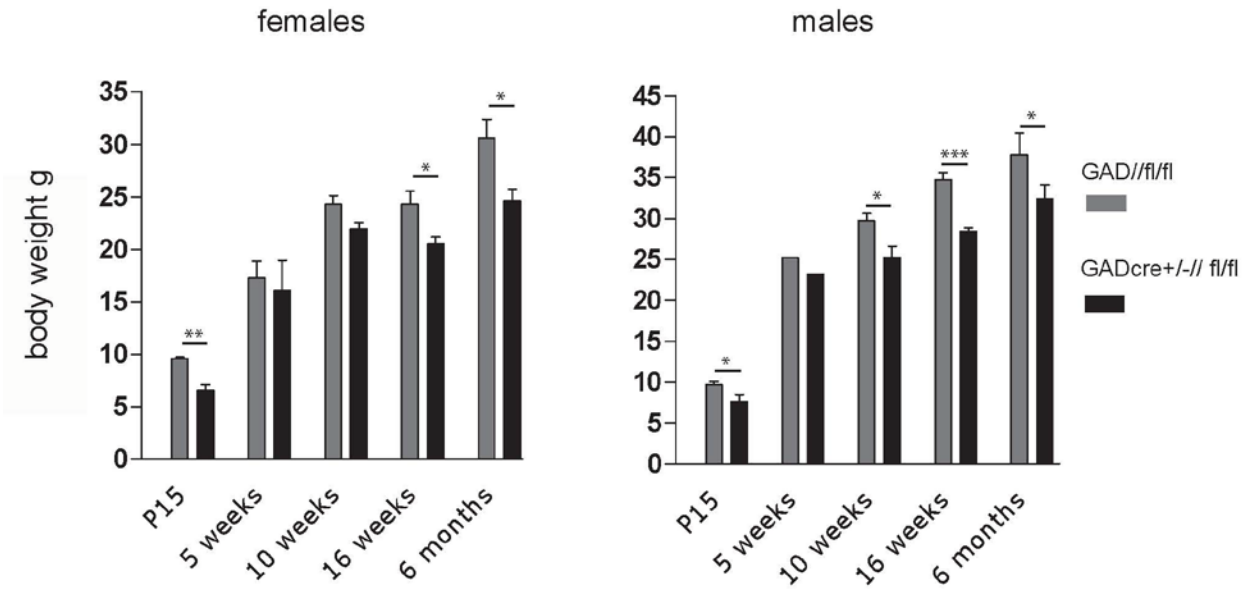

*Figure 20. Reduction in body weight of female and male mutants compared to controls. ***p < 0.0001, **p < 0.001, *p < 0.01. The histograms show mean + SEM for each age-group. Measurements were performed on at least two mice per group, although the group of 5 week old males consists of only one measure for each genotype. This datum is shown here to draw attention to the tendency of the values.*

From a sample of 400 mice genotyped at weaning, 24% were ChATcre+/-//fl/+, 28% were ChAT//fl/+, 28% were ChAT//fl/fl and 20% were ChATcre+/-//fl/fl mutant mice. No differences were found in the ratio between male and female mutants. In addition, weight was similar for all the genotypes at corresponding ages.

3.2.2. Nkx2-1-ablation leads to loss of ChAT- and PV-immunoreactive neurons in the basal forebrain

The efficiency of the two genetic manipulations was monitored by means of IHC and ISH. Conditional prenatal *Nkx2-1*-ablation in GAD67-expressing cells resulted in an almost complete loss of Nkx2-1 protein and mRNA throughout the ventral forebrain already at early embryonic stages (E14, not shown) and at all postnatal ages analyzed (Fig. 21).

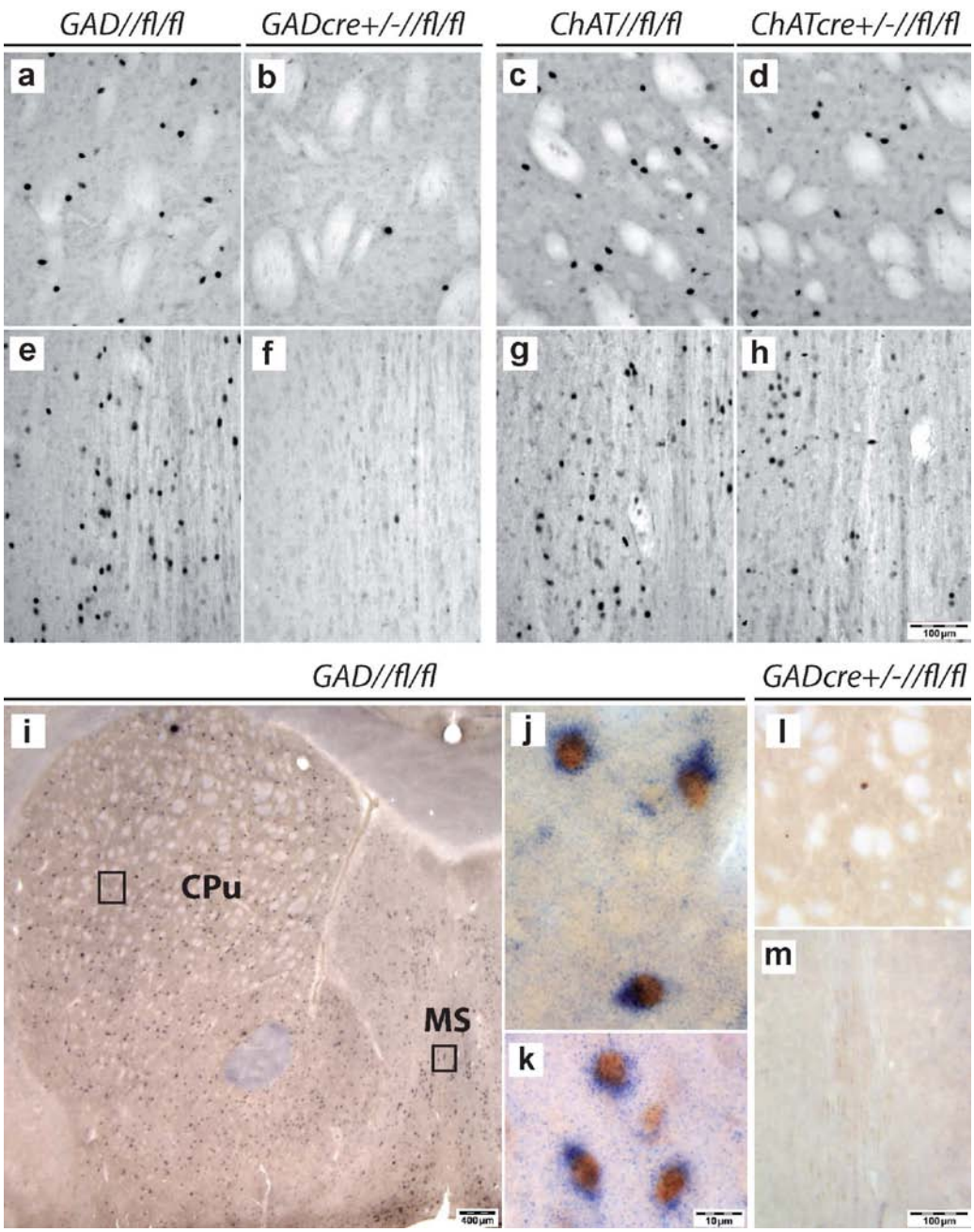

Figure 21. Loss of immunoreactive- / ISH-positive-Nkx2-1 cells in the ventral telencephalon of conditional mutants.

Nkx2-1 IHC in the MS (a-d), and CPu (e-h) of GADcre+/-//fl/fl and ChATcre+/-//fl/fl mutants and their corresponding controls. Note the almost total or partial loss of Nkx2-1 positive cells respectively in GADcre+/-//fl/fl and ChATcre+/-//fl/fl mutants.

IHC for Nkx2-1 combined with ISH for Nkx2-1 (i-m); boxed areas in "i" are shown at higher magnification in "j" (CPu), and "k" (MS), the corresponding regions are shown at lower magnification for GADcre+/-//fl/fl mice. No labeling for Nkx2-1 mRNA was detected in these regions.

To test whether Nkx2-1 loss leads to a corresponding reduction in the number of cholinergic and GABAergic neurons, we performed stereological cell counts on brain sections of 3 month old mice. The number of cholinergic and PV-positive neurons of the medial septum-ventral limb of the diagonal band complex, horizontal limb of the diagonal band-substantia innominata, caudate-putamen, and lateral globus pallidus (see Fig. 8 in Materials and methods for detailed description of the four regions investigated) was found to be dramatically reduced in mutant mice compared to controls at 3 months of age (Fig. 22; Tables 1 and 2 in Appendix) and P15 (data not shown). This was most prominent for the CPu, where an almost complete loss of neurons was observed (Figs. 22e; j). Identical results were obtained for these regions in mutants at P15, suggesting that the cells are already missing from the early stages (data not shown).

In ChATcre+/-//fl/fl mice, loss of Nkx2-1 expression was attenuated (Fig. 21d; h). In rodents, the staining pattern for cholinergic basal forebrain neurons is complete as early as P15 (cf. Bender et al., 1996). Therefore we expected Nkx2-1 mutation by the ChAT-Cre construct to occur in the cholinergic neurons not earlier than that time point. At this age the number of cholinergic neurons in the MSvBD, the HDB-SI, the CPu and the LGP of ChATcre+/-//fl/fl mice was comparable to that of adult control (ChAT//fl/fl) animals (Fig. 22k; Table 3 in Appendix). However, at 3 months of age the number of these neurons was found to be significantly reduced to about 50% in ChATcre+/-//fl/fl mice (Figs. 22k-o; Table 4 in Appendix), suggesting that the loss of neurons after Nkx2-1 mutation occurs in a progressive fashion.

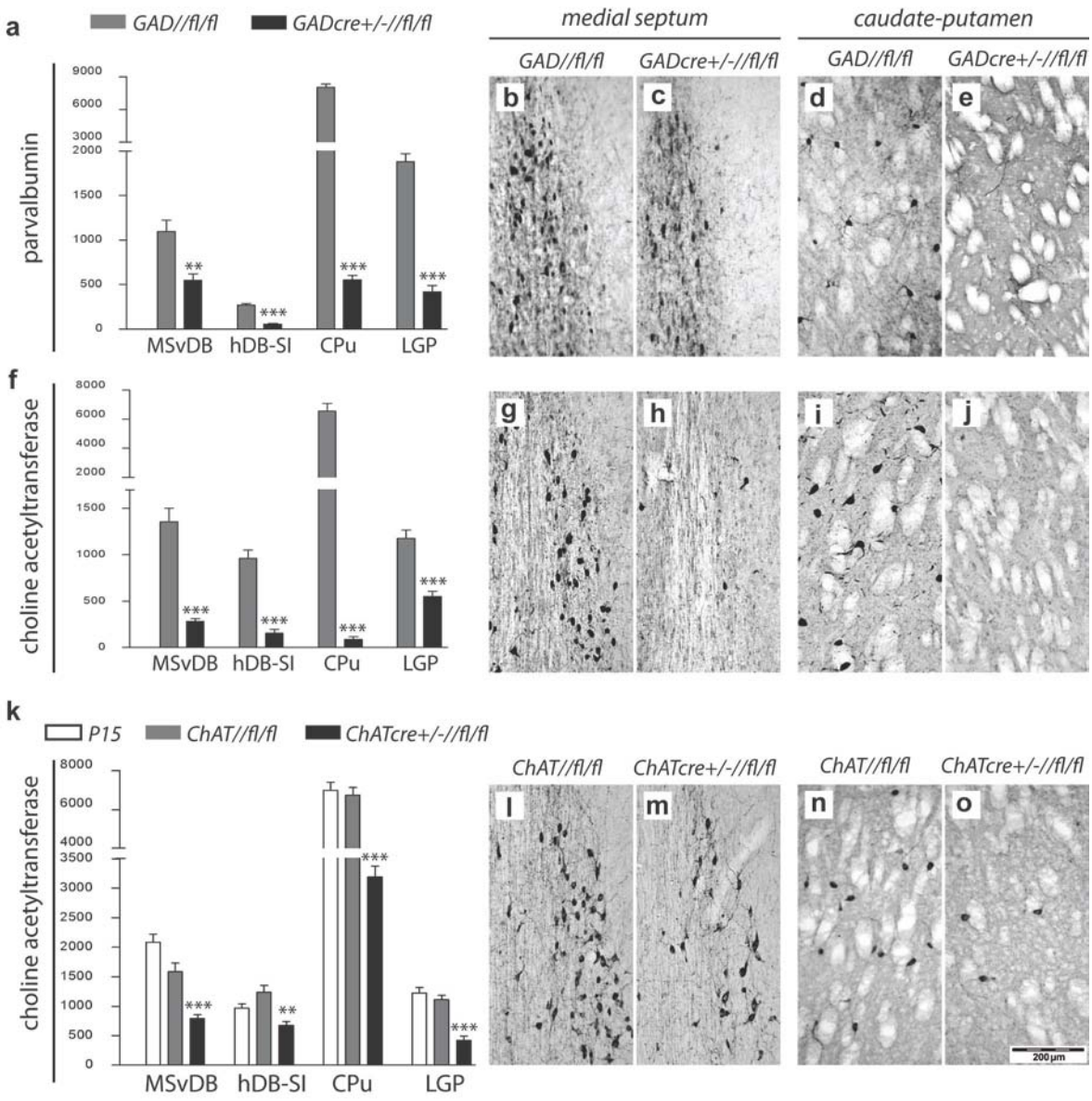

Figure 22. Reduction in the number of ChAT- and PV-immunoreactive neurons in the subcortical telencephalon of mutant mice.

*Stereological cell counts for PV- and ChAT- immunoreactive cells of GADcre+/-//fl/fl mice (a; f) and ChATcre+/-//fl/fl (k) in the four regions investigated, ***p < 0.0001; **p < 0.001. Histograms show mean + SEM.*

Representative coronal sections stained for PV (b-e) or ChAT (g-j and l-o) showing the loss of immunoreactive neurons in the MSvDB and the CPu of GADcre+/-//fl/fl and ChATcre+/-//fl/fl mice compared to the corresponding controls.

3.2.3 The loss of cholinergic neurons in the ventral forebrain is accompanied by target denervation

The cholinergic fibers from the septal complex and the other basal forebrain cholinergic centers innervate the entire neocortex and hippocampus. We therefore investigated whether the loss of cholinergic neurons is accompanied by a corresponding impairment of their axonal projections. Histochemistry for AChE at 3 months of age revealed a nearly complete absence of cholinergic fibers throughout the cortical mantle (Figs. 23a; b), including the hippocampal formation (Figs. 23e; f) in GADcre+/-//fl/fl mutants. In addition, severe alterations of the local cholinergic projections were found in the mutant CPu (Figs. 23i; j). Notably, the altered AChE staining of fibers was already observed in the mutants at 2 and 4 weeks of age (data not shown). Only in more latero-ventral parts of the cortex (e.g. the piriform cortex and the amygdaloid complex) the AChE staining pattern appeared as unchanged (data not shown).

Surprisingly, severe alterations of the AChE staining were also observed for the long cholinergic projections in the neocortex of 3 month old ChATcre+/-//fl/fl mice (Figs. 23c; d). The AChE-staining pattern was unexpectedly better preserved in the hippocampus proper (Figs. 23g; h). Finally, the fiber network of local interneuron projections is mostly maintained in the mutant CPu (not shown).

In conclusion, following prenatal mutation of Nkx2-1, extensive loss of cholinergic fibers was observed in all regions studied from P15 until adulthood. Postnatal ablation resulted in extensive loss of fibers in large parts of the neocortex; however the effect was attenuated in other regions, including the allocortical hippocampal formation and the basal ganglia.

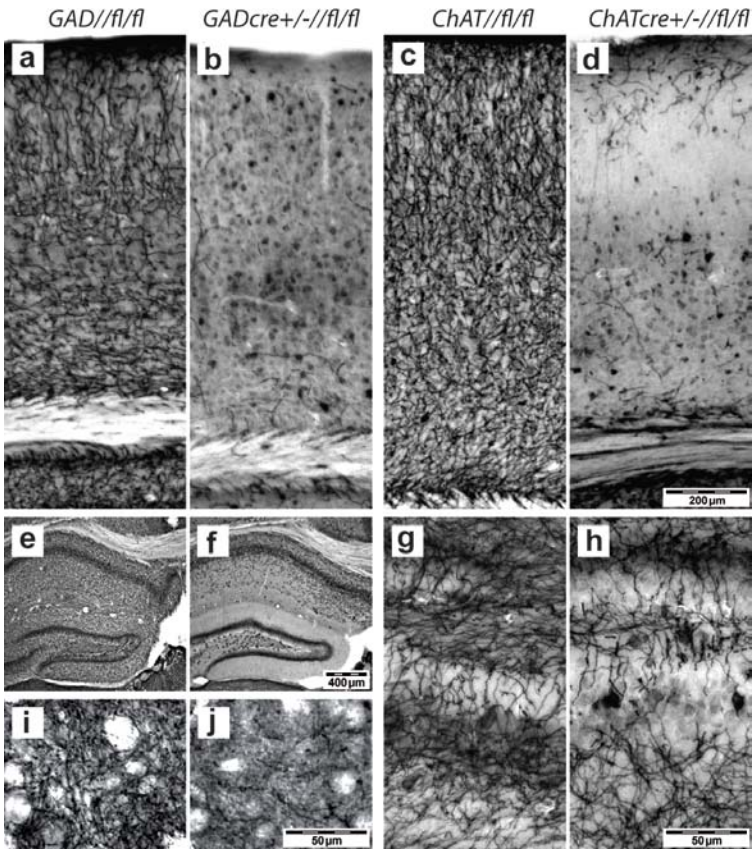

Figure 23. Loss of cholinergic fibers in the target regions.
AChE-histochemistry showing intense staining of fibers throughout the neocortical mantle (a; c), the hippocampal formation (e; g) and the CPu (i) in control animals (GAD//fl/fl and ChAT//fl/fl). Note the severe loss of fibers in the neocortical mantle (b), in the hippocampus (f) and in the CPu (j) of GADcre+/-//fl/fl mutant mice.
Only a few aberrant fibers mostly located in superficial and deep layers were detectable in the neocortex of ChATcre+/-//fl/fl mutants (d), and the AChE pattern exhibited defects in a "patch-like" fashion, as shown here for granule cell layer of the dentate gyrus (h).

3.2.4. Fate of basal forebrain neurons in GAD-cre//fl/fl and ChAT-cre//fl/fl mutants

Impairment of neuronal populations by *Nkx2-1* ablation may result in cell loss or a shift of their immunohistochemical profile (Butt et al., 2008). We therefore determined the total volume and number of neurons of the LGP, a structure known for its very high number of PV- and Nkx2-1-positive neurons (Magno et al., 2009) due to its embryonic origin (Sussel et al., 1999).The inspection of slices processed for immunohistochemistry experiments already indicated that the LGP of GADcre+/-//fl/fl mice was smaller.

Accordingly, both the total volume of the LGP (-47.6%; Fig. 24a) and the total number of NeuN-positive neurons (-58.3%; Fig. 24b) were substantially reduced in comparison to controls. We also investigated postnatal tissue samples of GADcre+/-//fl/fl animals using fine-structural methods. Cells showing signs of degeneration were occasionally observed in all four regions investigated (see below).

Cholinergic and GABAergic basal forebrain neurons can be further characterized by the expression of two transcription factors acting downstream of Nkx2-1, namely Lhx7 and Lhx6, respectively (ref. Sussel et al., 1999). As shown for the CPu of a GADcre+/-//fl/fl mouse at 3 months of age, double-labelings for *Lhx7* mRNA and Nkx2-1 confirmed an almost complete loss of cholinergic neurons (Fig. 24). In contrast, *Lhx6* labeling was partially maintained (Fig. 24), and most Lhx6-positive cells could subsequently be double-labeled by IHC for SOM (Fig. 24i).

As discussed above, in postnatal ChATcre+/-//fl/fl mice, a substantial loss of cholinergic basal forebrain neurons was detected at 3 months of age. Likewise, most of the remaining ChAT-positive cells in various subcortical regions were weakly stained and/or had shrunk. These degenerative changes were preferentially examined using fine-structural methods. Indeed, a large number of “dark” neurons was found in semithin preparations (Figs. 24j; k). These neurons showed fine-structural characteristics typical of prolonged degenerative processes rather than apoptotic cell death (Fig. 24m; cf. Naumann et al., 1992a).

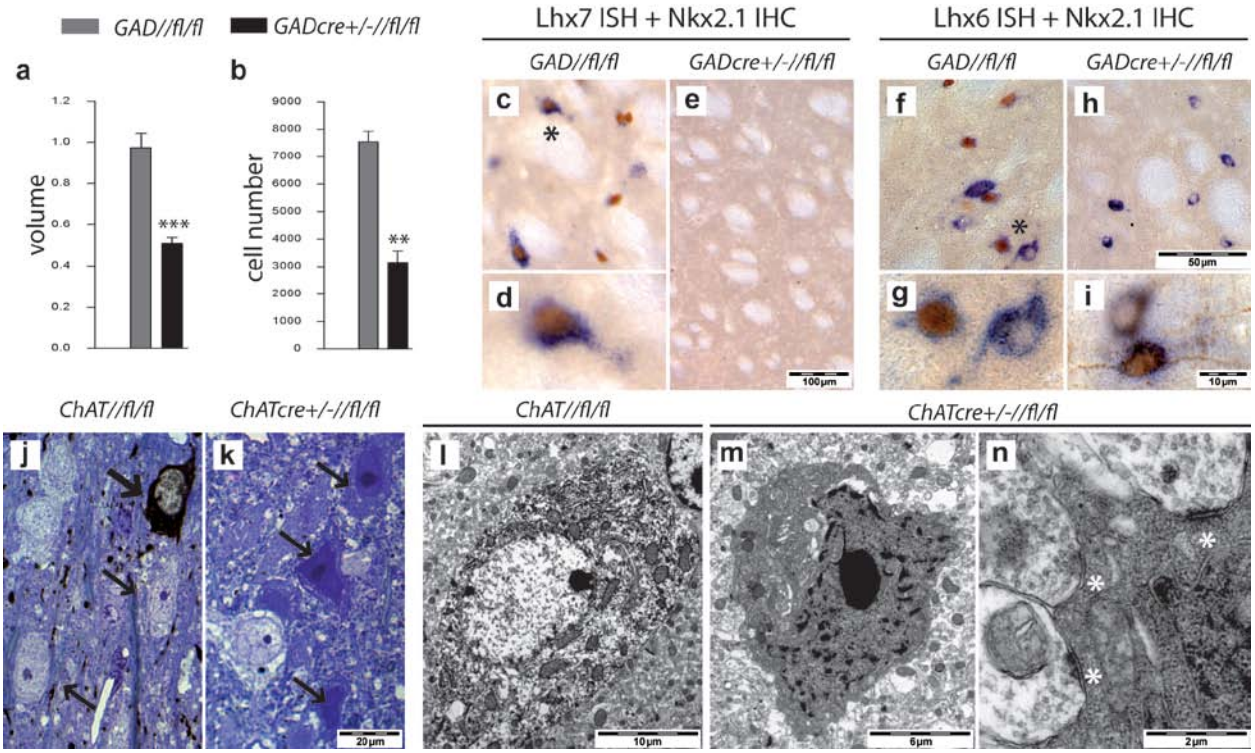

Figure 24. Fate of basal forebrain neurons in GAD-cre//fl/fl and ChAT-cre//fl/fl mice.
*Histograms showing quantification of the total volume (a) and the total number of NeuN-positive cells (b) in the LGP at 3 months of age, ***p < 0.0001, **p < 0.001.*
ISH for Lhx7 combined with Nkx2-1-IHC in the CPu (c-e). A neuron co-labeled for Nkx2-1 and Lhx7 is shown at higher magnification below (d, black asterisk in c).
ISH for Lhx6 combined with IHC for Nkx2-1 in the CPu (see also higher magnification in g; black asterisk in f). ISH for Lhx6 combined with IHC for SOM (see higher magnification in i).
Semithin (j; k) and ultrathin (l-n) sections following IHC for ChAT. Electron micrographs of septal neurons in mutant mice showing severe degenerative changes (m). At ultrastructural level, these cells proved to be very electron-dense and, thus, organelles could hardly be detected. Many, however, still bore intact nuclei membranes and, at least partially, input synapses (n; white asterisks).

3.2.5. Behavioral impairments following inactivation of Nkx2-1

The cholinergic centers of the basal forebrain were strongly affected in the brain of prenatal and postnatal mutants. Since these centers are related to cognitive functions such as learning and memory, but also motor coordination we tested the behavior according to the Morris Water Maze (MWM) and the rota-rod tasks. The MWM is used to assess spatial memory and learning (see Materials and Methods for a detailed

description; Morris et al., 1982), while the rota-rod test assesses the ability of an animal to balance on a rotating rod, therefore providing a measurement of motor coordination and balance.

GADcre+/-//fl/fl mice of both sexes showed significant deficits in the spatial version of the MWM task (Fig. 25). Additionally, the swimming paths of female mutants were significantly longer and their average speed slightly lower compared to female control mice (Fig. 26). The learning deficit was reflected by the probe trial after removing the platform. However, female control mice displayed equal swimming times in all quadrants during the spatial probe trial (Fig. 25b). In the cued version, female mutant mice displayed longer escape latencies, pointing to disturbed visual-motor integrity or reduced overall learning capacity (Fig. 25a, left).

Male mutant mice showed no significant decreases in escape latencies during the place version of the MWM, whereas male control mice learned to locate the platform (Fig. 25a). The swimming speed was only slightly lower in male mutant mice compared to male control mice, whereas no differences in the swim path length were observed between both genotypes (Fig. 26). The spatial probe trial revealed that neither male control nor GADcre+/-//fl/fl mice were able to remember the previous platform location (Fig. 25b). Learning and memory impairment is due in part to either a deficit in vision / motor activity, as suggested by the results of the cued version (Fig. 25a), or general learning deficits, as the severe loss of cholinergic innervation of the cortices indicates.

GADcre+/-//fl/fl mice of both sexes additionally showed deficits in the rota-rod test, the most frequently applied test for detecting disturbances of subcortical organization of motor functions (Fig. 25c). The time spent on the rotating rod was significantly lower for mutant mice than for the corresponding controls. Again, females seemed to be more strongly affected than their male counterparts (Fig. 25c).

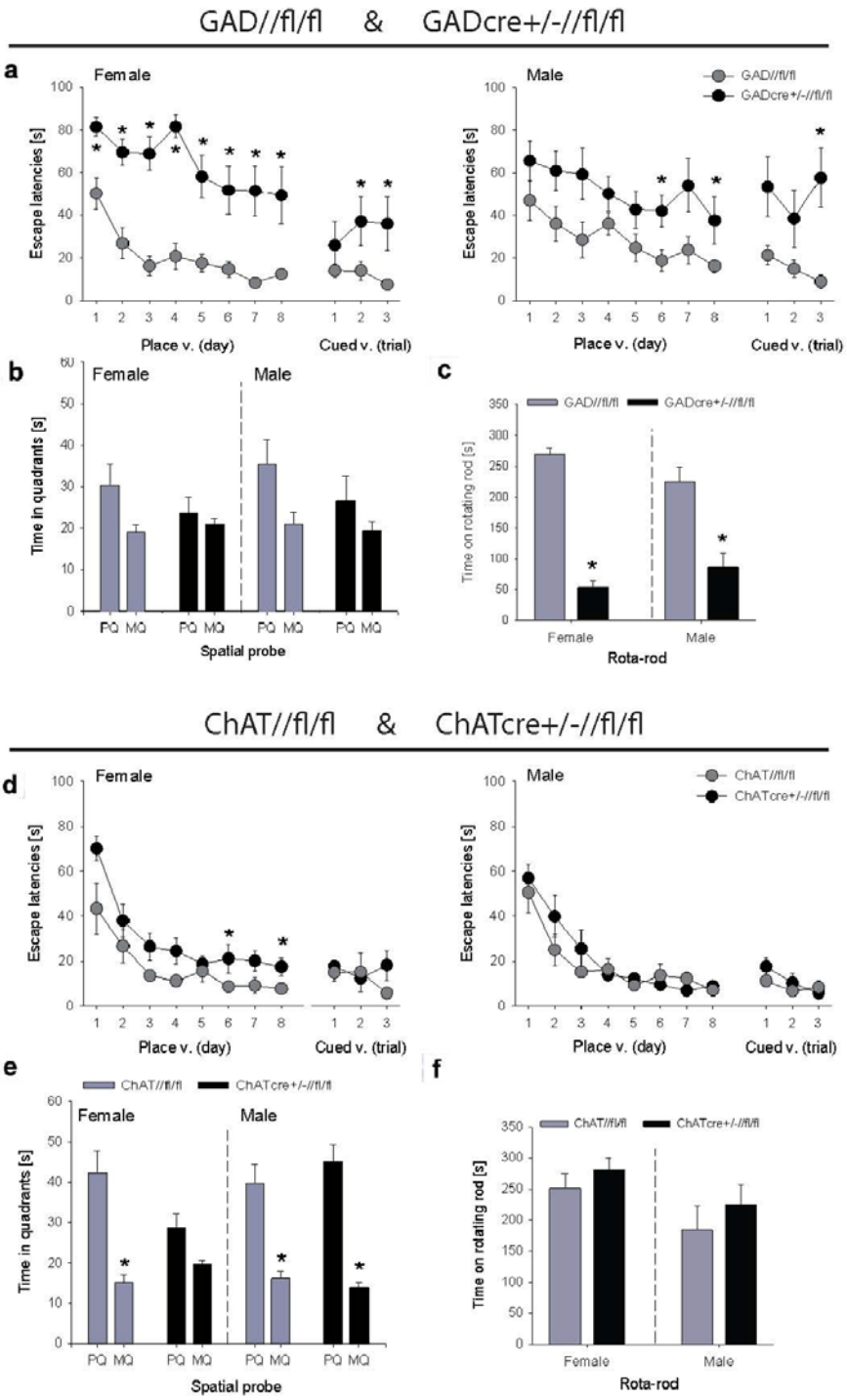

Figure 25. Impaired spatial memory and motor deficits in GADcre+/-//fl/fl mice, and learning deficits in female ChATcre+/-//fl/fl mice.

Escape latencies during the place and cued version (v.) of the MWM are shown for GADcre+/-//fl/fl (a), ChATcre+/-//fl/fl (d) mice and their corresponding controls. Detailed analysis of each day revealed that female GADcre+/-//fl/fl mice showed significantly higher escape latencies than female control mice (a, left,) and day-by-day comparison of the performances revealed significant differences between mutant and control males for days 6 and 8 (5a, right). For

ChATcre+/-//fl/fl mice direct comparison with controls revealed that on day 6 and 8 female mutants needed significantly more time to locate the platform.
The time (spatial probe of the MWM) spent in the platform quadrant (PQ) and the mean time spent in the three other quadrants (MQ) is presented for GADcre+/-//fl/fl (b), ChATcre+/-//fl/fl (e) mice and their corresponding controls. Female GADcre+/-//fl/fl (b) and ChATcre+/-//fl/fl (e) mutant mice spent similar swimming times in all quadrants.
The time spent on the rotating rod is plotted on the diagram for female and male mutant and control mice (c; f). GADcre+/-//fl/fl male and female mutant mice spent significantly less time on the rotating rod than the corresponding GADcre//fl/fl control mice (c).
*Data are presented as means ± SEM; or means + SEM; *p < 0.05 vs controls.*

Postnatal Nkx2-1 deletion in ChAT-expressing cells caused sex-specific deficits in spatial learning. Both female ChATcre+/-//fl/fl and control mice learned to locate the platform during the place version, however female mutant mice showed a mild impairment in the performance of the place version which was reflected by the probe trial (Fig.25). This deficit observed for the female mutant mice is not related to a visual-motor deficit since they showed performance comparable to female control mice in the cued version (Fig. 25d). It should be noted that female mutant mice display longer swimming paths at higher swim speed than female control mice (Fig. 26).
With regards to male mice, both mutant and control groups demonstrated good performance in the place version of the MWM (Fig 25). This was also reflected by the probe trial (Fig. 25e). Nor was there any difference in the cued version of the MWM (see Fig. 25d). Finally, the rota-rod test showed no motor deficit between female and male ChATcre+/-//fl/fl mice and their corresponding control mice (Fig. 25f).

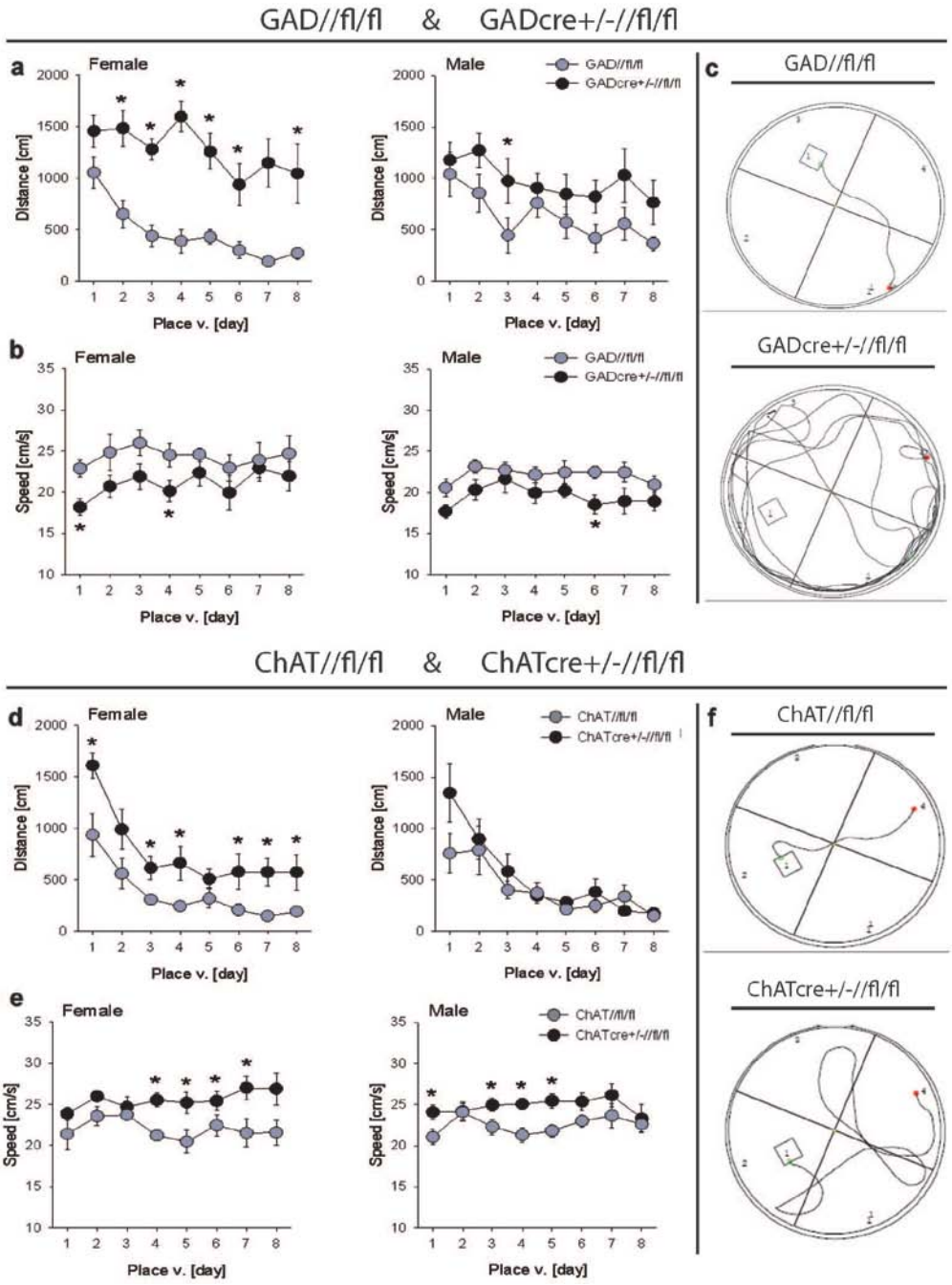

Figure 26. Impaired spatial memory in GADcre+/-//fl/fl mice and female ChATcre+/-//fl/fl mice.
The average swim path (a; d) and speed (b; e) during the place version (v.) are shown for GADcre+/-//fl/fl, ChATcre+/-//fl/fl mice and their corresponding controls. Representative paths followed by female mutant and control mice on the third day of the place version (c; f).
Note the longer path and lower average speed of the female GADcre+/-//fl/fl mutants to find the platform (a, left; c, below).
*Data are presented as mean ± SEM. *p < 0.05 vs. controls.*

3.3. EXPRESSION OF NKX2-1 IN THE HUMAN BASAL GANGLIA

Nkx2-1 is required during pre- and postnatal life for the proper differentiation and maintenance of cholinergic and PV-expressing GABAergic neurons in the mouse basal forebrain. Can this finding be applied to humans? To answer this question IHC for NKX2-1 was performed on tissue samples of the human basal ganglia. Staining for NKX2-1 resulted in a more intense darkening of the external part of the globus pallidus compared to its internal part (Fig. 27a). Accordingly, many more NKX2-1-immunoreactive cell nuclei could be detected in the GPe (inset in Fig. 27a).

Triple-immunofluorescence showed that NKX2-1 immunoreactivity is localized in the nucleus of cells, as demonstrated by co-localization with DAPI, and all NKX2-1-positive profiles are neurons, as shown by co-localization with NeuN (Fig. 27a).

Few studies investigated the distribution of distinct neurochemical markers in the human basal forebrain. Analysis of the basal ganglia demonstrated that ChAT- and PV-immunoreactive neurons are present in the human striatum (Holt et al., 1997; Bernacer et al., 2008), as described in rodents. In contrast, it remains controversial whether cholinergic neurons, in addition to the GABAergic counterparts, populate the human globus pallidus (Morel et al., 2002).

Double-immunofluorescence experiments on the human GPe showed that NKX2-1-immunoreactive neurons were GABAergic, and a smaller proportion of these cells co-expressed PV (Figs. 27e-j). Immunofluorescence for NKX2-1 and ChAT was less successful, and only a few neurons, localized at the border between the putamen and the GPe, were found to be double-labeled.

Fluorescence labeling experiments on human tissue always resulted, in addition to the specific antibody staining, in a punctuate pattern. The intense fluorescence is due to lipofucsin particles which are frequently detected in human neurons (Buhl and Schlote, 1987).

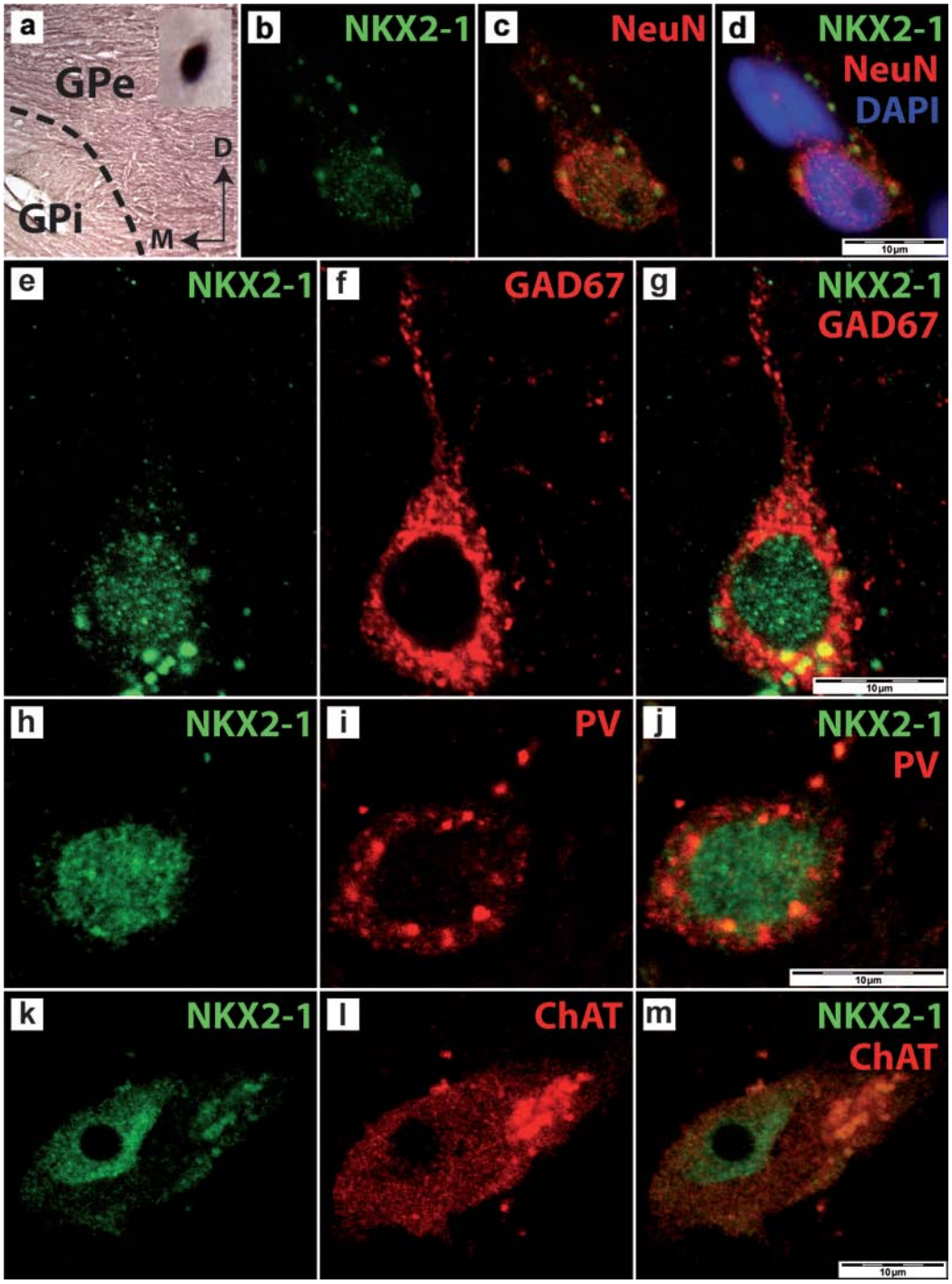

Figure 27. NKX2-1 expressing neurons in the human basal banglia.

IHC for NKX2-1 in the globus pallidus (a; GPe and GPi are separated by a dashed line; inset in "a" showing a NKX2-1 positive cell profile). Triple or double immunofluorescence for NKX2-1 (b; e; h; k; nuclear staining), NeuN (c), DAPI (d, overlay), GAD67 (f), PV (i), ChAT (l); overlays (d; g; j; m). Scale bars 10 um. PV (in the GPe; Figures 27h-j) or ChAT (in the putamen bordering the GPe; Figs. 27k-m). Note intense fluorescence of lipofucsion particles, which are detectable in every staining on human tissue.

4. DISCUSSION

Major divisions of the mammalian subpallium are known to be involved in the regulation of various brain functions such as motor behavior, learning and memory, motivation and hormone homeostasis, and are severely affected in psychiatric and neurological human disorders. In most cases, however, the underlying morphological alterations are not fully understood. Motor functions, for instance, are known to depend upon correct neuronal transmission within the basal ganglia (for review: Gerfen, 2004). Although all patients exhibiting heterozygous deletions of the *NKX2-1* gene show symptoms described as choreoathetosis, malformations within the basal ganglia, as revealed by MRI images, were found only in some of them (Krude et al., 2002; do Carmo Costa et al., 2005). These few cases thus cannot explain the complex motor disturbances described for all haploinsufficient patients.

The neurological symptoms due to *NKX2-1*-mutations first emerge approximately one year after birth, suggesting that specific neuronal defects become obvious during full maturation of neuronal circuitries. At molecular level an involvement of the basal ganglia in this disease has been confirmed by experiments performed in rodents. Numerous studies have shown that prenatal expression of the transcription factor Nkx2-1 in the medial ganglionic eminence is a prerequisite for the correct differentiation of some neuronal subtypes of both the striatum and the globus pallidus (Sussel et al., 1999; Marin et al., 2000). It is reasonable that *NKX2-1*-haploinsufficiency might affect the postnatal maturation of such neurons and their integration into neuronal circuitries, in addition to their prenatal differentiation. To discover which mechanisms and cell types are affected by Nkx2-1 mutation we first investigated which neurons express Nkx2-1 postnatally. In the adult mouse forebrain, cholinergic and PV-expressing GABAergic neuron maintain expression of the transcription factor. Therefore, through the analysis of cell-type-specific mutations of Nkx2-1, we assessed the impact of the transcription factor during the prenatal and postnatal period on the development and maintenance of cholinergic and parvalbumin-expressing GABAergic neurons.

4.1. PRENATAL FUNCTION OF NKX2-1

4.1.1. The fate of Nkx2-1-dependant PV-expressing GABAergic and cholinergic neurons

The regionalization of the developing brain is firstly accomplished by graded signaling of secreted morphogenic molecules which define dorsal-ventral and anterior-posterior patterning of the neuroepitelium. Subsequently, direct or indirect interactions between the morphogens' signaling and the transcription factors establish distinct proliferative regions (for review: Hebert and Fishell, 2008). Thus, via the spatial and temporal patterning, particular combinations of transcription factors orchestrate the specification of neuronal subtypes, hence generating a large neuronal diversity (Schuurmans and Guillemot, 2002; Flames et al., 2007). Several reports (Sussel et al., 1999; Marin et al., 2000; Pleasure et al., 2000; Xu et al., 2004; Butt et al., 2005; Flames et al., 2007; Fogarty et al., 2007; Butt et al., 2008; Wonders et al., 2008; this study), including a recent fate-mapping study (Xu et al., 2008), have shown that Nkx2-1-lineage cells of the subpallium mostly differentiate into GABAergic neurons. Nkx2-1 could determine cell fate by directly regulating the expression of other transcription factors, such as two members of the LIM homeobox family Lhx6 and Lhx7 (Sussel et al., 1999; Marin et al., 2000; Fig. 5 in Introduction). New findings confirmed that Lhx6 acts downstream Nkx2-1 in the subventricular zone (SVZ) of the MGE to specify the fate of PV and SOM-expressing cortical interneurons (Liodis et al., 2007; Du et al., 2008). Moreover, Lhx6, in combination with Lhx7 and Islet-1, two factors involved in the specification of basal forebrain cholinergic neurons (Sussel et al., 1999; Marin et al., 2000; Fragkouli et al., 2005), regulates the differentiation of GABAergic and cholinergic interneurons in the striatum (Fragkouli et al., 2009a).

A *GAD67-cre* line was chosen to conditionally mutate *Nkx2-1* in GABAergic neurons. As outlined in the introduction, GAD67 expression becomes detectable in the developing forebrain already at E10. Thus, GAD67-driven inactivation Nkx2-1 occurs in the ventral forebrain since early embryonic stages. The nearly complete loss of PV-positive GABAergic neurons, in the basal ganglia, the septal complex, and the related magnocellular nuclei, as observed for *GAD67cre+/-//fl/fl* mice, corresponds with the findings of the earlier studies. On the other hand, the number of PV-expressing neurons appeared as unchanged in the cortex and hippocampus of the mutant mice. This could

be explained considering the fact that precursors of cortical GABAergic interneurons (Butt et al., 2005; 2008) must downregulate *Nkx2-1* for migrating to the cortical regions (Nobrega-Pereira et al., 2008). GAD67-driven inactivation of Nkx2-1 occurs in the differentiation zones of the ventral telencephalon, when cells become post-mitotic and start their migration. Most likely, at this stage, precursor cells destined to the cortical regions have already downregulated the synthesis of the transcription factor and, therefore, are no more sensitive to Nkx2-1 ablation. Similarly, no obvious cell loss was observed for striatal SOM-expressing GABAergic neurons which are known to downregulate the expression of Nkx2-1 as they exit the neuroepithelium (Marin et al., 2000).

To our surprise, ablation of Nkx2-1 in GAD67-expressing cells affected also the development of basal forebrain cholinergic neurons, in addition to the GABAergic population. This finding suggests that most of cholinergic and GABAergic neurons of the basal forebrain derive from a common GABAergic progenitor which depends on the expression of Nkx2-1. Analysis of Lhx6 and Lhx7 expression patterns further confirmed that cholinergic neurons and the PV-positive subpopulation of GABAergic neurons were almost completely absent in the ventral telencephalon. This could have two possible explanations: first, the mutated cells are arrested in their immature state and persist, at least for a limited time period, in an atrophic, shrunken state or, secondly, they died rapidly and are removed by phagocytic processes within a very short time. However, the lack of corresponding cell profiles or fine-structural hallmarks in tissue samples (e.g., long-lasting activation of microglia, cell debris; cf. Hollerbach et al., 1998) does not support the latter hypothesis.

The persistence of some neurons immunoreactive for ChAT or PV, despite a complete lack of Nkx2-1 protein and mRNA in the ventral telencephalon of *GADcre+/-//fl/fl* mice at 3 months of age, can be explained by two possibilities: either they derived from Nkx2-1-negative domains (Flames et al., 2007; Garcia-Lopez et al., 2008), or they represent small, less sensitive, subpopulations.

Recent studies revealed that Nkx2-1 plays an important role in the cell-type specification by suppressing the surrounding cell fate programs (Butt et al., 2008). The effect of prenatal *Nkx2-1* ablation could be therefore compensated, at least partially, by the generation of non-Nkx2-1-dependant neurons. However, as shown for the LGP, a strong reduction of both volume and total neuronal cell number suggests that prenatal

deletion of *Nkx2-1* is unlikely accompanied by the generation of other, functionally different, neurons in the affected regions.

4.1.2. Motor deficits following Nkx2-1 prenatal inactivation

Patients suffering from NKX2-1-haploinsufficiency show severe deficit of coordinated movement. This motor dysfunction is at least partially caused by alteration in the development of the basal ganglia: a brain structure controlling voluntary movement and posture. The two major components of the basal ganglia are the striatum and the globus pallidus. The striatum receives inputs directly from the motor cortex and sends most of the outputs to the globus pallidus (indirect pathway), and to the substantia nigra pars reticulata (direct pathway). The globus pallidus is subdivided into an external and internal segment (in humans) or a lateral and a medial part (in mice). The external segment is involved in the indirect pathway, while the internal is an input station of the direct pathway. The external segment projects to the subthalamic nuclei that, in turn, send the information to the SNr and to the thalamus (for review: Nambu et al., 2000). Signaling from the putamen to the external segment of the globus pallidus through the so-called indirect pathway limits the stimulation of the thalamus whereas the direct pathway results in an inhibition of the tonic inhibitory output of the basal ganglia (for review Gerfen, 2004). Therefore, alterations in these circuits could lead to higher degree of inhibition (direct pathway) or excitation (indirect pathway) of the thalamic outflow to the cortex, thus generating hyperkinesia and choreic movements.

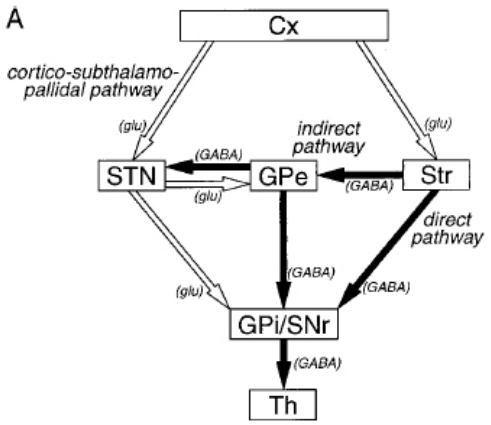

Figure 28. Schematic diagram illustrating the basal ganglia circuitry in mammals.
Cortico-striato-pallidal direct and indirect pathways and their balance are involved in control of fine movements in primates. White and black arrows indicate respectively excitatory or inhibitory

projections (Nambu et al., 2000). Cx, cortex; Str, striatum; STN, subthalamic nucleus; SNr, substantia nigra pars reticulata; Th, thalamus

At cellular level, the CPu consists of about 95% of GABAergic medium spiny projection neurons mainly co-expressing the calcium-binding protein calbindin, with at least 4 different classes of interneurons contributing to the small number of remaining neurons (Reiner et al., 1998; Schlosser et al., 1999). Striatal interneurons have been characterized by electrophysiological approaches (e. g. Kawaguchi, 1993; Calabresi et al., 2000), but their specific functional roles within the generation and control of movements have not been determined yet. On the other hand the majority of the LGP neurons are GABAergic projection neurons but, in contrast to the striatum, about two-thirds of them co-express PV (Kita, 1994) and Nkx2-1.

Expression of Nkx2-1 is of fundamental importance for the specification of the striatal interneurons and most of the pallidal projection neurons during development (Sussel et al., 1999; Marin et al., 2000; Butt et al., 2008). Ablation of Nkx2-1 in GAD67-expressing cells at early embryonic stages caused a severe loss of striatal cholinergic and PV-positive interneurons without affecting the 95% component of GABAergic projection neurons. In addition, Nkx2-1 targeting leads to a severe loss of the projection neurons in the LGP. Not surprisingly, *GADcre+/-//fl/fl* mice display a dramatic impairment of motor abilities due to the alteration of the motorcortex-CPu-LGP axis.

Similarly, the choreoathetosis in humans could be a result of disturbed processing of information (1) within the striatum because of the impairment of GABAergic and cholinergic interneurons, and (2) at the level of the pallidal GABAergic neurons projecting to the substantia nigra and the subthalamic nucleus (for review: Gerfen, 2004).

4.1.3. Cognitive impairments due to prenatal loss of Nkx2-1

No deficits have been yet described for NKX2-1–haploinsufficient patients that could be related to limbic structures including the septohippocampal system. However, these regions exhibit large numbers of Nkx2-1-positive cells since early prenatal stages, and they are associated with higher cognitive functions (for review: Aggleton, 1993; Davis et al., 1994; Heimer et al., 1997; Harding et al., 2000; Mufson et al., 2003; Vann and Aggleton, 2004).

The various septal nuclei extend widely within the interventricular wall and into ventral parts of the telencephalon. This complex is not clearly defined for several nuclei are regarded, depending on the various functional aspects in question, as parts of other neuronal assemblies such as the basal ganglia (e. g. the nucleus accumbens) or the extended amygdala (e. g. the bed nuclei of the stria terminalis; for review: Andy, 1976; Risold, 2004). However, the septal region, as an important relay station, is part of neuronal loops that interconnect the limbic telencephalon with the hypothalamus and brain stem (for review: Swanson and Cowan, 1979; Risold and Swanson, 1997a; Risold, 2004). In vertebrates, the various septal nuclei, in particular the lateral septal nucleus and the medial septum-diagonal band complex, largely comprise GABAergic neurons (e.g., Panula et al., 1984; Kohler et al., 1985; Onteniente et al., 1986; Alonso and Frotscher, 1989a; Alonso and Frotscher, 1989b; Leranth and Frotscher, 1989). A second large population, the cholinergic neurons, is distributed within the medial septal nucleus and the vertical limb of the diagonal band. These neurons, together with those located more caudally in the horizontal extension of the diagonal band and a less clearly defined area that includes the nucleus basalis magnocellularis (Meynert) and the medial preoptic area (cf. Riedel et al., 2002), are the major sources of far-reaching cholinergic axons targeting nearly all regions of the cortex (for review: Mesulam et al., 1983; 1983b; Sofroniew et al., 1987). The neighboring lateral septum, another large part of the septal complex which is strongly interconnected with the MSDB locally and with several hypothalamic nuclei (for review: Risold and Swanson, 1997b), is described as GABAergic as a whole. Accordingly, high levels of *GAD65* and *GAD67* mRNAs were observed throughout the three main compartments of this nucleus (e. g. Bender et al., 1996; present study). In addition, several studies have shown that LS neurons are very heterogeneous due to the expression of a wide range of hormones and peptides in addition to GABA (cf. Dutar et al., 1995; for review: Risold and Swanson, 1997b).

The early developing septal area consists of different proliferative domains. Within these regions Nkx2-1-positive and Nkx2-1-negative septal subdomains can be distinguished according to their positions to neighboring proliferative zones, e. g. the LGE, the MGE, or POA (Flames et al., 2007). In addition, it has been shown that part of the cholinergic corticopetal ventral forebrain neurons derive from the more caudal-located commissural-preoptic area, another subdivision of the subpallium expressing *Nkx2-1* (Garcia-Lopez et al., 2008). In line with this, prenatal inactivation of Nkx2-1 caused a

reduction in the number of cholinergic and PV-expressing GABAergic neurons in the MSDB-complex.

The almost complete loss of cholinergic neurons resulted in a nearly complete lack of AChE-positive fibers for target structures of the cholinergic basal forebrain neurons and within the striatum at all postnatal ages analyzed. These alterations caused severe impairment of learning and spatial memory functions in *GAD67cre+/-//fl/fl* mice. This correlates with the results of many excellent studies that have highlighted the central role of the cholinergic projection systems, which extend to nearly all parts of the telencephalon, including the cortical mantle and the amygdaloid complex (for review: Berger-Sweeney, 2003; McKinney and Jacksonville, 2005). It is now clear that early impairment of the development of these fiber systems results in permanent morphological alterations of the target structures followed by long-lasting and more global alterations in cognitive behaviors, including attention and mnemonic functions (for review: Berger-Sweeney, 2003). These results are only partially comparable to those obtained with other prenatal mutations of the cholinergic basal forebrain system, e.g. following deletion of *Lhx7* (Fragkouli et al., 2005; 2009b). Although *Lhx7* mutation has also been described as causing severe impairments in spatial learning and memory, Lhx7-deficient mice displayed normal locomotor activity and motor coordination in these studies (Fragkouli et al., 2005; 2009b). This discrepancy could be explained by the fact that we targeted PV-positive GABAergic neurons in addition to their cholinergic counterparts. Moreover, it should be kept in mind that GABAergic projection neurons of the ventral forebrain always contribute to the projections that originate in the large magnocellular nuclei, which are often described as “cholinergic centers” (e.g., Gritti et al., 1997). It remains unclear to which extent the GABAergic neurons might have contributed to the deficits in higher cognitive functions, as their role in the latter has been less intensively investigated than that of the cholinergic projection systems (e.g., Schwegler et al., 1996).

4.1.4. Deficits related to the diencephalic nuclei

Few preliminary data described the presence of hypothalamic dysfunctions in some NKX2-1-haploinsufficient patients. Nevertheless, the hypothalamic deficits are not a major feature of the syndrome, as they were not detected in all patients. Moreover, the

symptoms described so far are very heterogeneous with respect to the various hypothalamic functions (S. Schrittert, Doctoral dissertation).
The hypothalamic primordium is described as one of the main regions with high prenatal *Nkx2-1* expression in the brain and, accordingly, morphological alterations were found in the *Nkx2-1* null mutants (see introduction; Kimura et al., 1996; Marin et al., 2002). Although co-expression of Nkx2-1 and GAD67 by neurons was found to be limited in the hypothalamus, it cannot be excluded that GAD67-driven inactivation of Nkx2-1 led to alteration in the hypothalamic nuclei. In fact, the number of mutants is slightly lower compared to that of the other genotypes suggesting a loss of mice. Thus, probably in some cases early Nkx2-1 ablation in GABAergic neurons causes general impairments of vegetative functions (cf. Swaab et al., 1993). One of the structure bearing a high number of Nkx2-1-positive GABAergic neurons is the nucleus arcuatus (Yee et al., 2009). Dysfunction of this nucleus, which is involved in feeding behavior (for review: Valassi et al., 2008), could explain the reduced body weight of *GAD67cre+/-//fl/fl* mutant. As the diencephalon was not the main focus of this study, the findings described above will be further investigated in another study.

4.2. POSTNATAL EXPRESSION OF NKX2-1

Nkx2-1 expression is not only maintained in various brain regions of early postnatal mice, but also in adult and aged animals throughout the ventral forebrain. Despite a substantial downregulation of the mRNA during the first two weeks after birth, quantification of *Nkx2-1* by realtime PCR revealed that its synthesis is maintained to a stable level after the second postnatal week.
The ventral tips of the lateral ventricles are one of the regions that showed strong expression, but also downregulation of Nkx2-1 during the first two postnatal weeks. Fate mapping studies suggest that this region is a remnant of the MGE, a region that strongly expresses Nkx2-1 during development (Young et al., 2007). The ganglionic eminences are regarded as transient prenatal structures of the forebrain (Bulfone et al., 1993; Rubenstein et al., 1994), however, their derivates persist into postnatal life (Wichterle et al., 2001; Young et al., 2007; Lledo et al., 2008). The lateral part (LGE) gives rise to most of the adult subventricular zone, which continuously generates olfactory bulb interneurons throughout life (Doetsch and Alvarez-Buylla, 1996; Lois et al., 1996;

Wichterle et al., 1999; 2001; Stenman et al., 2003; Yun et al., 2003). On the other hand, derivates of the MGE have been less investigated. In this study, at P0, but also during the first postnatal weeks after birth, the number of Nkx2-1-immunoreactive profiles is very high in the ventral tips of the lateral ventricles. Fine-structural analysis revealed that these cells still exhibit characteristics of progenitors. In older animals, the extent of labeling for Nkx2-1-positive cells is much lower, suggesting that the generation of new neurons or glial cells from this source decreases substantially during postnatal maturation of the brain. It is known that progenitors residing in the ventral tips of the lateral ventricles give rise, in addition to those of the LGE remnants, to subsets of neurons populating the olfactory bulb, the nucleus accumbens, and other subcortical neuronal structures (Das and Altman, 1970; De Marchis et al., 2004; Merkle et al., 2004; Inta et al., 2008). As shown for the prenatal ventral forebrain, Nkx2-1 positive precursors in the ventral tips of the lateral ventricles could be a potential source of GABAergic and cholinergic neurons for the ventral forebrain throughout life.

Most intense labeling for both Nkx2-1 protein and mRNA on postnatal and adult tissue was found in the mammillary bodies. Nonetheless, the functional relevance of the strong Nkx2-1 expression by mature neurons of the mammillary bodies remains to be elucidated. This might be of some interest because the mammillary complex, as a relay station within the so-called Papez-circuit, is interconnected with limbic structures including the hippocampal formation, the septal complex, and the anterior thalamic nuclei. The involvement of this structure in the processing of higher limbic functions has been described extensively, and a damage of these nuclei was observed in patients suffering from Korsakoff-syndome (for review: Harding et al., 2000; Vann and Aggleton, 2004). However, a few is known about the function of this structure in rodents. Remarkably, no dysfunctions that correlate with the mammillary complex and its functions have been reported for *NKX2-1*-haploinsufficient patients.

4.2.1. Permanent expression of Nkx2-1 by cholinergic and PV-expressing GABAergic neurons of the ventral telencephalon

In the adult telencephalon Nkx2-1 expression is particularly maintained by cholinergic and PV-positive GABAergic neurons. Depending on the region in question, these neurons belong either to the class of interneurons (e.g. in the CPu), or are known to be projection neurons (e.g. in the LGP and MSvDB).

In the early postnatal period, cholinergic and PV-positive GABAergic neurons of the caudate-putamen co-express Nkx2-1 whereas only a small number of CR- and CB-positive cells was found to be co-labeled (Marin et al., 2000). The present study shows that robust synthesis of Nkx2-1 in the CPu is not restricted to the early postnatal period. Between 2 weeks and 6 months after birth, PV-positive, but also cholinergic, striatal interneurons maintain synthesis of Nkx2-1.

Throughout the septal complex, intense labeling for Nkx2-1 was not only observed at birth, but also during further maturation of the brain. In the MSDB-complex, the overwhelming majority of Nkx2-1-expressing cells could be identified as PV-containing GABAergic and cholinergic neurons known to be the origin of the septohippocampal projection (e.g. Mesulam et al., 1983; Amaral and Kurz, 1985; Freund, 1989; Naumann et al., 1992a; Kermer et al., 1995) and, vice versa, neurons co-labeled with other marker proteins were rarely found. It should be mentioned that a large number of neurons, mainly located in the intermediate part of the LS in close proximity to the lateral ventricles, was regularly found to be immunoreactive for ChAT. It is not known whether these neurons belong to GABAergic neurons or they form an own subclass of cholinergic neurons within the LS (cf. Birthelmer et al., 2003). However, they were never found to be positive for the transcription factor.

4.3. POSTNATAL FUNCTION OF NKX2-1

Several studies have provided evidences that *Nkx2-1* expression by mature neurons and glial cells of the hypothalamus and other diencephalic structures controls various vegetative functions (see Introduction). One of the most important questions of my study was to determine whether Nkx2-1 exerts a relevant function in the ventral forebrain during postnatal life. To address this matter *Nkx2-1* was inactivated in ChAT-expressing cells. Several studies performed in rodents have shown that ChAT-synthesis reaches mature levels around P15 (Bender et al., 1996; Korsching, 1993). However, evidence of ChAT expression has also been described for the prenatal ventral forebrain (Schambra et al., 1989). As revealed by the present cell counts, targeting of *Nkx2-1* in *ChATcre+/-//fl/fl* mice had no effect on the number of ChAT-immunoreactive neurons until P15, and first impairments of these cells were evident 2 weeks later.

Postnatal targeting of *Nkx2-1* in *ChATcre+/-//fl/fl* mice resulted in the loss of about 50% of the cholinergic neurons in the MSvDB, hDB-SI, CPu and LGP, and this reduction is a result of prolonged degeneration. Electron microscopy analysis of the magnocellular nuclei revealed the presence of many neurons exhibiting fine-structural characteristics as observed for axotomized MSvDB neurons (Naumann et al., 1992b). In addition, no apoptotic cell profiles could be detected in the four subcortical compartments analyzed in this study (cf. Clarke, 1990; Naumann et al., 1992b). In line with this, partial loss of Nkx2-1 in follicular cells of the adult thyroid was described to cause atrophy / degeneration of the follicles, without signs of apoptotic cell death (Kusakabe et al., 2006).

In contrast to the prenatal mutation, postnatal ablation of Nkx2-1 caused only a partial reduction in cell number. The partial loss of cholinergic neurons might be caused by the existence of subpopulations with different sensitivity to Nkx2-1. Little is known about the function of these cholinergic subpopulations (Calabresi et al., 2000; Dutar et al., 1995), however the remaining neurons are obviously sufficient to compensate for the cell loss, at least until 3 months of age. Accordingly, the mutant mice don't display any defect in motor coordination.

Previous studies have shown that the deficits in higher cognitive functions resulting from manipulation of the cholinergic fiber systems are less severe when performed in adult rodents compared to prenatal targeting (e.g., Berger-Sweeney, 2003). Indeed, in this study, the cognitive impairment observed in *ChATcre+/-//fl/fl* mice was rather moderate and also sex-dependent, as described in previous reports (cf. Berger-Sweeney, 2003; Fragkouli et al., 2009b). Only a minor deficit in the spatial learning and memory was observed for female mutants, which was independent of motor ability, as the mice were found to perform normally in these tests. Partial loss of cholinergic projection neurons, as observed following postnatal deletion of *Nkx2-1*, does not result in similar impairment of higher cognitive functions, as described for the *GADcre+/-//fl/fl* mice. Thus, the various impairments observed for the two mutations reflect the extent of cell loss. On the other hand GABAergic forebrain neurons, which also contribute to the septal complex and Meynert nucleus, have not been affected in *ChATcre+/-//fl/fl* mice. Therefore, a combined inactivation of Nkx2-1 in both the ventral forebrain cholinergic and GABAergic populations could better reflect the postnatal lack of the transcription factor.

4.4. NKX2-1 HAPLOINSUFFICIENCY IN HUMANS

This study shows that the transcription factor Nkx2-1 is required during pre- and postnatal life for the proper differentiation and maintenance of cholinergic neurons in the mouse basal forebrain. Reasonably, PV-positive GABAergic neurons are similarly dependent on permanent synthesis of Nkx2-1. Moreover, these cell types express NKX2-1 in adult human brain, suggesting that Nkx2-1 synthesis by these neuronal populations is conserved amongst mammals.

NKX2-1-haploinsufficiecy might affect the prenatal differentiation and the postnatal maturation of all Nkx2-1-dependent neurons and non-neuronal cells. The widespread distribution of Nkx2-1 positive cells in the telencephalon is only partially reflected by the symptoms observed in human patients. This could have many possible explanations. First, it should be mentioned that mutations of transcription factors in humans result in a stronger effect in comparison to the corresponding mutation in mice. This species-specific sensitivity to gene dosage was also detected for Nkx2-1 mutations (Krude et al., 2002). Haploinsufficiency of NKX2-1 resulted in a syndrome, while heterozygous mutations in mice did not cause corresponding defects. Homozygous mutations of the transcription factor have not been described in humans, while Nkx2-1$^{-/-}$ mice reach birth and die immediately after. This difference in sensitivity to gene-dosage could also exist among the various populations of Nkx2-1-expressing cells. Secondly, in humans, these less sensitive neuronal populations could originate from Nkx2-1-negative domains and therefore would not be affected by the loss of Nkx2-1.

Finally, the presence of cognitive dysfunctions in *NKX2-1*-haploinsufficient patients cannot be excluded, as the performance of the patients tested for learning and memory skills could be hampered by the motor dysfunction. Indeed, the early onset of deficits in motor coordination could impair the ability of the patients to learn at school. Thus, cognitive skills of NKX2-1-haploinsufficient patients could be compared only to a control group consisting of subjects with a comparable phenotype in terms of movement defect, with no underlying genetic condition.

4.5. CONCLUSIONS

The outcome of this work can be summarized with the following points:

1. The transcription factor Nkx2-1 is expressed by cholinergic and PV-positive GABAergic neurons of the ventral telencephalon throughout life.

2. Development of these neurons is heavily impaired following prenatal *Nkx2-1* ablation in GAD67-expressing cells.

3. Prenatal loss of function leads to severe deficits in motor coordination and impairments of the spatial memory and learning.

4. As shown for cholinergic neurons, permanent Nkx2-1 expression is essential for the integrity and functioning of these neurons.

5. Postnatal inactivation of *Nkx2-1* is accompanied by degeneration and mild deficits in cognitive skills.

6. NKX2-1 is expressed by mature neurons of the basal ganglia in the human brain.

7. Haploinsufficiency in humans is a result of pre- and post-natal lack of NKX2-1, which impairs development and maturation of cholinergic and PV-positive GABAergic neurons of the ventral forebrain.

5. SUMMARY

Coordinated movements require the caudate-putamen and the globus pallidus, two nuclei belonging to the basal ganglia, to be intact and functioning properly. Many neurons populating these regions derive from the medial ganglionic eminence (MGE), a transient structure that expresses the transcription factor Nkx2-1 during prenatal development. Nkx2-1 synthesis is essential for the determination of the cell fate and the migration of cortical interneurons, as well as several classes of neurons of the ventral forebrain. Interestingly, heterozygous mutation of the *NKX2-1* gene in humans has been described as causing an unusual disorder, from the first year of life onwards, which is mainly characterized by disturbances of motor abilities and delayed speech development. These symptoms suggest that both prenatal and postnatal lack of NKX2-1 could be responsible for the motor dysfunction observed in these patients.

So far, data obtained from rodents have been unable to explain convincingly the symptoms of human NKX2-1-haploinsufficiency. Interestingly, postnatal conditional mutation of the *Nkx2-1* gene in mature neurons led to hypothalamic dysfunctions such as delayed puberty and reduced reproductive capacity, but no impairments regarding motor coordination or cognitive functions were detected in these mutants.

This study shows for the first time which neurons are affected by NKX2-1 haploinsufficiency and it demonstrates that the development of these cells is heavily impaired following prenatal *Nkx2-1* deletion in GAD67-expressing cells. As shown for cholinergic neurons, permanent Nkx2-1 expression is essential for the integrity of the cholinergic projection systems. In line with this, predominately prenatal, but also postnatal inactivation of *Nkx2-1* in these neurons is accompanied by impairments of the spatial memory and learning. The disturbed motor abilities as observed for NKX2-1-haploinsufficient patients could be explained by the deficits of the intra-striatal neuronal loops and GABAergic projection neurons of the lateral globus pallidus. This assumption is further supported by the observation that the same cell types express NKX2-1 in the adult human basal ganglia. It remains to be elucidated why no memory and learning deficits have been described for the patients so far.

6. REFERENCES

1 Gruters A, Krude H, and Biebermann H. Molecular genetic defects in congenital hypothyroidism. Eur J Endocrinol. 2004;151 Suppl 3:U39-44.

2 Moya CM, Perez de Nanclares G, Castano L, et al. Functional study of a novel single deletion in the TITF1/NKX2.1 homeobox gene that produces congenital hypothyroidism and benign chorea but not pulmonary distress. The Journal of clinical endocrinology and metabolism. 2006;91:1832-1841.

3 Devriendt K, Vanhole C, Matthijs G, and de Zegher F. Deletion of thyroid transcription factor-1 gene in an infant with neonatal thyroid dysfunction and respiratory failure. N Engl J Med. 1998;338:1317-1318.

4 Iwatani N, Mabe H, Devriendt K, Kodama M, and Miike T. Deletion of NKX2.1 gene encoding thyroid transcription factor-1 in two siblings with hypothyroidism and respiratory failure. The Journal of pediatrics. 2000;137:272-276.

5 Breedveld GJ, Percy AK, MacDonald ME, et al. Clinical and genetic heterogeneity in benign hereditary chorea. Neurology. 2002a;59:579-584.

6 Krude H, Schutz B, Biebermann H, et al. Choreoathetosis, hypothyroidism, and pulmonary alterations due to human NKX2-1 haploinsufficiency. The Journal of clinical investigation. 2002;109:475-480.

7 Asmus F, Horber V, Pohlenz J, et al. A novel TITF-1 mutation causes benign hereditary chorea with response to levodopa. Neurology. 2005;64:1952-1954.

8 do Carmo Costa M, Costa C, Silva AP, et al. Nonsense mutation in TITF1 in a Portuguese family with benign hereditary chorea. Neurogenetics. 2005;6:209-215.

9 Devos D, Vuillaume I, de Becdelievre A, et al. New syndromic form of benign hereditary chorea is associated with a deletion of TITF-1 and PAX-9 contiguous genes. Mov Disord. 2006;21:2237-2240.

10 Provenzano C, Veneziano L, Appleton R, Frontali M, and Civitareale D. Functional characterization of a novel mutation in TITF-1 in a patient with benign hereditary chorea. Journal of the neurological sciences. 2008;264:56-62.

11 Kleiner-Fisman G, and Lang AE. Benign hereditary chorea revisited: a journey to understanding. Mov Disord. 2007;22:2297-2305; quiz 2452.

12Breedveld GJ, van Dongen JW, Danesino C, et al. Mutations in TITF-1 are associated with benign hereditary chorea. Human molecular genetics. 2002b;11:971-979.

13 Willemsen MA, Breedveld GJ, Wouda S, et al. Brain-Thyroid-Lung syndrome: a patient with a severe multi-system disorder due to a de novo mutation in the thyroid transcription factor 1 gene. European journal of pediatrics. 2005;164:28-30.

14 Pohlenz J, Dumitrescu A, Zundel D, et al. Partial deficiency of thyroid transcription factor 1 produces predominantly neurological defects in humans and mice. The Journal of clinical investigation. 2002;109:469-473.

15 Nutt SL, and Busslinger M. Monoallelic expression of Pax5: a paradigm for the haploinsufficiency of mammalian Pax genes? Biol Chem. 1999;380:601-611.

16 Civitareale D, Lonigro R, Sinclair AJ, and Di Lauro R. A thyroid-specific nuclear protein essential for tissue-specific expression of the thyroglobulin promoter. The EMBO journal. 1989;8:2537-2542.

17 Mizuno K, Gonzalez FJ, and Kimura S. Thyroid-specific enhancer-binding protein (T/EBP): cDNA cloning, functional characterization, and structural identity with thyroid transcription factor TTF-1. Molecular and cellular biology. 1991;11:4927-4933.

18 Guazzi S, Price M, De Felice M, Damante G, Mattei MG, and Di Lauro R. Thyroid nuclear factor 1 (TTF-1) contains a homeodomain and displays a novel DNA binding specificity. The EMBO journal. 1990;9:3631-3639.

19 Kim JG, Nam-Goong IS, Yun CH, et al. TTF-1, a homeodomain-containing transcription factor, regulates feeding behavior in the rat hypothalamus. Biochemical and biophysical research communications. 2006;349:969-975.

20 Gehring WJ, Affolter M, and Burglin T. Homeodomain proteins. Annu Rev Biochem. 1994;63:487-526.

21 Kim Y, and Nirenberg M. Drosophila NK-homeobox genes. Proc Natl Acad Sci U S A. 1989;86:7716-7720.

22 Vollmer JY, and Clerc RG. Homeobox genes in the developing mouse brain. J Neurochem. 1998;71:1-19.

23 Mark M, Rijli FM, and Chambon P. Homeobox genes in embryogenesis and pathogenesis. Pediatr Res. 1997;42:421-429.

24 Kissinger CR, Liu BS, Martin-Blanco E, Kornberg TB, and Pabo CO. Crystal structure of an engrailed homeodomain-DNA complex at 2.8 A resolution: a framework for understanding homeodomain-DNA interactions. Cell. 1990;63:579-590.

25 Price M, Lazzaro D, Pohl T, et al. Regional expression of the homeobox gene Nkx-2.2 in the developing mammalian forebrain. Neuron. 1992;8:241-255.

26 Bingle CD. Thyroid transcription factor-1. Int J Biochem Cell Biol. 1997;29:1471-1473.

27 Albert BJ, A.; Lewis, J.; Raff, M.; Roberts, K.; Walter, P. Molecoular Biology of the Cell, 4th ed. ed. New York, USA: Garland Science, 2002.

28 Endo T, Ohta K, Saito T, et al. Structure of the rat thyroid transcription factor-1 (TTF-1) gene. Biochemical and biophysical research communications. 1994;204:1358-1363.

29 Ikeda K, Clark JC, Shaw-White JR, Stahlman MT, Boutell CJ, and Whitsett JA. Gene structure and expression of human thyroid transcription factor-1 in respiratory epithelial cells. J Biol Chem. 1995;270:8108-8114.

30 Oguchi H, Pan YT, and Kimura S. The complete nucleotide sequence of the mouse thyroid-specific enhancer-binding protein (T/EBP) gene: extensive identity of the deduced amino acid sequence with the human protein. Biochim Biophys Acta. 1995;1261:304-306.

31 Hamdan H, Liu H, Li C, et al. Structure of the human Nkx2.1 gene. Biochim Biophys Acta. 1998;1396:336-348.

32 Li C, Cai J, Pan Q, and Minoo P. Two functionally distinct forms of NKX2.1 protein are expressed in the pulmonary epithelium. Biochemical and biophysical research communications. 2000;270:462-468.

33 Lazzaro D, Price M, de Felice M, and Di Lauro R. The transcription factor TTF-1 is expressed at the onset of thyroid and lung morphogenesis and in restricted regions of the foetal brain. Development (Cambridge, England). 1991;113:1093-1104.

34 Shimamura K, Hartigan DJ, Martinez S, Puelles L, and Rubenstein JL. Longitudinal organization of the anterior neural plate and neural tube. Development (Cambridge, England). 1995;121:3923-3933.

35 Sussel L, Marin O, Kimura S, and Rubenstein JL. Loss of Nkx2.1 homeobox gene function results in a ventral to dorsal molecular respecification within the basal telencephalon: evidence for a transformation of the pallidum into the striatum. Development (Cambridge, England). 1999;126:3359-3370.

36 Puelles L, Kuwana E, Puelles E, et al. Pallial and subpallial derivatives in the embryonic chick and mouse telencephalon, traced by the expression of the genes Dlx-2, Emx-1, Nkx-2.1, Pax-6, and Tbr-1. The Journal of comparative neurology. 2000;424:409-438.

37 Flames N, Pla R, Gelman DM, Rubenstein JL, Puelles L, and Marin O. Delineation of multiple subpallial progenitor domains by the combinatorial expression of transcriptional codes. J Neurosci. 2007;27:9682-9695.

38 Garcia-Lopez M, Abellan A, Legaz I, Rubenstein JL, Puelles L, and Medina L. Histogenetic compartments of the mouse centromedial and extended amygdala based on gene expression patterns during development. The Journal of comparative neurology. 2008;506:46-74.

39 Abellan A, and Medina L. Subdivisions and derivatives of the chicken subpallium based on expression of LIM and other regulatory genes and markers of neuron subpopulations during development. The Journal of comparative neurology. 2009;515:465-501.

40 Kimura S, Hara Y, Pineau T, et al. The T/ebp null mouse: thyroid-specific enhancer-binding protein is essential for the organogenesis of the thyroid, lung, ventral forebrain, and pituitary. Genes & development. 1996;10:60-69.

41 Marin O, Anderson SA, and Rubenstein JL. Origin and molecular specification of striatal interneurons. J Neurosci. 2000;20:6063-6076.

42 Lee BJ, Cho GJ, Norgren RB, Jr., et al. TTF-1, a homeodomain gene required for diencephalic morphogenesis, is postnatally expressed in the neuroendocrine brain in a developmentally regulated and cell-specific fashion. Molecular and cellular neurosciences. 2001;17:107-126.

43 Son YJ, Hur MK, Ryu BJ, et al. TTF-1, a homeodomain-containing transcription factor, participates in the control of body fluid homeostasis by regulating angiotensinogen gene transcription in the rat subfornical organ. J Biol Chem. 2003;278:27043-27052.

44 Nakamura K, Kimura S, Yamazaki M, Kawaguchi A, Inoue K, and Sakai T. Immunohistochemical analyses of thyroid-specific enhancer-binding protein in the fetal and adult rat hypothalami and pituitary glands. Brain Res Dev Brain Res. 2001;130:159-166.

45 Kusakabe T, Kawaguchi A, Hoshi N, Kawaguchi R, Hoshi S, and Kimura S. Thyroid-specific enhancer-binding protein/NKX2.1 is required for the maintenance of ordered architecture and function of the differentiated thyroid. Molecular endocrinology (Baltimore, Md. 2006;20:1796-1809.

46 Mastronardi C, Smiley GG, Raber J, et al. Deletion of the Ttf1 gene in differentiated neurons disrupts female reproduction without impairing basal ganglia function. J Neurosci. 2006;26:13167-13179.

47 Wichterle H, Turnbull DH, Nery S, Fishell G, and Alvarez-Buylla A. In utero fate mapping reveals distinct migratory pathways and fates of neurons born in the mammalian basal forebrain. Development (Cambridge, England). 2001;128:3759-3771.

48 Rakic P. Neurons in rhesus monkey visual cortex: systematic relation between time of origin and eventual disposition. Science (New York, N.Y. 1974;183:425-427.

49 Nadarajah B, Brunstrom JE, Grutzendler J, Wong RO, and Pearlman AL. Two modes of radial migration in early development of the cerebral cortex. Nature neuroscience. 2001;4:143-150.

50 Anderson SA, Qiu M, Bulfone A, et al. Mutations of the homeobox genes Dlx-1 and Dlx-2 disrupt the striatal subventricular zone and differentiation of late born striatal neurons. Neuron. 1997;19:27-37.

51 Wichterle H, Garcia-Verdugo JM, Herrera DG, and Alvarez-Buylla A. Young neurons from medial ganglionic eminence disperse in adult and embryonic brain. Nature neuroscience. 1999;2:461-466.

52 Lavdas AA, Grigoriou M, Pachnis V, and Parnavelas JG. The medial ganglionic eminence gives rise to a population of early neurons in the developing cerebral cortex. J Neurosci. 1999;19:7881-7888.

53 Marin O, and Rubenstein JL. A long, remarkable journey: tangential migration in the telencephalon. Nature reviews. 2001;2:780-790.

54 Letinic K, Zoncu R, and Rakic P. Origin of GABAergic neurons in the human neocortex. Nature. 2002;417:645-649.

55 Schlosser B, Klausa G, Prime G, and Ten Bruggencate G. Postnatal development of calretinin- and parvalbumin-positive interneurons in the rat neostriatum: an immunohistochemical study. The Journal of comparative neurology. 1999;405:185-198.

56 Bender R, Plaschke M, Naumann T, Wahle P, and Frotscher M. Development of cholinergic and GABAergic neurons in the rat medial septum: different onset of choline acetyltransferase and glutamate decarboxylase mRNA expression. The Journal of comparative neurology. 1996;372:204-214.

57 Pleasure SJ, Anderson S, Hevner R, et al. Cell migration from the ganglionic eminences is required for the development of hippocampal GABAergic interneurons. Neuron. 2000;28:727-740.

58 Miyoshi G, Butt SJ, Takebayashi H, and Fishell G. Physiologically distinct temporal cohorts of cortical interneurons arise from telencephalic Olig2-expressing precursors. J Neurosci. 2007;27:7786-7798.

59 Butt SJ, Sousa VH, Fuccillo MV, et al. The requirement of Nkx2-1 in the temporal specification of cortical interneuron subtypes. Neuron. 2008;59:722-732.

60 Grigoriou M, Tucker AS, Sharpe PT, and Pachnis V. Expression and regulation of Lhx6 and Lhx7, a novel subfamily of LIM homeodomain encoding genes, suggests a role in mammalian head development. Development (Cambridge, England). 1998;125:2063-2074.

61 Nobrega-Pereira S, Kessaris N, Du T, Kimura S, Anderson SA, and Marin O. Postmitotic Nkx2-1 controls the migration of telencephalic interneurons by direct repression of guidance receptors. Neuron. 2008;59:733-745.

62 Soriano P. Generalized lacZ expression with the ROSA26 Cre reporter strain. Nat Genet. 1999;21:70-71.

63 Hollerbach EH, Haas CA, Hildebrandt H, Frotscher M, and Naumann T. Region-specific activation of microglial cells in the rat septal complex following fimbria-fornix transection. The Journal of comparative neurology. 1998;390:481-496.

64 Adams JC. Heavy metal intensification of DAB-based HRP reaction product. J Histochem Cytochem. 1981;29:775.

65 Paxinos G FK. The Mouse Brain in Stereotaxic Coordinates, 2 ed. San Diego: Academic Press, 2001.

66 Naumann T, Casademunt E, Hollerbach E, et al. Complete deletion of the neurotrophin receptor p75NTR leads to long-lasting increases in the number of basal forebrain cholinergic neurons. J Neurosci. 2002;22:2409-2418.

67 Mesulam MM, Mufson EJ, Levey AI, and Wainer BH. Cholinergic innervation of cortex by the basal forebrain: cytochemistry and cortical connections of the septal area, diagonal band nuclei, nucleus basalis (substantia innominata), and hypothalamus in the rhesus monkey. The Journal of comparative neurology. 1983;214:170-197.

68 Kermer P, Naumann T, Bender R, and Frotscher M. Fate of GABAergic septohippocampal neurons after fimbria-fornix transection as revealed by in situ hybridization for glutamate decarboxylase mRNA and parvalbumin immunocytochemistry. The Journal of comparative neurology. 1995;362:385-399.

69 Bonnerot C, and Nicolas JF. Application of LacZ gene fusions to postimplantation development. Methods Enzymol. 1993;225:451-469.

70 Erlander MG, Tillakaratne NJ, Feldblum S, Patel N, and Tobin AJ. Two genes encode distinct glutamate decarboxylases. Neuron. 1991;7:91-100.

71 Meldgaard M, Fenger C, Lambertsen KL, Pedersen MD, Ladeby R, and Finsen B. Validation of two reference genes for mRNA level studies of murine disease models in neurobiology. J Neurosci Methods. 2006;156:101-110.

72 Bert B, Dere E, Wilhelmi N, et al. Transient overexpression of the 5-HT1A receptor impairs water-maze but not hole-board performance. Neurobiol Learn Mem. 2005;84:57-68.

73 Bert B, Fink H, Huston JP, and Voits M. Fischer 344 and wistar rats differ in anxiety and habituation but not in water maze performance. Neurobiol Learn Mem. 2002;78:11-22.

74 Allen GV, and Hopkins DA. Mamillary body in the rat: a cytoarchitectonic, Golgi, and ultrastructural study. The Journal of comparative neurology. 1988;275:39-64.

75 Yee CL, Wang Y, Anderson S, Ekker M, and Rubenstein JL. Arcuate nucleus expression of NKX2.1 and DLX and lineages expressing these transcription factors in neuropeptide Y(+), proopiomelanocortin(+), and tyrosine hydroxylase(+)

neurons in neonatal and adult mice. The Journal of comparative neurology. 2009;517:37-50.

76 Naumann T, Linke R, and Frotscher M. Fine structure of rat septohippocampal neurons: I. Identification of septohippocampal projection neurons by retrograde tracing combined with electron microscopic immunocytochemistry and intracellular staining. The Journal of comparative neurology. 1992a;325:207-218.

77 Mugnaini E, Oertel, W.H. . An Atlas of the Distribution of GABAergic Neurons and Terminals in the Rat CNS as revealed by GAD Immunohistochemistry. In A. Bjorklund, Hoekfelt, T.,GABA and Neuropeptides in the CNS, Part I, ed. Amsterdam: Elsevier Science Publishers B.V., 1985:p.^pp. 436-608.

78 Kohler C, and Chan-Palay V. Distribution of gamma aminobutyric acid containing neurons and terminals in the septal area. An immunohistochemical study using antibodies to glutamic acid decarboxylase in the rat brain. Anat Embryol (Berl). 1983;167:53-65.

79 Xu Q, Tam M, and Anderson SA. Fate mapping Nkx2.1-lineage cells in the mouse telencephalon. The Journal of comparative neurology. 2008;506:16-29.

80 Doetsch F, and Alvarez-Buylla A. Network of tangential pathways for neuronal migration in adult mammalian brain. Proc Natl Acad Sci U S A. 1996;93:14895-14900.

81 Young KM, Fogarty M, Kessaris N, and Richardson WD. Subventricular zone stem cells are heterogeneous with respect to their embryonic origins and neurogenic fates in the adult olfactory bulb. J Neurosci. 2007;27:8286-8296.

82 Katarova Z, Sekerkova G, Prodan S, Mugnaini E, and Szabo G. Domain-restricted expression of two glutamic acid decarboxylase genes in midgestation mouse embryos. The Journal of comparative neurology. 2000;424:607-627.

83 Korsching S. The neurotrophic factor concept: a reexamination. J Neurosci. 1993;13:2739-2748.

84 Madisen L, Zwingman TA, Sunkin SM, et al. A robust and high-throughput Cre reporting and characterization system for the whole mouse brain. Nature neuroscience. 13:133-140.

85 Magno L, Catanzariti V, Nitsch R, Krude H, and Naumann T. Ongoing expression of Nkx2.1 in the postnatal mouse forebrain: potential for understanding NKX2.1 haploinsufficiency in humans? Brain research. 2009;1304:164-186.

86 Morris RG, Garrud P, Rawlins JN, and O'Keefe J. Place navigation impaired in rats with hippocampal lesions. Nature. 1982;297:681-683.

87 Holt DJ, Graybiel AM, and Saper CB. Neurochemical architecture of the human striatum. The Journal of comparative neurology. 1997;384:1-25.

88 Bernacer J, Prensa L, and Gimenez-Amaya JM. Chemical architecture of the posterior striatum in the human brain. J Neural Transm. 2008;115:67-75.

89 Morel A, Loup F, Magnin M, and Jeanmonod D. Neurochemical organization of the human basal ganglia: anatomofunctional territories defined by the distributions of calcium-binding proteins and SMI-32. The Journal of comparative neurology. 2002;443:86-103.

90 Buhl EH, and Schlote W. Intracellular lucifer yellow staining and electron microscopy of neurones in slices of fixed epitumourous human cortical tissue. Acta Neuropathol. 1987;75:140-146.

91 Gerfen CR. Basal Ganglia. In G. Paxinos,The Rat Nervous System, ed.: Elsevier Academic Press, 2004:p.^pp. 458-508.

92 Hebert JM, and Fishell G. The genetics of early telencephalon patterning: some assembly required. Nature reviews. 2008;9:678-685.

93 Schuurmans C, and Guillemot F. Molecular mechanisms underlying cell fate specification in the developing telencephalon. Current opinion in neurobiology. 2002;12:26-34.

94 Xu Q, Cobos I, De La Cruz E, Rubenstein JL, and Anderson SA. Origins of cortical interneuron subtypes. J Neurosci. 2004;24:2612-2622.

95 Butt SJ, Fuccillo M, Nery S, et al. The temporal and spatial origins of cortical interneurons predict their physiological subtype. Neuron. 2005;48:591-604.

96 Fogarty M, Grist M, Gelman D, Marin O, Pachnis V, and Kessaris N. Spatial genetic patterning of the embryonic neuroepithelium generates GABAergic interneuron diversity in the adult cortex. J Neurosci. 2007;27:10935-10946.

97 Wonders CP, Taylor L, Welagen J, Mbata IC, Xiang JZ, and Anderson SA. A spatial bias for the origins of interneuron subgroups within the medial ganglionic eminence. Developmental biology. 2008;314:127-136.

98 Liodis P, Denaxa M, Grigoriou M, Akufo-Addo C, Yanagawa Y, and Pachnis V. Lhx6 activity is required for the normal migration and specification of cortical interneuron subtypes. J Neurosci. 2007;27:3078-3089.

99 Du T, Xu Q, Ocbina PJ, and Anderson SA. NKX2.1 specifies cortical interneuron fate by activating Lhx6. Development (Cambridge, England). 2008;135:1559-1567.

100 Fragkouli A, Hearn C, Errington M, et al. Loss of forebrain cholinergic neurons and impairment in spatial learning and memory in LHX7-deficient mice. Eur J Neurosci. 2005;21:2923-2938.

101 Fragkouli A, van Wijk NV, Lopes R, Kessaris N, and Pachnis V. LIM homeodomain transcription factor-dependent specification of bipotential MGE

progenitors into cholinergic and GABAergic striatal interneurons. Development (Cambridge, England). 2009a;136:3841-3851.

102 Nambu A, Tokuno H, Hamada I, et al. Excitatory cortical inputs to pallidal neurons via the subthalamic nucleus in the monkey. J Neurophysiol. 2000;84:289-300.

103 Reiner A, Medina L, and Veenman CL. Structural and functional evolution of the basal ganglia in vertebrates. Brain Res Brain Res Rev. 1998;28:235-285.

104 Kawaguchi Y. Physiological, morphological, and histochemical characterization of three classes of interneurons in rat neostriatum. J Neurosci. 1993;13:4908-4923.

105 Calabresi P, Centonze D, Gubellini P, Pisani A, and Bernardi G. Acetylcholine-mediated modulation of striatal function. Trends in neurosciences. 2000;23:120-126.

106 Kita H. Parvalbumin-immunopositive neurons in rat globus pallidus: a light and electron microscopic study. Brain research. 1994;657:31-41.

107 Aggleton JP. The contribution of the amygdala to normal and abnormal emotional states. Trends in neurosciences. 1993;16:328-333.

108 Davis M, Rainnie D, and Cassell M. Neurotransmission in the rat amygdala related to fear and anxiety. Trends in neurosciences. 1994;17:208-214.

109 Heimer L, Harlan RE, Alheid GF, Garcia MM, and de Olmos J. Substantia innominata: a notion which impedes clinical-anatomical correlations in neuropsychiatric disorders. Neuroscience. 1997;76:957-1006.

110 Harding A, Halliday G, Caine D, and Kril J. Degeneration of anterior thalamic nuclei differentiates alcoholics with amnesia. Brain. 2000;123 (Pt 1):141-154.

111 Mufson EJ, Ginsberg SD, Ikonomovic MD, and DeKosky ST. Human cholinergic basal forebrain: chemoanatomy and neurologic dysfunction. J Chem Neuroanat. 2003;26:233-242.

112 Vann SD, and Aggleton JP. The mammillary bodies: two memory systems in one? Nature reviews. 2004;5:35-44.

113 Andy OJ, Stephan, H. Septum Development in Primates, Vol N. 20, The Septal Nuclei New York: Plenum Press, 1976.

114 Risold PY. The Septal Region. In Paxinos G.,The Rat Nervous System, ed. San Diego: Elsevier Academic Press, 2004:p.^pp. 602-636.

115 Swanson LW, and Cowan WM. The connections of the septal region in the rat. The Journal of comparative neurology. 1979;186:621-655.

116 Risold PY, and Swanson LW. Chemoarchitecture of the rat lateral septal nucleus. Brain Res Brain Res Rev. 1997a;24:91-113.

117 Panula P, Revuelta AV, Cheney DL, Wu JY, and Costa E. An immunohistochemical study on the location of GABAergic neurons in rat septum. The Journal of comparative neurology. 1984;222:69-80.

118 Kohler C, Wu JY, and Chan-Palay V. Neurons and terminals in the retrohippocampal region in the rat's brain identified by anti-gamma-aminobutyric acid and anti-glutamic acid decarboxylase immunocytochemistry. Anat Embryol (Berl). 1985;173:35-44.

119 Onteniente B, Tago H, Kimura H, and Maeda T. Distribution of gamma-aminobutyric acid-immunoreactive neurons in the septal region of the rat brain. The Journal of comparative neurology. 1986;248:422-430.

120 Alonso JR, and Frotscher M. Hippocampo-septal fibers terminate on identified spiny neurons in the lateral septum: a combined Golgi/electron-microscopic and degeneration study in the rat. Cell Tissue Res. 1989a;258:243-246.

121 Alonso JR, and Frotscher M. Organization of the septal region in the rat brain: a Golgi/EM study of lateral septal neurons. The Journal of comparative neurology. 1989b;286:472-487.

122 Leranth C, and Frotscher M. Organization of the septal region in the rat brain: cholinergic-GABAergic interconnections and the termination of hippocampo-septal fibers. The Journal of comparative neurology. 1989;289:304-314.

123 Riedel A, Hartig W, Seeger G, Gartner U, Brauer K, and Arendt T. Principles of rat subcortical forebrain organization: a study using histological techniques and multiple fluorescence labeling. J Chem Neuroanat. 2002;23:75-104.

124 Sofroniew MV, Pearson RC, and Powell TP. The cholinergic nuclei of the basal forebrain of the rat: normal structure, development and experimentally induced degeneration. Brain research. 1987;411:310-331.

125 Risold PY, and Swanson LW. Connections of the rat lateral septal complex. Brain Res Brain Res Rev. 1997b;24:115-195.

126 Dutar P, Bassant MH, Senut MC, and Lamour Y. The septohippocampal pathway: structure and function of a central cholinergic system. Physiological reviews. 1995;75:393-427.

127 Berger-Sweeney J. The cholinergic basal forebrain system during development and its influence on cognitive processes: important questions and potential answers. Neurosci Biobehav Rev. 2003;27:401-411.

128 McKinney M, and Jacksonville MC. Brain cholinergic vulnerability: relevance to behavior and disease. Biochem Pharmacol. 2005;70:1115-1124.

129 Gritti I, Mainville L, Mancia M, and Jones BE. GABAergic and other noncholinergic basal forebrain neurons, together with cholinergic neurons, project to the mesocortex and isocortex in the rat. The Journal of comparative neurology. 1997;383:163-177.

130 Schwegler H, Boldyreva M, Linke R, Wu J, Zilles K, and Crusio WE. Genetic variation in the morphology of the septo-hippocampal cholinergic and GABAergic systems in mice: II. Morpho-behavioral correlations. Hippocampus. 1996;6:535-545.

131 Marin O, Baker J, Puelles L, and Rubenstein JL. Patterning of the basal telencephalon and hypothalamus is essential for guidance of cortical projections. Development (Cambridge, England). 2002;129:761-773.

132 Swaab DF, Hofman MA, Lucassen PJ, Purba JS, Raadsheer FC, and Van de Nes JA. Functional neuroanatomy and neuropathology of the human hypothalamus. Anat Embryol (Berl). 1993;187:317-330.

133 Valassi E, Scacchi M, and Cavagnini F. Neuroendocrine control of food intake. Nutr Metab Cardiovasc Dis. 2008;18:158-168.

134 Bulfone A, Puelles L, Porteus MH, Frohman MA, Martin GR, and Rubenstein JL. Spatially restricted expression of Dlx-1, Dlx-2 (Tes-1), Gbx-2, and Wnt-3 in the embryonic day 12.5 mouse forebrain defines potential transverse and longitudinal segmental boundaries. J Neurosci. 1993;13:3155-3172.

135 Rubenstein JL, Martinez S, Shimamura K, and Puelles L. The embryonic vertebrate forebrain: the prosomeric model. Science (New York, N.Y. 1994;266:578-580.

136 Lledo PM, Merkle FT, and Alvarez-Buylla A. Origin and function of olfactory bulb interneuron diversity. Trends in neurosciences. 2008;31:392-400.

137 Lois C, Garcia-Verdugo JM, and Alvarez-Buylla A. Chain migration of neuronal precursors. Science (New York, N.Y. 1996;271:978-981.

138 Stenman J, Toresson H, and Campbell K. Identification of two distinct progenitor populations in the lateral ganglionic eminence: implications for striatal and olfactory bulb neurogenesis. J Neurosci. 2003;23:167-174.

139 Yun K, Garel S, Fischman S, and Rubenstein JL. Patterning of the lateral ganglionic eminence by the Gsh1 and Gsh2 homeobox genes regulates striatal and olfactory bulb histogenesis and the growth of axons through the basal ganglia. The Journal of comparative neurology. 2003;461:151-165.

140 Das GD, and Altman J. Postnatal neurogenesis in the caudate nucleus and nucleus accumbens septi in the rat. Brain research. 1970;21:122-127.

141 De Marchis S, Fasolo A, and Puche AC. Subventricular zone-derived neuronal progenitors migrate into the subcortical forebrain of postnatal mice. The Journal of comparative neurology. 2004;476:290-300.

142 Merkle FT, Tramontin AD, Garcia-Verdugo JM, and Alvarez-Buylla A. Radial glia give rise to adult neural stem cells in the subventricular zone. Proc Natl Acad Sci U S A. 2004;101:17528-17532.

143 Inta D, Alfonso J, von Engelhardt J, et al. Neurogenesis and widespread forebrain migration of distinct GABAergic neurons from the postnatal subventricular zone. Proc Natl Acad Sci U S A. 2008;105:20994-20999.

144 Amaral DG, and Kurz J. An analysis of the origins of the cholinergic and noncholinergic septal projections to the hippocampal formation of the rat. The Journal of comparative neurology. 1985;240:37-59.

145 Freund TF. GABAergic septohippocampal neurons contain parvalbumin. Brain research. 1989;478:375-381.

146 Birthelmer A, Lazaris A, Riegert C, et al. Does the release of acetylcholine in septal slices originate from intrinsic cholinergic neurons bearing p75(NTR) receptors? A study using 192 IgG-saporin lesions in rats. Neuroscience. 2003;122:1059-1071.

147 Schambra UB, Sulik KK, Petrusz P, and Lauder JM. Ontogeny of cholinergic neurons in the mouse forebrain. The Journal of comparative neurology. 1989;288:101-122.

148 Naumann T, Peterson GM, and Frotscher M. Fine structure of rat septohippocampal neurons: II. A time course analysis following axotomy. The Journal of comparative neurology. 1992b;325:219-242.

149 Clarke PG. Developmental cell death: morphological diversity and multiple mechanisms. Anat Embryol (Berl). 1990;181:195-213.

150 Fragkouli A, Pachnis V, and Stylianopoulou F. Sex differences in water maze performance and cortical neurotrophin levels of LHX7 null mutant mice. Neuroscience. 2009b;158:1224-1233.

ACKNOWLEDGEMENTS

First I would like to thank my “Doktorvater” Dr. Thomas Naumann for the supervision and the fruitful discussions during these last four years.

I would like to gratefully acknowledge Prof. Nitsch and all collaborators which contributed to the development of the project: Dr. Oliver Kretz, Dr. Bettina Bert, Prof. Heidrun Fink, Prof. Hannah Monyer, Prof. Heiko Krude, Katharina Paulick, Dr. Johannes Vogt.

Vielen Dank to my “direct colleagues” Gudrun Thomaschek, Christian Gujjarro, Sara Ersoezlue and all the “indirect colleagues” of the Institut für Zell- und Neurobiologie (Anatomie, Charite´ Campus Mitte).

All this work was not possible without the support of my family and friends. I owe them for their constancy, niceness, tolerance and support throughout. I am especially grateful to Greg for the proofreading of this text.

Last but not least a very special thank to my partner Vincenzo Catanzariti. Thank you so much for supporting me all the time, for contributing to the formatting and proofreading of all my works and for being a cardinal point of my life.

APPENDIX

Appendix 1: List of regions where Nkx2-1-positive profiles have been identified.

TELENCEPHALON

accumbens nucleus

Acb accumbens nu

AcbC accumbens nu, core

AcbSh accumbens nu, shell

CPu caudate putamen

E/OV ependymal and subependymal layer /olfactory tubercle

hippocampal formation:

CA1 field CA1 of the hippocampus

CA3 field CA3 of the hippocampus

CA2 field CA2 of the hippocampus

LGP Lateral globus pallidus

septal complex

MS medial septal nu

LS lateral septal nu

LSI lateral septal nu, intermediate part

LSV lateral septal nu, ventral part

LSD lateral septal nu, dorsal part

HDB nu of the horizontal limb of the diagonal band

VDB nu of the vertical limb of the diagonal band

SHi septohippocampal nu

SI substantia innominata

DIENCEPHALON

third ventricle

AVPe anteroventral periventricular nu

Pe periventricular hypothalamic nucleus

Arc arcuate nucleus

amygdala

AAV anterior amygdaloid area, ventral part

BLA basolateral amygdaloid nu

BMP basomedial amygdaloid nu, posterior part

La lateral amygdaloid nu

Me Medial amygdaloid nu

BST bed nu stria terminalis

hypothalamus

AHP anterior hypothalamic area, posterior part

DMH dorsomedial hypothalamic nu

LH lateral hypothalamic area

MCLH magnocellular nu of the lateral hypothalamus

PH posterior hypothalamic area

VMH ventromedial hypothalamic nu

Mammillary bodies

LM Lateral mammillary nucleus

MM Medial mammillary nucleus

ME median eminence

MGP medial globus pallidus

POA preoptic area

MPA Medial preoptic area

MPO Medial preoptic nucleus

LPO lateral preoptic area

ADP anterodorsal preoptic nu

MnPO median preoptic nu

SFO subfornical organ

Appendix 2: Table of cell numbers

Table 1. Total number of ChAT-immunoreactive neurons in the regions investigated of *GAD//fl/fl* and *GADcre+/-//fl/fl* (3 months of age) as obtained by stereological cell counts.

MSvBD		**hDB-SI**		**CPu**		**LGP**	
GAD//fl/fl	*GADcre+/-//fl/fl*	*GAD//fl/fl*	*GADcre+/-//fl/fl*	*GAD//fl/fl*	*GADcre+/-//fl/fl*	*GAD//fl/fl*	*GADcre+/-//fl/fl*
1049	284	622	249	5191	0	800	409
1280	249	782	71	7467	71	1316	551
2073	160	1137	18	4693	160	1084	302
1291	320	1185	142	7217	190	1413	711
1237	373	1073	356	7807	49	1244	604
1190	231	948	89	6963	0	1203	676

Table 2.Total number of PV-immunoreactive neurons in the regions investigated of *GAD//fl/fl* and *GADcre+/-//fl/fl* (3 months of age) as obtained by stereological cell counts.

MSvBD		**hDB-SI**		**CPu**		**LGP**	
GAD//fl/fl	*GADcre+/-//fl/fl*	*GAD//fl/fl*	*GADcre+/-//fl/fl*	*GAD//fl/fl*	*GADcre+/-//fl/fl*	*GAD//fl/fl*	*GADcre+/-//fl/fl*
1333	853	267	18	7538	853	1742	818
480	533	213	53	9312	512	2240	489
1209	729	284	36	7844	602	1867	516
1170	338	302	71	8312	392	1983	160
1288	640	216	62	7201	592	1610	422
1093	402	328	36	7973	427	1843	269

Table 3. Total number of ChAT-immunoreactive neurons in the regions investigated of *ChATcre+/-//fl/fl mice* (P15) as obtained by stereological cell counts.

MSvBD	**hDB-SI**	**CPu**	**LGP**
1809	747	8533	1493
2044	907	7538	1458
1938	1120	6187	1013
2649	800	7467	942
1778	1191	5902	1138
2293	1031	6314	1287

Table 4. Total number of ChAT-immunoreactive neurons in the regions investigated of *ChAT//fl/fl* and *ChATcre+/-//fl/fl* mice (3 months of age) as obtained by stereological cell counts.

MSvBD		**hDB-SI**		**CPu**		**LGP**	
ChAT//fl/fl	*ChATcre+/-//fl/fl*	*ChAT//fl/fl*	*ChATcre+/-//fl/fl*	*ChAT//fl/fl*	*ChATcre+/-//fl/fl*	*ChAT//fl/fl*	*ChATcre+/-//fl/fl*
1191	667	1262	818	5902	2606	1013	516
2014	800	1458	480	7431	3015	836	427
1636	853	1102	800	5689	3164	1137	285
1458	1067	1529	480	6400	2951	1227	142
1240	644	1315	715	6852	3920	1055	451
1973	708	748	755	8179	3467	1387	692

CURRICULUM VITAE

Mein Lebenslauf wird aud datenschutzrechtlichen Gruenden in der elektonischen Version meiner Arbeit nicht veroeffentlich.

LIST OF PUBLICATIONS

Articles:

"**Pattern of Tau forms in CSF is altered in progressive supranuclear palsy**."
Borroni B., Gardoni F., Parnetti L., Magno L., Malinverno M., Maggese E., Calabresi P., Spillantini M.G., Padovani A., Di Luca M.
Neurobiol Aging. 2009 Jan 30 (1):34-40. PMID: 17709155

"**Ongoing expression of Nkx2.1 in the postnatal mouse forebrain: potential for understanding *NKX2.1* haploinsufficiency in humans?**"
Magno L., Catanzariti V., Nitsch R., Krude H., Naumann T.
Brain Research. 2009 Dec 22;1304:164-86. PMID: 19766601

"**The integrity of central cholinergic neurons depends on prenatal *and* postnatal expression of Nkx2-1**."
Magno L., Kretz O., Bert B., Ersözlü S., Vogt J., Fink H., Kimura S., Vogt A., Monyer H., Nitsch R., Naumann T.
(under revision at Brain)

Abstracts:

SfN Neuroscience 2009
Chicago, IL, October 17-21, 2009
"Nkx2.1 transcription factor is necessary for the proper devepolment and maintenance of the basal forebrain cholinergic neurons" *Magno L., Kretz O., Monyer H., Bert B., Kimura S., Nitsch R., Naumann T.*

Gordon Conference "Inhibition in the CNS"
Waterville, ME, July 26-31, 2009
"Inactivation of Nkx2.1 in GAD-67 expressing neurons leads to deficits in movement coordination" *Magno L., Kretz O., Bert B., Monyer H., Kimura S., Nitsch R., Naumann T.*

Berlin Brain Days 2008

5th International PhD student symposium – Berlin, December 9-10, 2008

"Development and maturation of cholinergic and GABAergic neurons require Nkx2.1 expression" *Magno L., Nitsch R., Naumann T.*

6th FENS Forum of European Neuroscience

Geneva, July 12-16, 2008

"Postnatal expression of the transcription factor Nkx2.1 in mouse telencephalon" *Magno L., Krude H., Nitsch R., Naumann T.*

SFB 665 Symposium 2007

Berlin, November 15-17, 2007

"The ontogeny, phylogeny and pathology of Nkx2.1 gene function in the brain" *Magno L., Paulick K., Schnittert S., Naumann T., Birchmeier C., Nitsch R., Krude H.*

Berlin Brain Days 2007

4th International PhD student symposium & Seminar on Neuroinflammation – Berlin, November 26-29, 2007

"The role of Nkx2.1 gene in human and mouse brain" *Magno L.*

Berlin Brain Days 2006

3rd International PhD student symposium & Seminar on Imaging in Neuroscience – Berlin, October 29 - November 1, 2006

"Pathology of Nkx2.1 gene function in the brain" *Magno L.*

IX Annual Meeting ITINAD

Italian Interdisciplinary Network on Alzheimer Disease – Sorrento, May 26-28, 2005

"Decreased levels of Adam 10 in AD patients' platelets are paralleled by a decrease in mRNA." *Magno L., Borroni B., Marcello E., Gardoni F., Padovani A., Cattabeni F., DiLuca M.*

ERKLÄRUNG

„Ich, Lorenza Magno, erkläre, dass ich die vorgelegte Dissertation mit dem Thema: „The integrity of basal forebrain neurons depends on permanent expression of Nkx2-1: potential for understanding haploinsufficiency in humans.“ selbst verfasst und keine anderen als die angegebenen Quellen und Hilfsmittel benutzt, ohne die (unzulässige) Hilfe Dritter verfasst und auch in Teilen keine Kopien anderer Arbeiten dargestellt habe.“

01.11.2010 Lorenza Magno